

# Historic climate extremes analysis for the Wellington Region

*Prepared for Greater Wellington Regional Council*

*December 2020*

Prepared by:

John-Mark Woolley  
Richard Turner  
Neelesh Rampal  
Trevor Carey-Smith  
Ed Yang  
Petra Pearce



For any information regarding this report please contact:

Petra Pearce  
Manager - Climate, Atmosphere and Hazards  
Climate and Environmental Applications  
+64-9-375 2052  
petra.pearce@niwa.co.nz

National Institute of Water & Atmospheric Research Ltd  
Private Bag 99940  
Viaduct Harbour  
Auckland 1010

Phone +64 9 375 2050

NIWA CLIENT REPORT No: 2020089AK  
Report date: December 2020  
NIWA Project: WRC20101

Quality Assurance Statement		
	Reviewed by:	Dr Nicolas Fauchereau Climate Scientist NIWA Hamilton
	Formatting checked by:	John-Mark Woolley
	Approved for release by:	Dr Andrew Tait Chief Scientist – Climate, Atmosphere and Hazards NIWA Wellington

© All rights reserved. This publication may not be reproduced or copied in any form without the permission of the copyright owner(s). Such permission is only to be given in accordance with the terms of the client's contract with NIWA. This copyright extends to all forms of copying and any storage of material in any kind of information retrieval system.

Whilst NIWA has used all reasonable endeavours to ensure that the information contained in this document is accurate, NIWA does not give any express or implied warranty as to the completeness of the information contained herein, or that it will be suitable for any purpose(s) other than those specifically contemplated during the Project or agreed by NIWA and the Client.

## Contents

<b>Executive summary .....</b>	<b>9</b>
<b>1 Introduction .....</b>	<b>11</b>
<b>2 Wind .....</b>	<b>11</b>
2.1 Data and methods .....	11
2.2 Wellington.....	14
2.3 Wairarapa .....	22
<b>3 Rainfall intensity.....</b>	<b>26</b>
3.1 Historic rainfall threshold exceedances.....	27
3.2 Future changes in rainfall threshold exceedances .....	33
<b>4 Mean sea level pressure.....</b>	<b>40</b>
4.1 Methodology and data .....	40
4.2 Annual trends in pressure.....	43
4.3 Seasonal variability in pressure .....	46
4.4 Multi-year and Inter-decadal variability .....	48
<b>5 Dew point temperature .....</b>	<b>53</b>
5.1 Methodology and data .....	53
5.2 Wellington.....	56
5.3 Wairarapa .....	63
<b>6 Conclusions .....</b>	<b>72</b>
<b>7 Supplementary figures.....</b>	<b>73</b>
<b>8 Acknowledgements .....</b>	<b>75</b>
<b>9 References.....</b>	<b>76</b>

### Tables

Table 2-1:	Details on the climate stations in this section, including station name, NIWA Climate Database Agent No, longitude, latitude, and comments.	12
Table 2-2:	Details about the wind sensors at the climate stations in this paper, including base elevation, height of sensor, and remarks.	12
Table 2-3:	Table listing the annual maximum homogenised gust ( $\text{ms}^{-1}$ ) at Wellington Aero for the decades 1960's to 2010's.	14

Table 2-4:	Table showing annual maximum gust speeds homogenised ( $\text{ms}^{-1}$ ) for Masterton in period 1991 to 2019.	23
Table 3-1:	Details of rainfall gauges used in this section. Gauges labelled with 'infill' were used for filling gaps in the main records for that location.	26
Table 3-2:	Annual rainfall thresholds analysed for Wellington Region sites from HIRDS.	27
Table 3-3:	Average annual rainfall threshold exceedances for all four Wellington Region sites, for the entire period of record.	32
Table 3-4:	Percentage change factors for a 2-year return period event to project rainfall depths derived from the current climate to a future climate that is 1 degree warmer. The values in brackets show the expected variability across New Zealand based on Regional Climate Modelling results (from Table 6 and Table 7 in Carey-Smith et al., 2018).	33
Table 3-5:	New Zealand land-average temperature increase ( $^{\circ}\text{C}$ ) relative to 1986—2005 for four future greenhouse gas concentration scenarios. Each projection is an average of six regional climate model simulations (from Table 8 in Carey-Smith et al., 2018).	33
Table 3-6:	Adjusted thresholds (in mm) used to account for model biases when estimating changes in event frequency from RCM rainfall.	35
Table 4-1:	Listing of Climate stations where 9 am (NZST) mean sea level pressure records were obtained for this section.	40
Table 4-2:	Pressure thresholds used for the analysis on a monthly basis.	42
Table 4-3:	5-highest years of annual mean pressure (hPa, Jan-Dec average) and associated relative humidity (RH, %), temperature ( $^{\circ}\text{C}$ ), and wind speed anomalies.	46
Table 4-4:	5-lowest years of annual mean pressure (hPa, Jan-Dec average) and associated relative humidity (RH, %), temperature ( $^{\circ}\text{C}$ ), and wind speed anomalies.	46
Table 4-5:	The correlation coefficient between the % of pressure events above and below the 90 <sup>th</sup> and 10 <sup>th</sup> percentile and the SOI (left column) and IPO (right column) indexes, respectively.	49
Table 4-6:	Decades with the highest percentage of pressure observations falling below the 10 <sup>th</sup> percentile (All Seasons).	51
Table 4-7:	Decades with the highest percentage of pressure observations exceeding the 90 <sup>th</sup> percentile (All Seasons).	52
Table 5-1:	Listing of Climate stations where 9 am (NZST) temperature and humidity records were obtained for this section.	54
Table 5-2:	Regression relationships and correlations between 8 am and 9 am temperature and humidity variables for stations where hourly records available. $T_a$ = dry bulb air temperature, $T_w$ = wet bulb air temperature, RH = relative humidity, $T_d$ = dew point temperature.	55
Table 5-3:	Change in average seasonal values in "9 am" dew-point temperature ( $T_d$ ), Relative Humidity (RH), dry bulb air temperature ( $T_a$ ) and wet-bulb air-temperature ( $T_w$ ) for the Kelburn, Wellington site between 1928 and 2020.	57
Table 5-4:	Top ten ranked months with highest average 9 am $T_d$ (6 <sup>th</sup> column) in the period 1928 to 2019 at Kelburn. Also listed are the average values $T_a$ , $T_w$ , RH in these months.	59
Table 5-5:	Bottom ten ranked months with lowest average 9 am $T_d$ (6 <sup>th</sup> column) in the period 1928 to 2019 at Kelburn. Also listed are the average values $T_a$ , $T_w$ , RH in these months.	60

Table 5-6:	Dates of extreme high values (top ten) of “9 am” $T_d$ (6th column) in the period 1928 to 2019 at Kelburn. Also listed are the values $T_a$ , $T_w$ , RH and Dew-point depression ( $DPP = T_a - T_d$ ) on these dates.	63
Table 5-7:	Dates of extreme low values (bottom ten) of “9 am” $T_d$ (6th column) in the period 1928 to 2019 at Kelburn. Also listed are the values $T_a$ , $T_w$ , RH and Dew-point depression ( $DPP = T_a - T_d$ ) on these dates.	63
Table 5-8:	Change in average seasonal values in “9 am” dew-point temperature ( $T_d$ ), Relative Humidity (RH), dry bulb air temperature ( $T_a$ ) and wet-bulb air-temperature ( $T_w$ ) for the Masterton, Wairarapa site between 1928 and 2019.	64
Table 5-9:	Top ten ranked months with highest average “9 am” $T_d$ (6th column) in the period 1928 to 2019 at Masterton. Also listed are the average values $T_a$ , $T_w$ , RH in these months.	67
Table 5-10:	Bottom ten ranked months with lowest average “9 am” $T_d$ (6th column) in the period 1928 to 2019 at Masterton. Also listed are the average values $T_a$ , $T_w$ , RH in these months.	67
Table 5-11:	Dates of extreme high values (top ten) of “9 am” $T_d$ (6th column) in the period 1928 to 2019 at Masterton. Also listed are the values $T_a$ , $T_w$ , RH and Dew-point depression ( $DPP = T_a - T_d$ ) on these dates.	70
Table 5-12:	Dates of extreme low (bottom ten) values of “9 am” $T_d$ (6th column) in the period 1928 to 2019 at Masterton. Also listed are the values $T_a$ , $T_w$ , RH and Dew-point depression ( $DPP = T_a - T_d$ ) on these dates.	71

## Figures

Figure 2-1:	Map showing location of wind gust observing sites at Wellington Airport.	13
Figure 2-2:	Map showing location of wind gust observing sites at East Taratahi and Masterton Aero AWS .	13
Figure 2-3:	Time-series plots showing annual maximum gusts ( $ms^{-1}$ ) (thick red lines) and annual maximum northerly (thin red line) and southerly (thin green line) sector gusts for Wellington Aero from 1960 to 2019.	15
Figure 2-4:	Maximum daily wind gusts ( $ms^{-1}$ ) plotted against mean daily temperatures ( $^{\circ}C$ ) for Wellington Aero from 13-April to 11-May 1974.	16
Figure 2-5:	Maximum daily wind gusts ( $ms^{-1}$ ) plotted against mean daily temperatures ( $^{\circ}C$ ) for Wellington Aero from 06-June to 04-July 2013.	16
Figure 2-6:	Time series of homogenised noon (12:00 pm NZST) gusts ( $ms^{-1}$ , blue dots) for Wellington Aero for the period 1994 through 2019.	17
Figure 2-7:	Time series of daily wind run (km) for Wellington Aero for the period 1994 through 2019.	17
Figure 2-8:	Time series of daily maximum wind gusts ( $ms^{-1}$ ) at Wellington Aero for the period 1972 through 2017 from N (top panel) and S (bottom panel).	18
Figure 2-9:	Annual and seasonal time-series of average maximum daily gust speeds ( $ms^{-1}$ ) for Wellington Aero from 1972 to 2017.	20
Figure 2-10:	Annual and seasonal time-series plotting the number of days exceeding the 90th, 95th, and 99th percentiles gust speeds ( $ms^{-1}$ ) for Wellington Aero from 1972 to 2017.	21
Figure 2-11:	Time series of the homogenised annual maximum gust ( $ms^{-1}$ , thick blue line) at Masterton for the period 1991 to 2020. Also shown are the annual maximum	

	southerly sector gust (SE through WSW - green line) and the maximum northerly (NW through NE – red line).	22
Figure 2-12:	Homogenised noon (12:00 pm NZST) gust record ( $\text{ms}^{-1}$ ) for Masterton, based on East Taratahi (green) and Masterton AWS (blue) gust records for the period 1995 to 2020.	23
Figure 2-13:	Time series of daily maximum wind gusts ( $\text{ms}^{-1}$ ) at Masterton (East Taratahi plus Masterton – Homogenised) for the period 1991 through 2019 from NW (top panel) and S (bottom panel).	24
Figure 2-14:	Count of days per year in which daily max gusts from the NW (top panel) and S (bottom panel) directions have occurred at Masterton in the period 1991 to 2019.	25
Figure 2-15:	Time series of daily wind run (km) for Masterton (East Taratahi plus Masterton AWS) for the period 1991 to 2019.	25
Figure 3-1:	Average annual rainfall threshold exceedances per decade for Kelburn.	28
Figure 3-2:	Average annual rainfall threshold exceedances per decade for Wellington Aero .	29
Figure 3-3:	Average annual rainfall threshold exceedances per decade for Paraparaumu.	30
Figure 3-4:	Average annual rainfall threshold exceedances per decade for Masterton.	31
Figure 3-5:	Average annual rainfall threshold exceedances for all four Wellington Region locations, for the entire period of record.	32
Figure 3-6:	The change in rainfall exceedances with climate change for Kelburn.	36
Figure 3-7:	As Figure 3-6 but for Wellington Aero.	37
Figure 3-8:	As Figure 3-6 but for Paraparaumu.	38
Figure 3-9:	As Figure 3-6 but for Masterton.	39
Figure 4-1:	Approximate locations of Wellington climate stations used in the pressure analysis.	41
Figure 4-2:	The probability distribution of all pressure observations from the combined pressure record.	42
Figure 4-3:	An illustration of the aggregated Wellington pressure record (hPa), with the records of each individual site color-coded.	43
Figure 4-4:	An illustration of the aggregated Wellington pressure record (hPa) as show in Figure 4-3, with the trend analysis for annual minimum pressure (red) and annual maximum pressure (blue).	44
Figure 4-5:	Trend analysis for annual minimum pressure (hPa, top), annual maximum pressure (middle), and annual mean pressure (bottom).	45
Figure 4-6:	The mean seasonal cycle (1868 – present) of the % of observations that fall below or exceed the 10 <sup>th</sup> and 90 <sup>th</sup> percentile, respectively .	47
Figure 4-7:	A comparison of the distribution of pressure for Summer (Dec-Feb) and Winter (Jun-Aug).	48
Figure 4-8:	The annual mean time-series for the SOI and percentage of observations of mean sea level pressure in Wellington below the 10th percentile (a) and above the 90th percentile (b) over the period 1950-2020. A two-year running mean is applied to both time-series. Dashed lines are trend lines obtained by linear regression.	50
Figure 4-9:	The annual mean time-series (10-year running mean) for the IPO and percentage of observations of mean sea level pressure in Wellington below the	

	10th percentile (a) and above the 90th percentile (b) over the period 1870 – 2020.	51
Figure 5-1:	Map showing location of Masterton climate stations with records used in the Dewpoint Temperature analysis.	55
Figure 5-2:	Time series of summer “9 am” averages for dry bulb air temperature ( $T_a$ ; red-line), wet-bulb air-temperature ( $T_w$ ; orange line), dew-point temperature ( $T_d$ ; blue line) and Relative Humidity ( $RH$ ; green line) for the Kelburn, Wellington site for the period 1928 to 2020.	57
Figure 5-3:	Time series of autumn “9 am” averages for dry bulb air temperature ( $T_a$ ; red-line), wet-bulb air-temperature ( $T_w$ ; orange line), dew-point temperature ( $T_d$ ; blue line) and Relative Humidity ( $RH$ ; green line) for the Kelburn, Wellington site for the period 1928 to 2020.	58
Figure 5-4:	Time series of winter “9 am” averages for dry bulb air temperature ( $T_a$ ; red-line), wet-bulb air-temperature ( $T_w$ ; orange line), dew-point temperature ( $T_d$ ; blue line) and Relative Humidity ( $RH$ ; green line) for the Kelburn, Wellington site for the period 1928 to 2020.	58
Figure 5-5:	Time series of spring “9 am” averages for dry bulb air temperature ( $T_a$ ; red-line), wet-bulb air-temperature ( $T_w$ ; orange line), dew-point temperature ( $T_d$ ; blue line) and Relative Humidity ( $RH$ ; green line) for the Kelburn, Wellington site for the period 1928 to 2020.	59
Figure 5-6:	Monthly “9 am” average (orange lines), minimum (blue lines), and maximum (red lines) time series (thin lines) of dry bulb air temperature ( $T_a$ ) for Kelburn, Wellington for the period 1929 to 2019.	61
Figure 5-7:	Monthly “9 am” average (orange lines), minimum (blue lines), and maximum (red lines) time series (thin lines) of wet bulb temperature ( $T_w$ ) for Kelburn, Wellington for the period 1929 to 2019.	61
Figure 5-8:	Monthly “9 am” average (orange lines), minimum (blue lines), and maximum (red lines) time series (thin lines) of relative humidity ( $RH$ ) for Kelburn, Wellington for the period 1929 to 2019.	62
Figure 5-9:	Monthly “9 am” average (orange lines), minimum (blue lines), and maximum (red lines) time series (thin lines) of dew-point temperature ( $T_d$ ) for Kelburn, Wellington for the period 1929 to 2019.	62
Figure 5-10:	Time series of “9 am” summer averages for dry bulb air temperature ( $T_a$ ; red-line), wet-bulb air-temperature ( $T_w$ ; orange line), dew-point temperature ( $T_d$ ; blue line) and Relative Humidity ( $RH$ ; green line) for the Masterton, Wairarapa site for the period 1928 to 2020.	65
Figure 5-11:	Time series of “9 am” autumn averages for dry bulb air temperature ( $T_a$ ; red-line), wet-bulb air-temperature ( $T_w$ ; orange line), dew-point temperature ( $T_d$ ; blue line) and Relative Humidity ( $RH$ ; green line) for the Masterton, Wairarapa site for the period 1928 to 2020.	65
Figure 5-12:	Time series of “9 am” winter averages for dry bulb air temperature ( $T_a$ ; red-line), wet-bulb air-temperature ( $T_w$ ; orange line), dew-point temperature ( $T_d$ ; blue line) and Relative Humidity ( $RH$ ; green line) for the Masterton, Wairarapa site for the period 1928 to 2020.	66
Figure 5-13:	Time series of “9 am” spring averages for dry bulb air temperature ( $T_a$ ; red-line), wet-bulb air-temperature ( $T_w$ ; orange line), dew-point temperature ( $T_d$ ; blue line) and Relative Humidity ( $RH$ ; green line) for the Masterton, Wairarapa site for the period 1928 to 2020.	66

Figure 5-14:	Monthly “9 am” average (orange lines), minimum (blue lines), and maximum (red lines) time series (thin lines) of dry bulb air temperature ( $T_a$ ) for Masterton, Wairarapa for the period 1929 to 2019.	68
Figure 5-15:	Monthly “9 am” average (orange lines), minimum (blue lines), and maximum (red lines) time series (thin lines) wet bulb temperature ( $T_w$ ) for Masterton, Wairarapa for the period 1929 to 2019.	69
Figure 5-16:	Monthly “9 am” average (orange lines), minimum (blue lines), and maximum (red lines) time series (thin lines) of relative humidity (RH) for Masterton, Wairarapa for the period 1929 to 2019.	69
Figure 5-17:	Monthly “9 am” average (orange lines), minimum (blue lines), and maximum (red lines) time series (thin lines) of dew-point temperature ( $T_d$ ) for Masterton, Wairarapa for the period 1929 to 2019.	70
Figure 7-1:	Standard deviation of annual mean sea level pressure through time	73
Figure 7-2:	Standard deviation of 3-year mean sea level pressure through time computed using 3-year bins.	74
Figure 7-3:	Standard deviation of mean sea level pressure through time computed using a 5-year bins.	74



## Executive summary

This report follows the 'Wellington Region Climate Change Extremes' report completed by NIWA for Greater Wellington Regional Council in 2019 (Pearce et al., 2019). This report is considered an appendix to the 2019 report, with additional analysis of historic climate extremes for Wellington sites of wind, rainfall, atmospheric pressure, and dew point temperature.

### Wind

Analyses of trends and records in maximum wind gusts at Wellington (1960-2019) and Masterton (1991-2019) were carried out. Homogenisation techniques were used to account for potential changes in exposure due to station location changes.

The time series of annual maximum gusts at Masterton shows a decreasing number of southerlies and an increasing number of northerlies.

North-westerly events dominate annual maxima events in Masterton and northerlies dominate the Wellington record.

The three annual maximum events in the Wellington record that are southerly include the strongest on record (the *Wahine* storm of 1968) and two other very strong events (2013 and 1974).

There is little in terms of temporal trends in strength of annual maxima, but some increasing trends in Wellington for spring.

### Rainfall

Changes in the frequency of extreme precipitation events for four locations in the Wellington Region were analysed using the following thresholds: number of events >5 mm in 10 minutes, events >10 mm in 30 minutes, events >15 mm in 1 hour, events >40 mm in 6 hours, events >50 mm in 12 hours, events >60 mm in 24 hours, and events >100 mm in 48, 72, and 120 hours.

There are no obvious consistent temporal trends in the frequency of historic extreme precipitation events within or between the analysed sites.

Of the stations that were analysed, Kelburn generally has the largest number of exceedances of extreme rainfall thresholds per year while Waingawa (Masterton) has the least.

### Atmospheric pressure

The analysis of atmospheric pressure was carried out for Wellington city, incorporating data from a group of sites in close proximity. Data for Wellington city goes back to the 1860s.

Extreme pressure observations were considered as those which fall below the 10<sup>th</sup> percentile (low pressure) or exceed the 90<sup>th</sup> percentile (high pressure) of all observations in the record.

Extreme low pressure events are more evenly distributed across the seasons whereas extreme high pressure events are more concentrated in autumn and winter.

More high pressure extremes are observed during La Niña and more low-pressure extremes occur during El Niño.

Extreme low-pressure events occur more frequently than average during the positive phase of the Interdecadal Pacific Oscillation (IPO). During the negative phase of the IPO extreme high-pressure events occur more frequently than average.

### **Dew point temperature**

Digitisation of daily wet and dry bulb temperature data for both Kelburn and Masterton sites was completed to enable this analysis.

Overall, there was a 0.7 °C increase in dew point temperature ( $T_d$ ) averaged over all seasons.

The strongest trend for an increase was in winter, amounting to +1.7 °C over 90 years at Kelburn, and +1.8 °C at Masterton over the same period. Autumn also saw increasing trends at both locations whereas summer and spring saw smaller increases.

January 2018 had the highest average  $T_d$  values of any month in both the Kelburn and Wairarapa records while February 1998 was ranked third in the Kelburn record. Both 1998 and 2018 are tied for 2<sup>nd</sup> warmest years on record for New Zealand (dry bulb air temperature).

Despite the long-term upward trend, average  $T_d$  values for February 1938 and February 1935 are ranked 2<sup>nd</sup> and 10<sup>th</sup> highest respectively in the Kelburn record. February 1935 is also ranked 8<sup>th</sup> highest in the Wairarapa record.

Extreme high summer and autumn values of  $T_d$  occurred in the 1930's where there seems to be considerable year to year variability.

Of the ten months with lowest average  $T_d$  values, seven occurred in the 1930's and 1940's for Wellington. At Masterton, six were in the 1930's and all ten had occurred by 1972.

# 1 Introduction

In 2019, NIWA completed a report for Greater Wellington Regional Council (GWRC) about projections and impacts of climate change extremes on the region (Pearce et al., 2019)<sup>1</sup>. This report is an extension to the 2019 report, presented as a standalone document but intended to serve as an appendix.

This report presents analyses for historic extremes of wind, rainfall, air pressure, and dew point temperature data for the Wellington Region.

## 2 Wind

### 2.1 Data and methods

The wind speed parameters analysed in this report are daily maximum gust speeds, 12 p.m. local time gust speeds and daily wind-run (equivalent to the daily average mean speed). Stations used in this study are Wellington Aero for Wellington, and East Taratahi and Masterton Aero Automatic Weather Station (AWS) for the Wairarapa. These stations were chosen because they have the longest running gust speed records and key station details are provided in Table 2-1 and Table 2-2. In order to get long-term records for the locations, combining records due to shifts in the location (Figure 2-1 and Figure 2-2) of the anemometer was required. To combine the records sensibly, homogenisation procedures as described in Turner et al. (2019) must be applied. These homogenization procedures account for changes in instrumentation (e.g. Munro MK II anemometers tended to overspeed in high wind situations), exposure, local hill-shape effect and upwind fetch, and produce speeds that approximate what would be observed at an airfield with short grass and flat terrain. Turner et al. (2019) provides extensive detail about this methodology and applied this process to Wellington Aero - some of those results are directly presented here. For Masterton, differences in exposure and fetch had to be accounted for in the homogenisation. Additionally, there was an eight-month period of overlap of the East Taratahi and Masterton records (26 February to 4 November 2009) which allowed calibration of the homogenisation (see Figure 2-12).

---

<sup>1</sup> NIWA client report 2019134AK. Available at <https://www.gw.govt.nz/assets/Climate-change/GWRC-NIWA-climate-extremes-FINAL3.pdf>

**Table 2-1: Details on the climate stations in this section, including station name, NIWA Climate Database Agent No, longitude, latitude, and comments. Note the datum for longitude and latitude is WGS84 and coordinates are for the anemometer masts.**

Name	Agent No	Longitude (deg E)	Latitude (deg S)	Comment
Wellington Aero	3445	174.8114	41.3317	Anemometer on mast above terminal at airfield, and gust records available from 1972-1993. Monthly Max gusts from 1961.
Wellington Aero	3445	174.8056	41.3314	Anemometer to west of runway and adjacent to road and seawall, gust records available from 1994 to present, flat and open exposure and near sea-level.
East Taratahi	2612	175.6225	41.0138	Rural setting – grass farmland and some trees. 5km south from edge of town. This station on outer edge of NW lee zone and gust records are for 1991-2009.
Masterton Aero AWS	36735	175.6389	40.9762	SE of airstrip and 900 m from edge of town. This station on outer edge of NW lee zone and gust records are available for 2009-2020.

**Table 2-2: Details about the wind sensors at the climate stations in this paper, including base elevation, height of sensor, and remarks.**

	Parameter	Base Elevation (m)	Height of sensor above Base Elevation (m)	Remarks
Wellington Aero	Wind Speed	3	11 (prior 1993)/7 (present)	MK II/WAA151
Wellington Aero	Wind Direction	3	11 (prior 1993)/7 (present)	MK II/WAV151
East Taratahi	Wind Speed	91	10	WAA151
East Taratahi	Wind Direction	91	10	WAV151
Masterton Aero AWS	Wind Speed	104	10	WAA151
Masterton Aero AWS	Wind Direction	104	10	WAV151

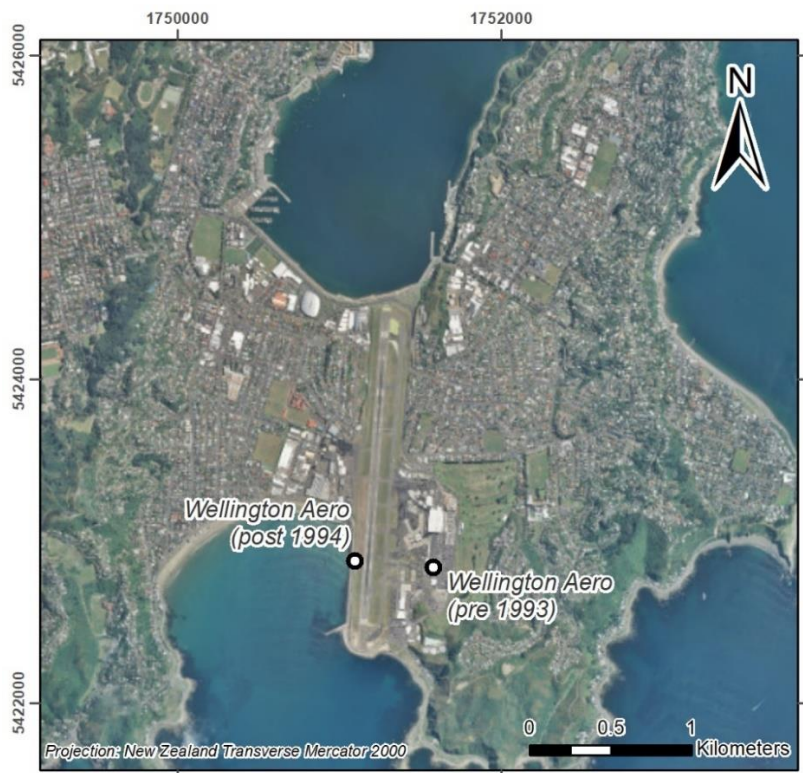


**Figure 2-1: Map showing location of wind gust observing sites at Wellington Airport.**

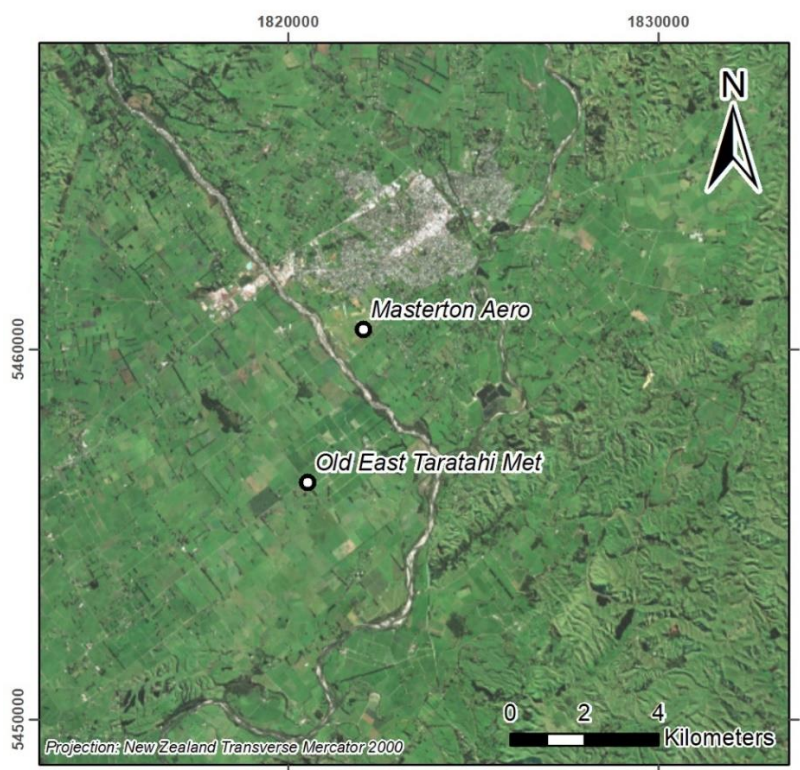


**Figure 2-2: Map showing location of wind gust observing sites at East Taratahi and Masterton Aero AWS .**

## 2.2 Wellington

The examination of homogenised gust records (Table 2-3 and Figure 2-3, bottom panel) shows that the annual maximum gusts are dominated by northerly (winds from NW through NE) events in the range of about 30-38 m/s (108-137 km/hr) with 58 of the peak annual maximum gusts over the last 60 years being northerlies. The other two events were southerly, and one of these, the *Wahine* Storm of 1968, was the most extreme event of the record. The peak homogenised gust of the *Wahine* Storm was 44 m/s (158 km/hr), which was 6 m/s (22 km/hr, or 16%) higher than the second most extreme event. The remaining annual maximum that was southerly occurred in 1974 and was the 15<sup>th</sup> highest annual maximum. It is also noted that in June 2013 a strong southerly occurred with a peak homogenised gust of 37.1 m/s (134 km/hr) (Figure 2-3). While this southerly did not rank as the annual maximum for 2013 in the homogenised gust record, it was stronger than 51 of the 60 annual maxima that occurred in other years in the homogenised record (Table 2-3; Figure 2-3). The 1974 and 2013 southerly maximum gusts had similar speeds (Figure 2-3) and Figure 2-4 and Figure 2-5 have therefore been presented to give a general impression/comparison of the effect of these southerly gusts on temperatures at the time.

A simple linear regression fitted to the annual corrected maximum shows a slight decrease of the annual maximum gust speed of around 1.5 m/s (5.4 km/hr) over the 60 years, but around 35% of this trend is due to the *Wahine* event occurring near the start of the record.

An examination of noon gust records (only possible since 1994 when hourly records became available) shows little change in the strength of noon gusts over the last 25 years (Figure 2-6). Additionally, there is little evidence of a trend in average wind speed in Wellington as can be seen by the time-series of daily wind run (Figure 2-7). Homogenised station records allow for more meaningful comparisons between wind records between storm events and at different stations across a region, and are important in design wind considerations, where they allow engineers to easily quantify exposures at different locations using well-established adjustments in wind-speeds due to hill-shape and terrain differences. For instance, structures on hill-tops and close to the sea have higher return period gust speeds. Further, for events such as the *Wahine* storm we can work backwards from the homogenised gust speed records to get better estimates of likely peak gusts experienced at different locations across the city from local (or site) estimates of surface roughness and topographic effects.

**Table 2-3: Table listing the annual maximum homogenised gust ( $\text{ms}^{-1}$ ) at Wellington Aero for the decades 1960's to 2010's.** Years with annual overall maximum being a southerly have bold red text, decadal maxima are yellow highlighted cells.

Year of decade	1960's	1970's	1980's	1990's	2000's	2010's
0	31.7	38.1	34.4	37.4	32.3	36.2
1	32.4	31.7	34.7	36.8	32.3	31.1
2	27.9	34.1	34.2	37.4	31.6	38.3
3	37.0	30.4	33.4	36.8	31.6	37.8
4	37.0	36.7	33.4	33.4	35.0	33.4
5	38.2	37.7	33.4	36.2	30.0	32.8
6	32.6	37.7	30.7	32.3	32.8	34.4
7	36.2	33.4	31.6	31.3	31.6	35.0
8	44.0	32.5	34.9	35.0	33.4	35.2
9	33.1	34.0	36.9	31.1	33.9	34.7



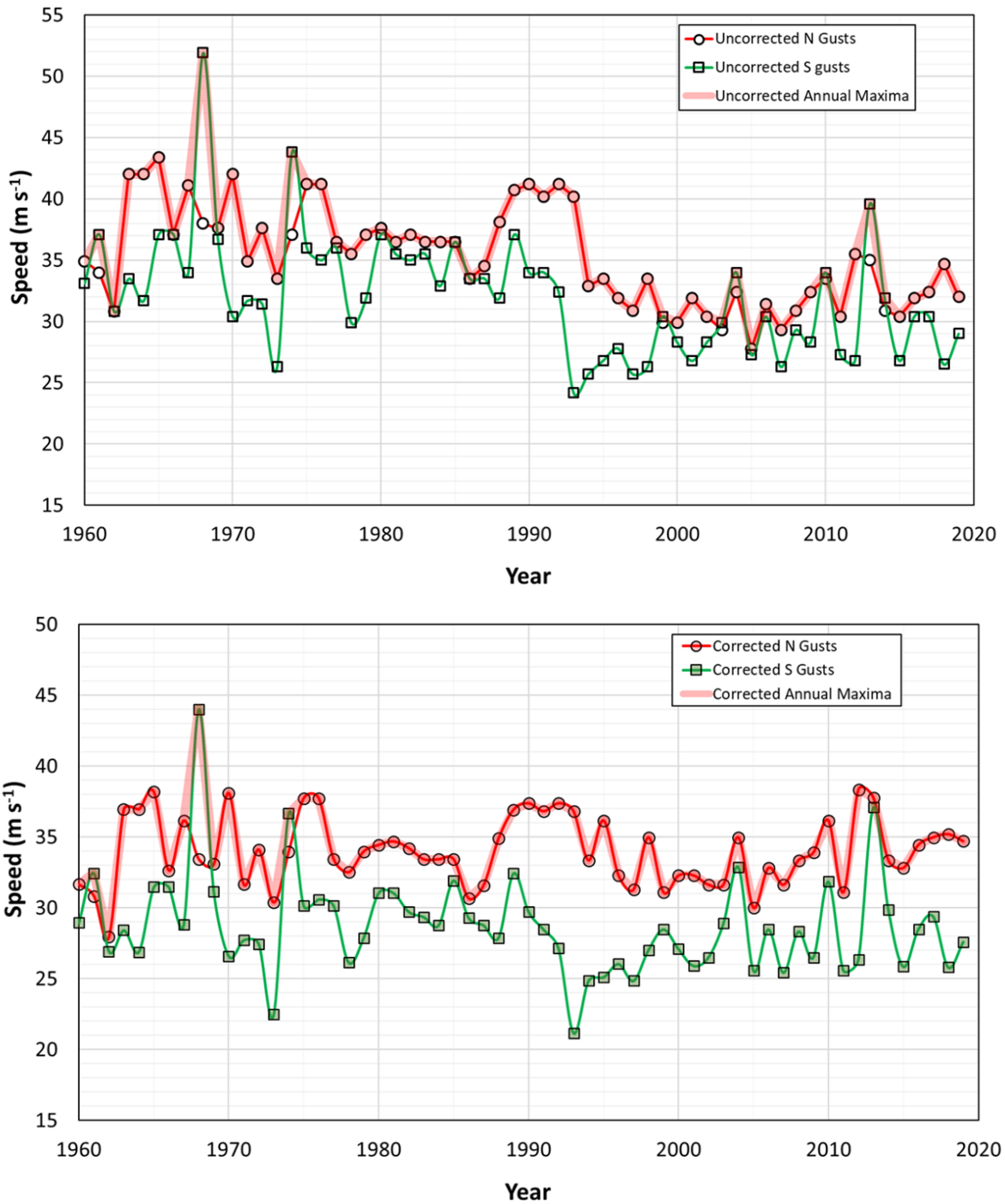


**Figure 2-3: Time-series plots showing annual maximum gusts ( $\text{ms}^{-1}$ ) (thick red lines) and annual maximum northerly (thin red line) and southerly (thin green line) sector gusts for Wellington Aero from 1960 to 2019. The upper panel shows the uncorrected (raw) time-series while the lower panel shows the corrected (homogenised) time-series.**

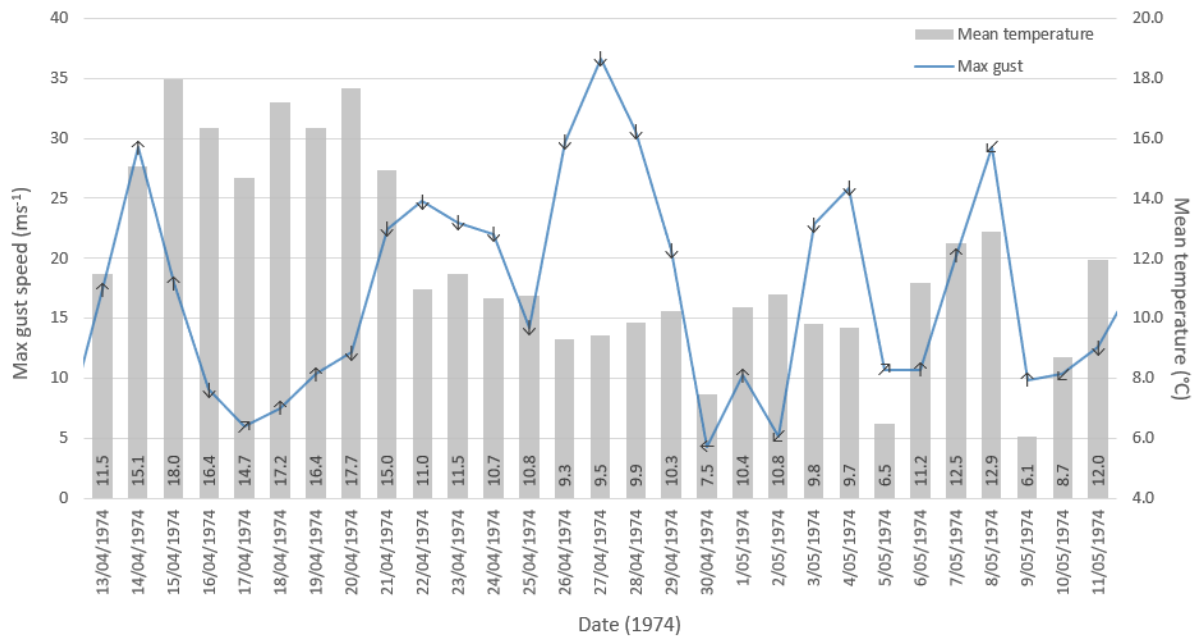


**Figure 2-4: Maximum daily wind gusts (ms<sup>-1</sup>) plotted against mean daily temperatures (°C) for Wellington Aero from 13-April to 11-May 1974.** Wind speeds are from the corrected (homogenised) gust time-series, with plotted arrows indicating the general direction from which the gust came. The southerly gust of 36.7 ms<sup>-1</sup> on 27-April 1974 was the highest wind gust for that year. The temperatures for each day are also listed at the base of each column.

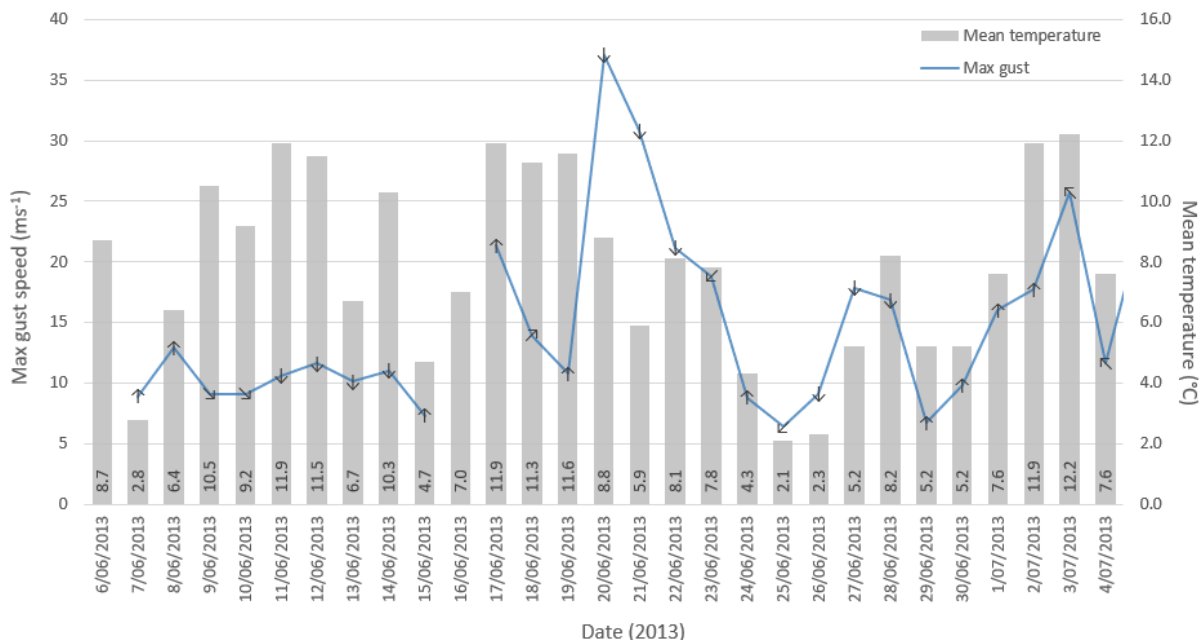


**Figure 2-5: Maximum daily wind gusts (ms<sup>-1</sup>) plotted against mean daily temperatures (°C) for Wellington Aero from 06-June to 04-July 2013.** Wind speeds are from the corrected (homogenised) gust time-series, with plotted arrows indicating the general direction from which the gust came. The southerly gust of 37.1 ms<sup>-1</sup> on 20-June 2013 was the strongest southerly gust for that year. The temperatures for each day are also listed at the base of each column. Where no directional arrow is shown for the gust record, no data exists.



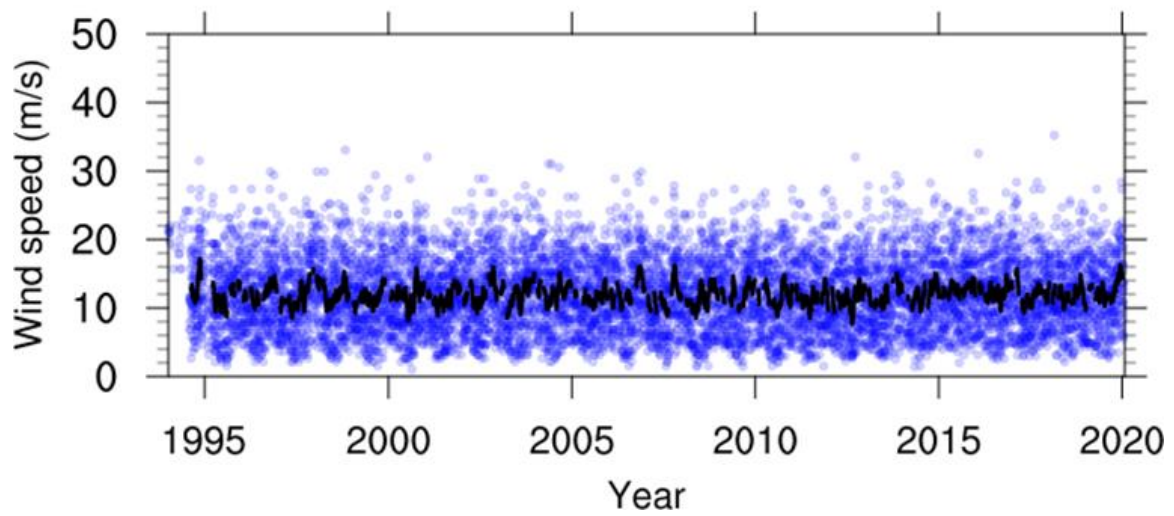


Figure 2-6: Time series of homogenised noon (12:00 pm NZST) gusts ( $\text{ms}^{-1}$ , blue dots) for Wellington Aero for the period 1994 through 2019. The thick black line is a 30-day moving average.

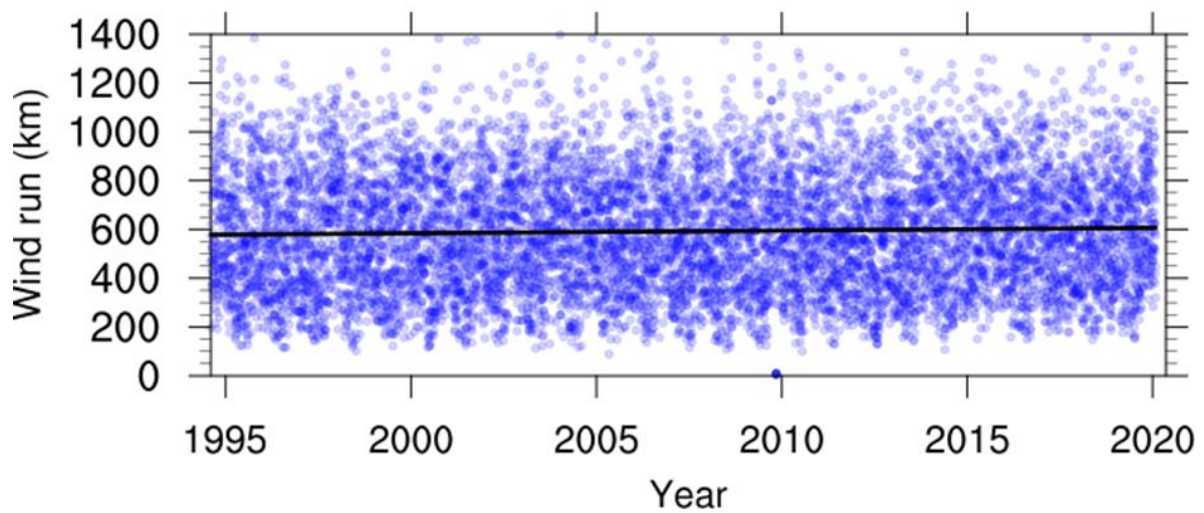
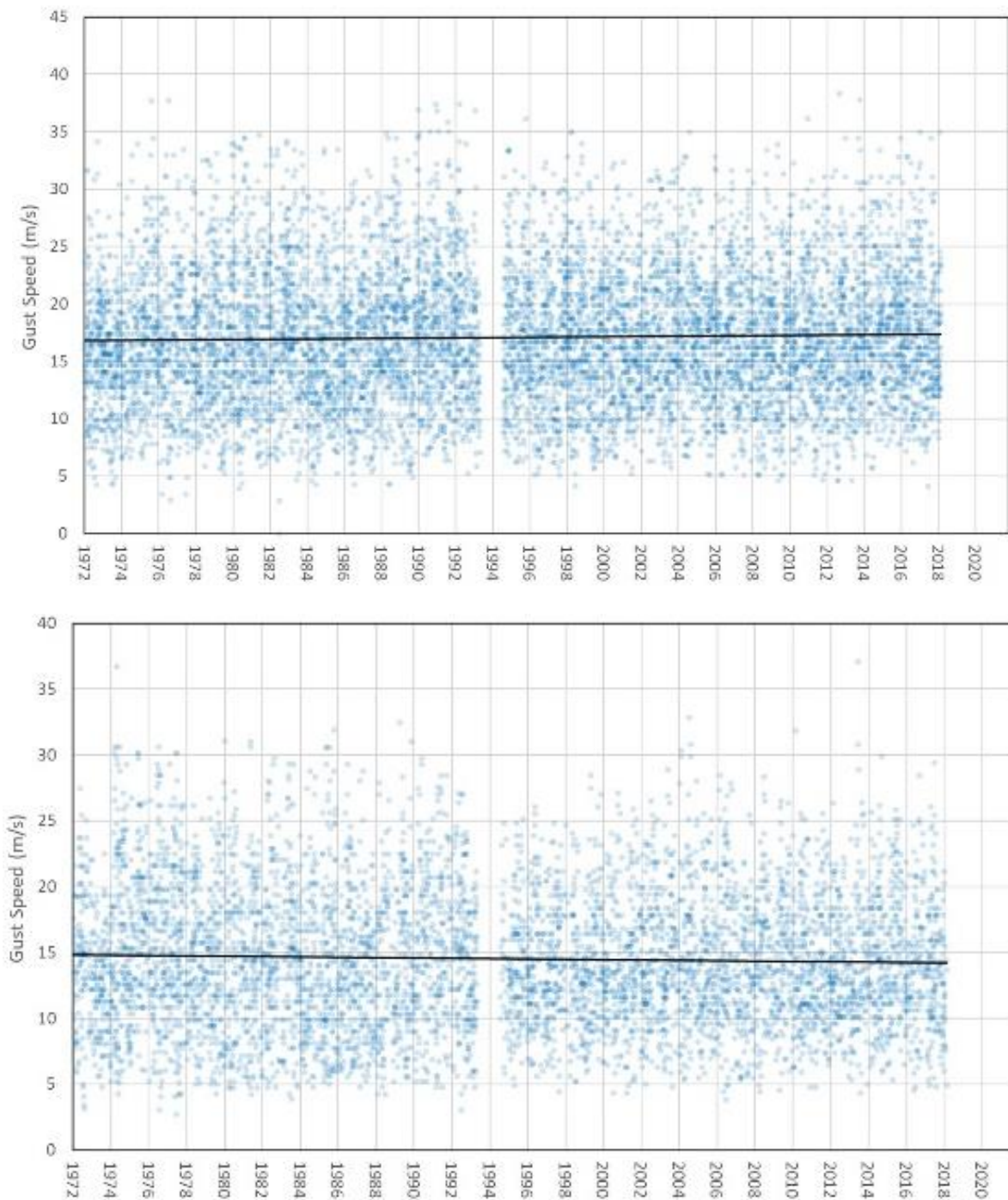


Figure 2-7: Time series of daily wind run (km) for Wellington Aero for the period 1994 through 2019. The black line is the regression line and shows no significant change in the mean wind.



**Figure 2-8: Time series of daily maximum wind gusts ( $\text{ms}^{-1}$ ) at Wellington Aero for the period 1972 through 2017 from N (top panel) and S (bottom panel).**

An examination of overall long-term trends for northerly and southerly gusts (Figure 2-8) shows only small and not significant trends. For seasonal trends however, Figure 2-9 and Figure 2-10 (taken from Figures 17 and 18 of Turner et al., 2019) show that average daily maximum gust speeds have increased in spring by around 0.5 m/s (1.8 km/hr) since 1972 at Wellington Aero. Spring was the only season with a marked trend and it also had an increase in days with max gusts exceeding the 90<sup>th</sup>, 95<sup>th</sup>, and 99<sup>th</sup> percentiles (noting that records indicate that average spring wind speeds have

decreased across this period). Interestingly, the other seasons all show a slight decrease in days of exceedance.

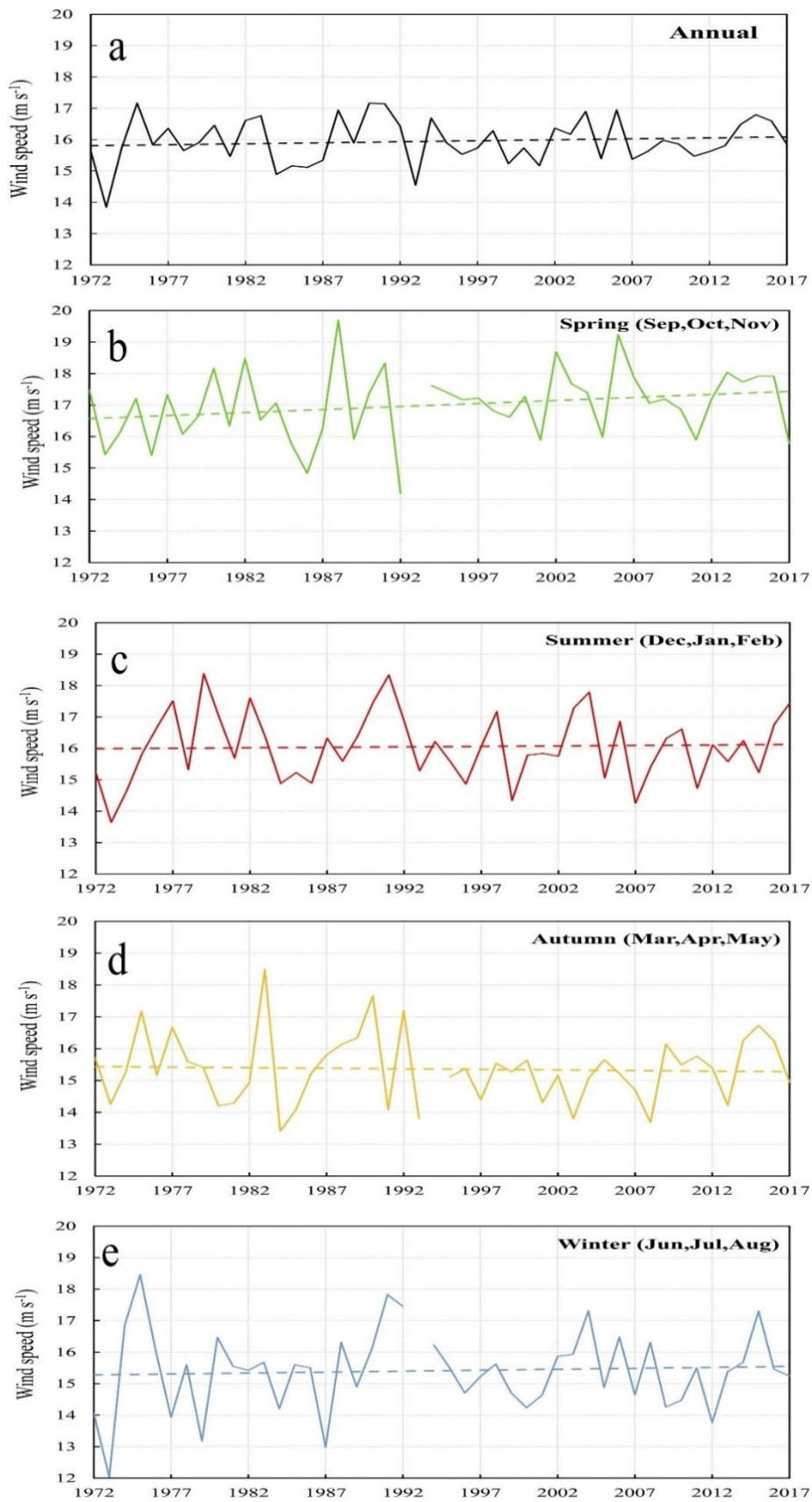


**Figure 2-9: Annual and seasonal time-series of average maximum daily gust speeds ( $\text{ms}^{-1}$ ) for Wellington Aero from 1972 to 2017. The dashed lines are trend lines obtained by linear regression. Figure from Turner et al. (2019)**



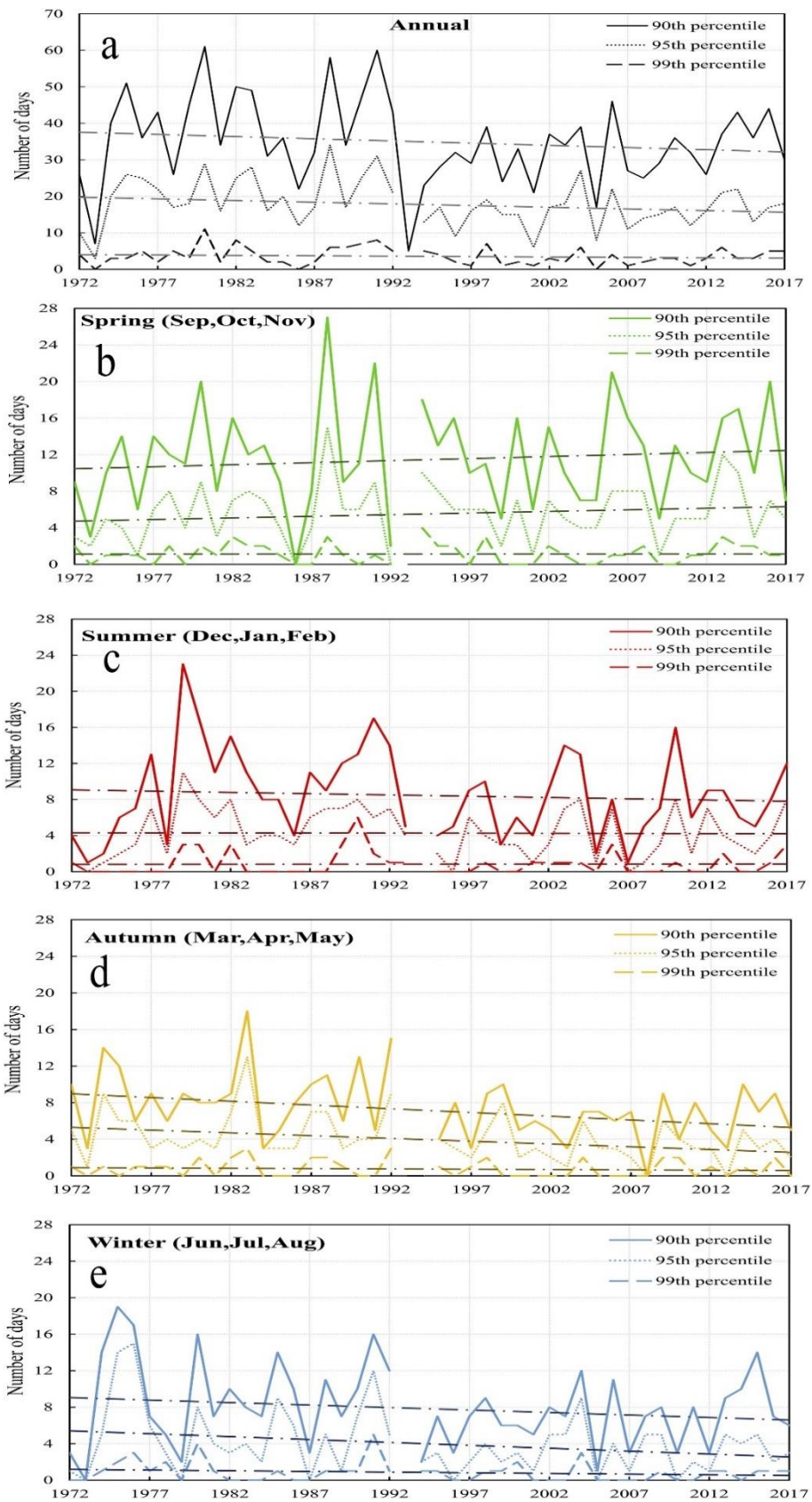


**Figure 2-10: Annual and seasonal time-series plotting the number of days exceeding the 90th, 95th, and 99th percentiles gust speeds ( $\text{ms}^{-1}$ ) for Wellington Aero from 1972 to 2017. The dashed lines are trend lines obtained by linear regression. Figure from Turner et al. (2019).**

## 2.3 Wairarapa

The record for daily maximum gusts at Masterton only extends back to 1991 (Figure 2-11 and Table 2-4). Similar to Wellington, there is little apparent trend with time and speeds varying in the range of 25 to 37 m/s (90-133 km/hr). For Masterton, the annual maximum gusts are dominated by Northerly sector winds which were primarily directed (> 90%) between WNW and NNW. The lack of a trend over the last 29 years is consistent with the time-series of noon gusts (Figure 2-12) and also consistent with the Wellington record over the same period. The time-series of noon gusts also clearly shows the seasonal cycle in gust speeds with a late autumn/early winter minima and late spring/early summer maxima. When considering more narrow directional sectors at Masterton from where the strongest daily max gusts frequently occur (NW: 292.5° to 337.5°, and S: 157.5° to 202.5°) (Figure 2-13), a similar picture is seen. However, it is interesting to note that the number of daily maximum S gusts per year show a decrease (linear regression) of around 10 days over the 1991-2019 period while the number of daily maximum NW gusts (292.5 to 337.5) per year shows an increase of around 10 days (Figure 2-14). There was little overall trend in the daily wind-run (Figure 2-15). Overall, it can therefore be inferred that any change in a site's exposure to wind in this period will be due to local in terrain surface roughness changes (e.g., housing developments or shelter belt removal) and differences in exposure in the NW or S directions.

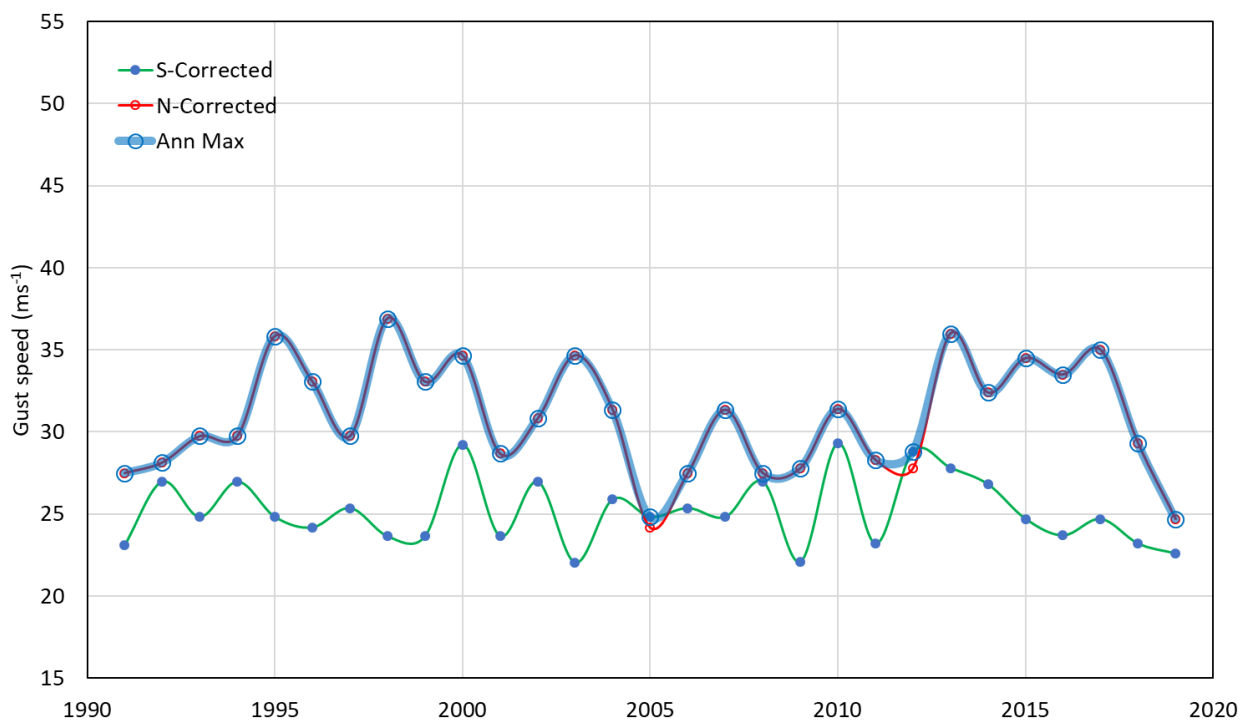


**Figure 2-11:** Time series of the homogenised annual maximum gust ( $\text{ms}^{-1}$ , thick blue line) at Masterton for the period 1991 to 2020. Also shown are the annual maximum southerly sector gust (SE through WSW - green line) and the maximum northerly (NW through NE - red line).

**Table 2-4: Table showing annual maximum gust speeds homogenised ( $\text{ms}^{-1}$ ) for Masterton in period 1991 to 2019. Years with annual overall maximum being a southerly have bold red text, decadal maxima are yellow highlighted cells.**

Year	Ann Max	Year	Ann Max	Year	Ann Max
		2000	34.7	2010	31.4
1991	<sup>1</sup> 27.5	2001	28.7	2011	28.3
1992	28.1	2002	30.8	2012	<b>28.8</b>
1993	29.7	2003	34.7	2013	36.0
1994	29.7	2004	31.4	2014	32.4
1995	35.8	2005	<b>24.8</b>	2015	34.5
1996	33.1	2006	27.5	2016	33.5
1997	29.7	2007	31.4	2017	35.0
1998	36.9	2008	27.5	2018	29.3
1999	33.1	2009	27.8	2019	24.7

<sup>1</sup> – from April 1991

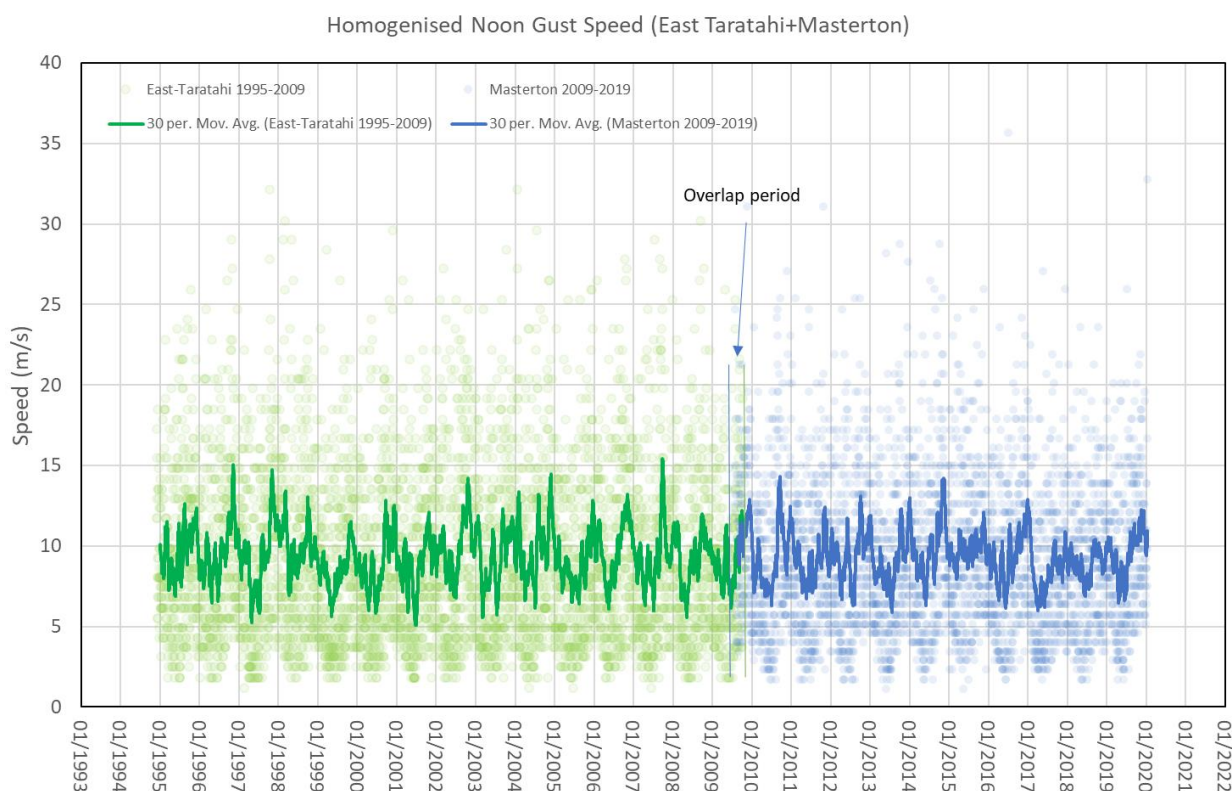


**Figure 2-12: Homogenised noon (12:00 pm NZST) gust record ( $\text{ms}^{-1}$ ) for Masterton, based on East Taratahi (green) and Masterton AWS (blue) gust records for the period 1995 to 2020. The thin blue vertical lines mark the period of overlap of records (26 Feb to 4 Nov 2009). The thick green and blue lines are the 30-day moving averages for the East Taratahi and Masterton sites respectively.**

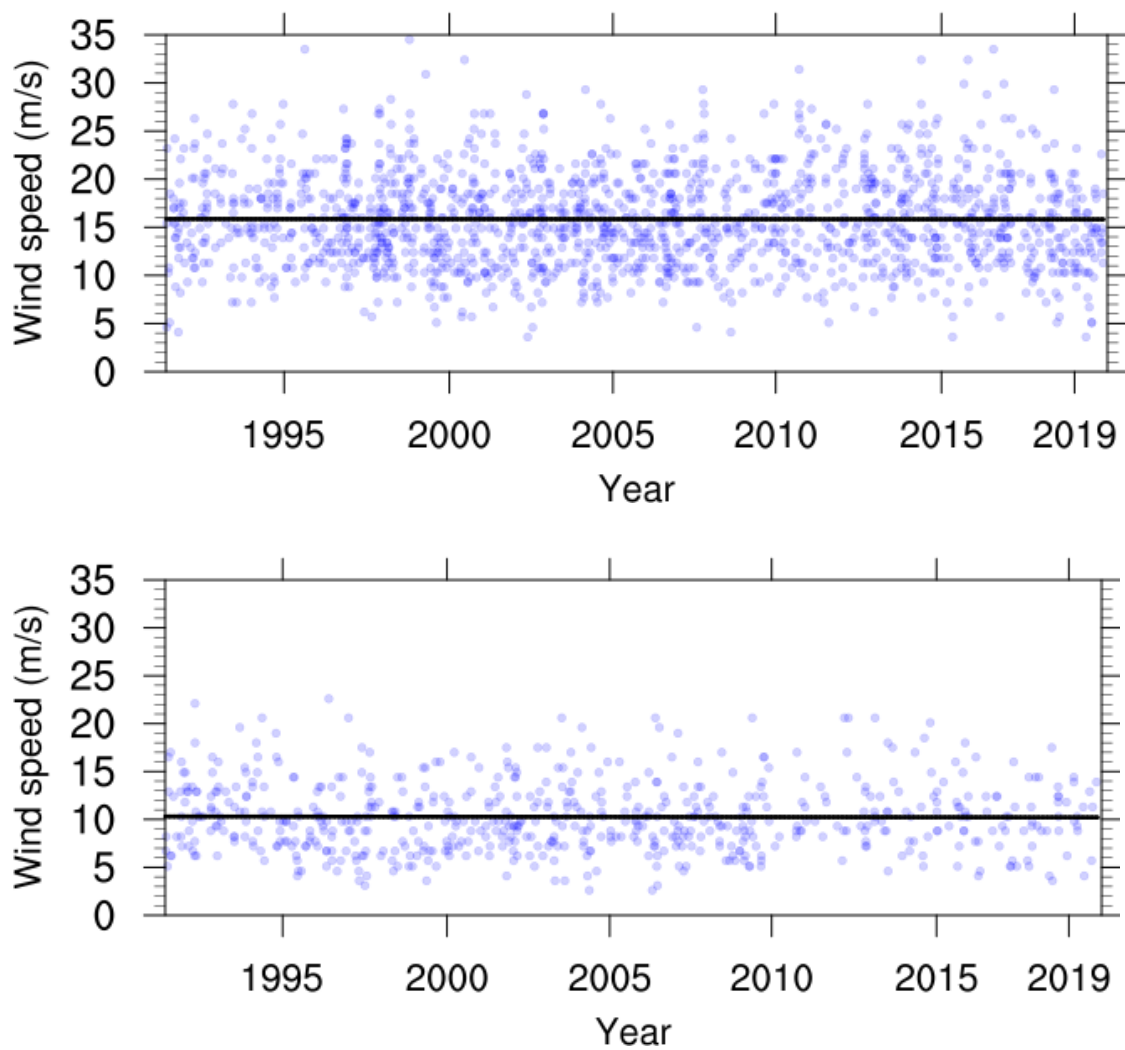


**Figure 2-13: Time series of daily maximum wind gusts ( $\text{ms}^{-1}$ ) at Masterton (East Taratahi plus Masterton – Homogenised) for the period 1991 through 2019 from NW (top panel) and S (bottom panel).**



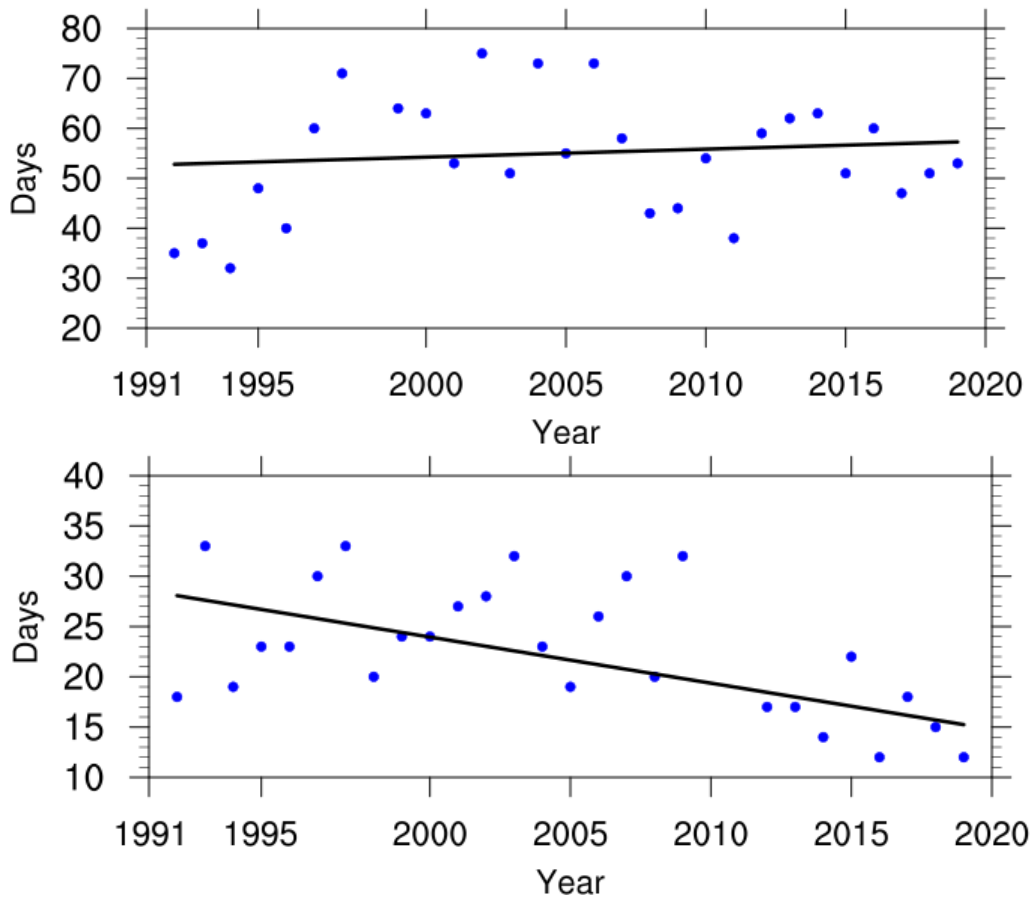


Figure 2-14: Count of days per year in which daily max gusts from the NW (top panel) and S (bottom panel) directions have occurred at Masterton in the period 1991 to 2019.

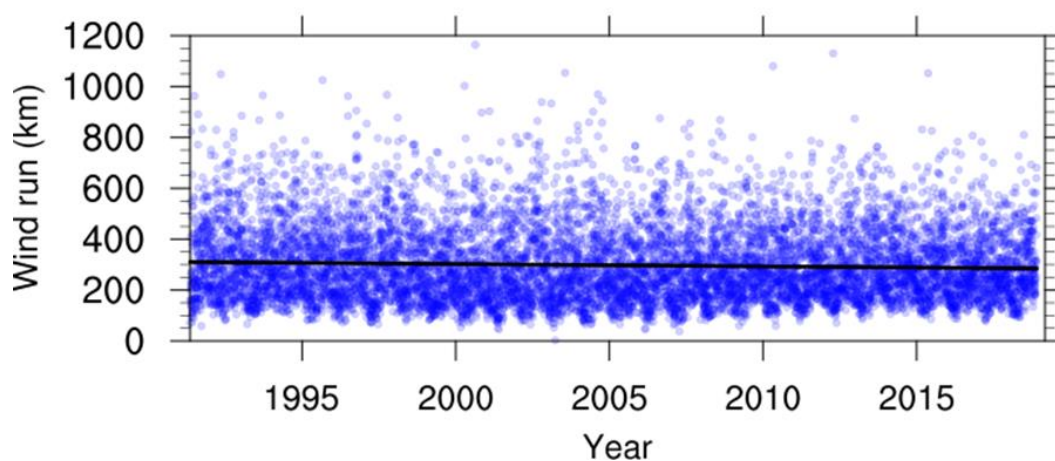


Figure 2-15: Time series of daily wind run (km) for Masterton (East Taratahi plus Masterton AWS) for the period 1991 to 2019. The black trend line was obtained by linear regression and indicates no significant change in the mean wind speed.

### 3 Rainfall intensity

This section considers the changes in the frequency of extreme precipitation events for four locations in the Wellington Region (Kelburn, Wellington Aero, Paraparaumu, and Masterton), based on digitised historic data held in NIWA’s National Climate Database (CliDB<sup>2</sup>) and records collated for the High Intensity Rainfall Design System (HIRDS<sup>3</sup>; Carey-Smith et al., 2018). To create long time-series at each of these locations, different gauge records have been combined as described in Table 3-1. Annual rainfall thresholds for analysis were chosen by GWRC and are listed in Table 3-2.

**Table 3-1: Details of rainfall gauges used in this section. Gauges labelled with ‘infill’ were used for filling gaps in the main records for that location.**

Location	Gauge	ID	Latitude	Longitude	Elevation	Details
Kelburn	WELLINGTON KELBURN	E14272	-41.286	174.767	125	1869-1906, 1927-2019 (sub-daily since 1940)
	WELLINGTON BUCKLE ST	E14370	-41.3	174.783	34	1906-1912 (daily)
	WELLINGTON THORNDON	E14278	-41.283	174.783	3	1912-1927 (daily)
Wellington Aero	WELLINGTON AERO	E14387	-41.322	174.804	4	1960-2019 (sub-hourly since 1967)
	WELLINGTON RONGOTAI (infill)	E14386	-41.321	174.801	5	1958-2010 (daily)
Paraparaumu	PARAPARAUMU AERO	E04991	-40.907	174.984	5	1951-2019 (sub-hourly since 1955)
	PARAPARAUMU EWS (infill)	E04995	-40.904	174.984	5	1996-2019 (sub-hourly)
Masterton	MASTERTON ESSEX ST	D05960	-40.967	175.65	118	1884-1942 (daily)
	WAINGAWA	D05964	-40.98	175.611	114	1926-1990 (sub-hourly since 1967)
	MASTERTON TE ORE ORE	D05973	-40.957	175.707	110	1992-2019 (sub-hourly)
	MASTERTON (infill)	D05962	-40.95	175.667	102	1946-1956 (daily)
	WAIRARAPA CADET FARM (infill)	D15061	-41.006	175.641	106	1951-2018 (daily)
	WRC Masterton Office (infill)	59646	-40.948	175.662	120	2000-2007 (sub-hourly)
	Ruamahanga at Wairarapa College (infill)	59616	-40.952	175.647	100	2003-2016 (sub-hourly)

<sup>2</sup> The National Climate Database (CliDB) can be accessed publicly through [www.cliflo.niwa.co.nz](http://www.cliflo.niwa.co.nz)

<sup>3</sup> The High Intensity Rainfall Design System (HIRDS) can be accessed as an online tool from <https://hirds.niwa.co.nz/>

**Table 3-2: Annual rainfall thresholds analysed for Wellington Region sites from HIRDS.**

---

<b>Annual rainfall thresholds</b>
Number of events >5mm in 10 min
Number of events >10 mm in 30 min
Number of events >15mm in 1 hour
Number of events >40mm in 6 hours
Number of events >50mm in 12 hours
Number of events >60mm in 24 hours
Number of events >100mm in 48, 72, and 120 hours

---

### 3.1 Historic rainfall threshold exceedances

The rainfall threshold exceedances for each of the four Wellington locations are displayed in Figure 3-1 to Figure 3-4. The plots show the average annual rainfall threshold exceedances by decade. Essentially, the plots indicate that there are no obvious consistent temporal trends within or between the sites. When examining extreme events at this scale, the inter-decadal variability is very large so any trend that may exist in these data is difficult to detect. The only statistically significant trends in these observed threshold exceedances are for the sub-hourly Kelburn time series.

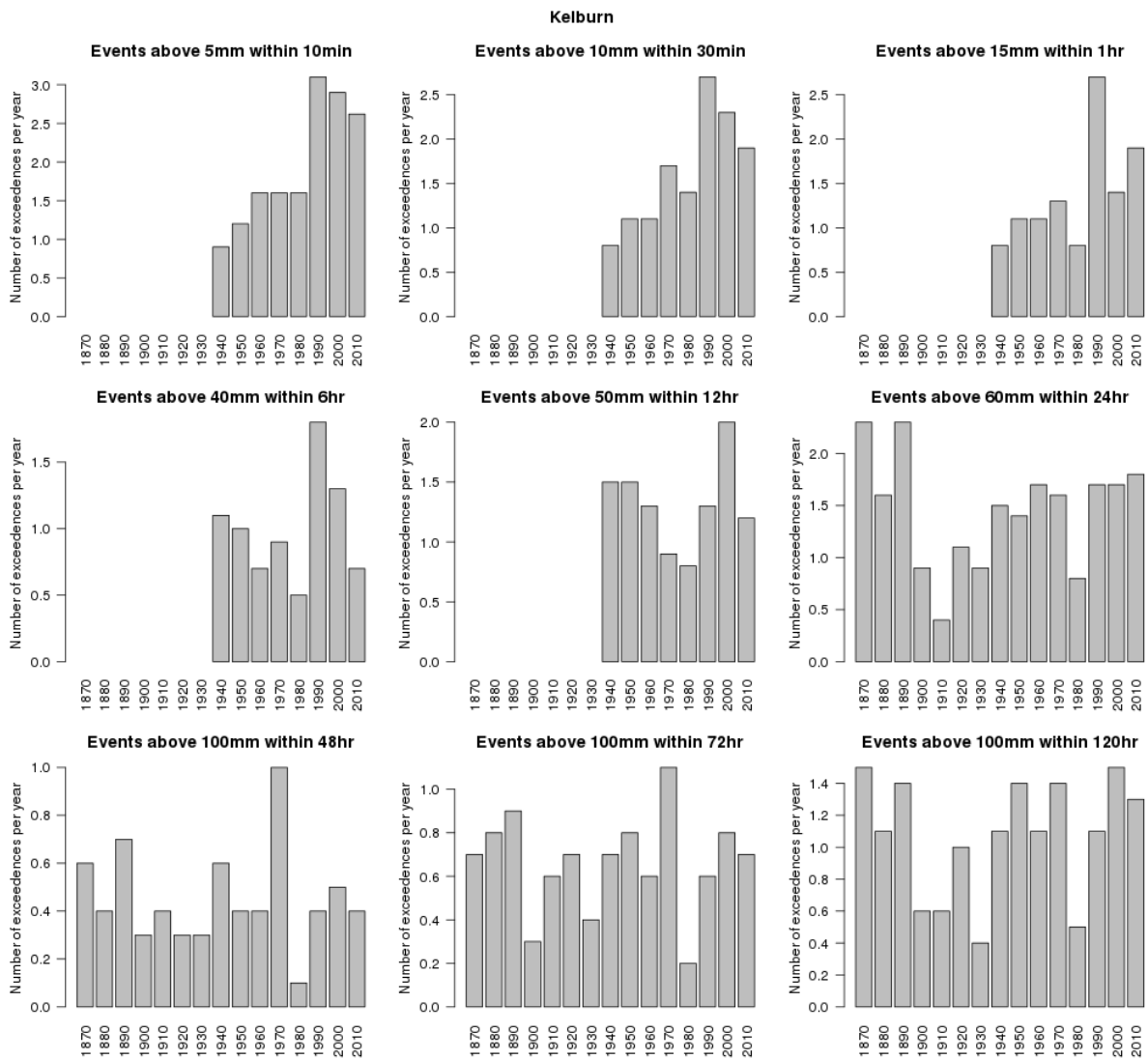


**Figure 3-1: Average annual rainfall threshold exceedances per decade for Kelburn. Where no bar is shown, data is not available for this decade.**

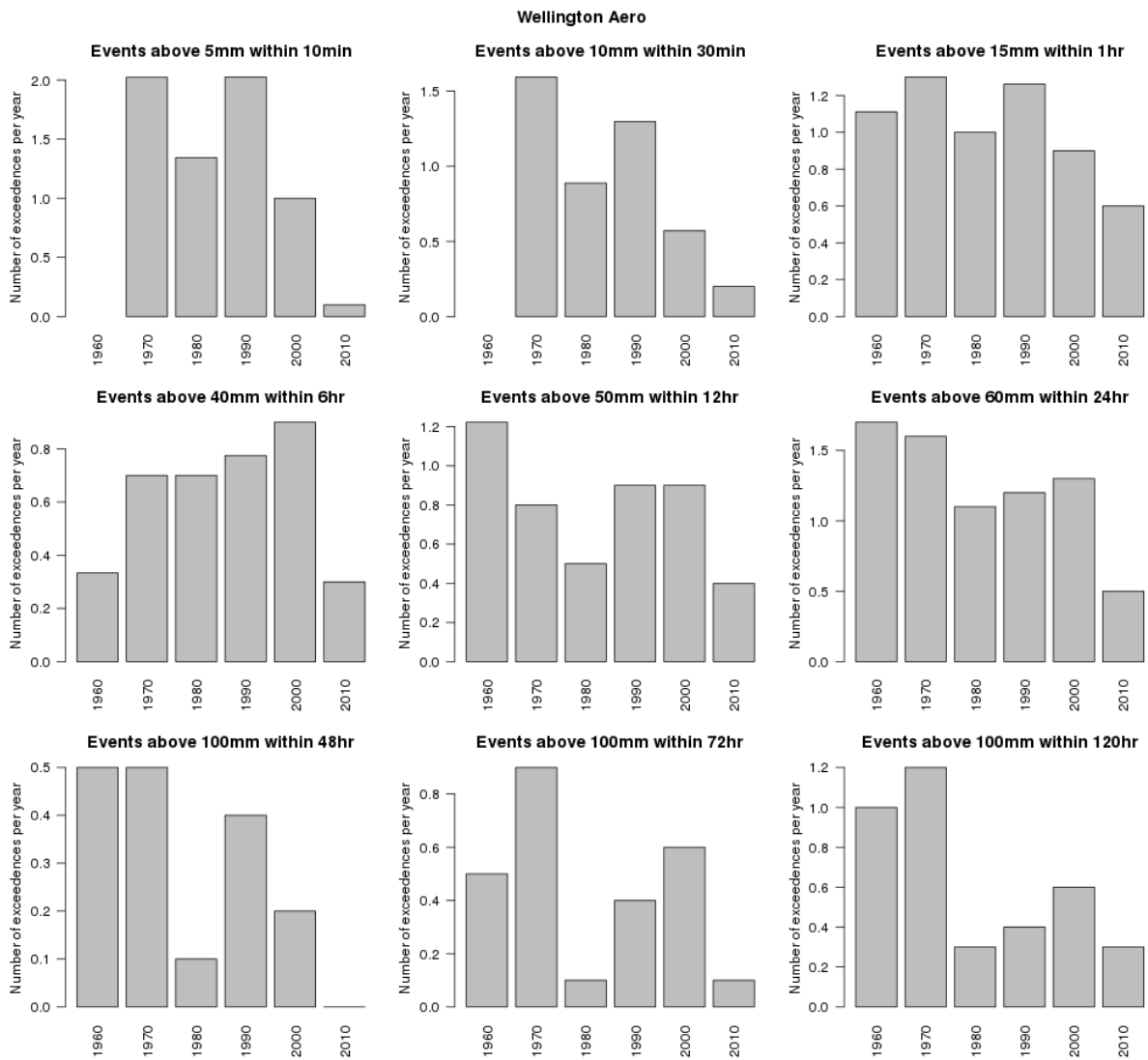


**Figure 3-2: Average annual rainfall threshold exceedances per decade for Wellington Aero .** Where no bar is shown, data is not available for this decade. Where there is a thin horizontal line (e.g. the decade starting in 2010 for the 48-hour duration) data is available, but the threshold was not reached.

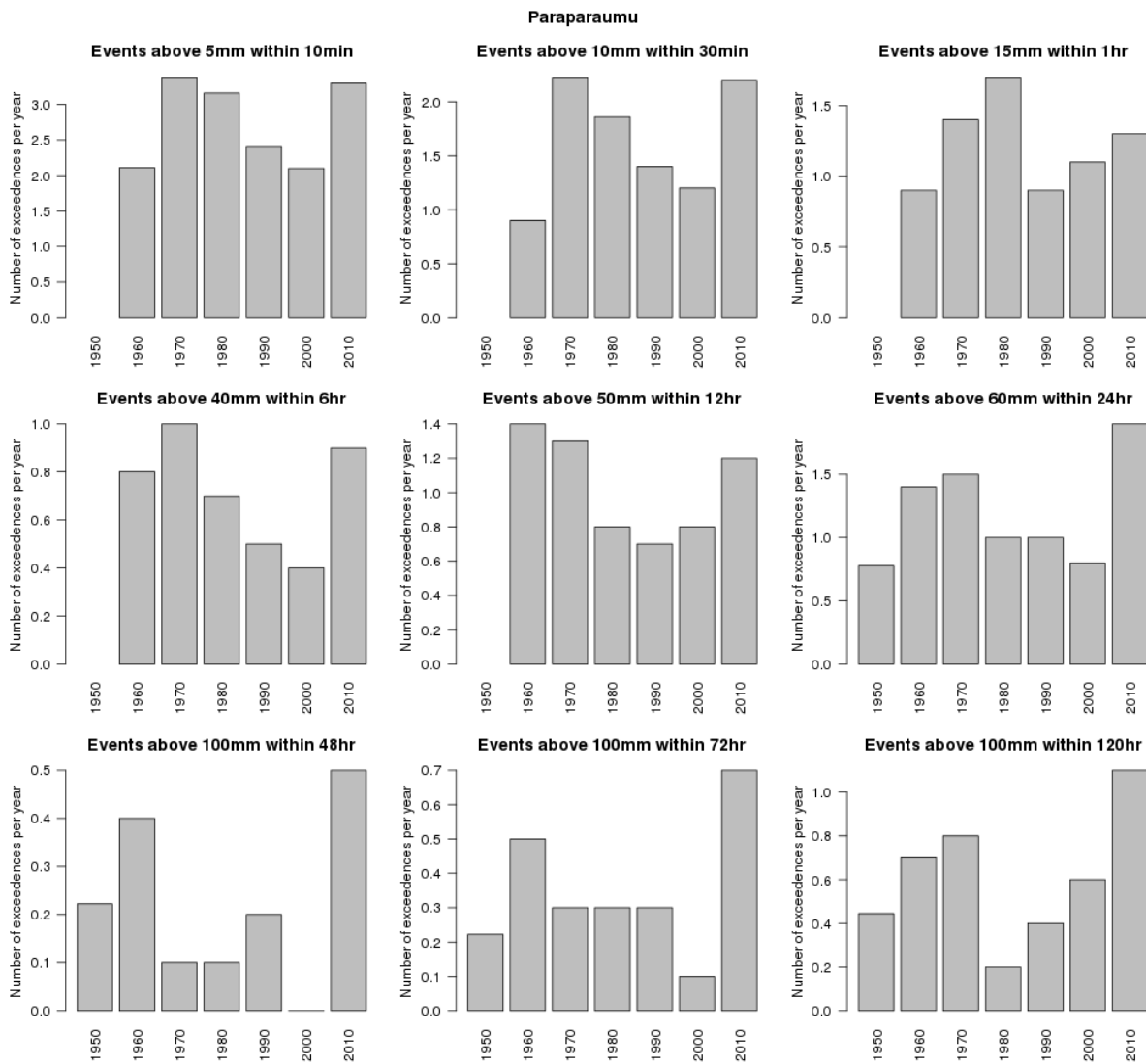


**Figure 3-3: Average annual rainfall threshold exceedances per decade for Paraparaumu.** Where no bar is shown, data is not available for this decade. Where there is a thin horizontal line (e.g. the decade starting in 2000 for the 48-hour duration) data is available, but the threshold was not reached.

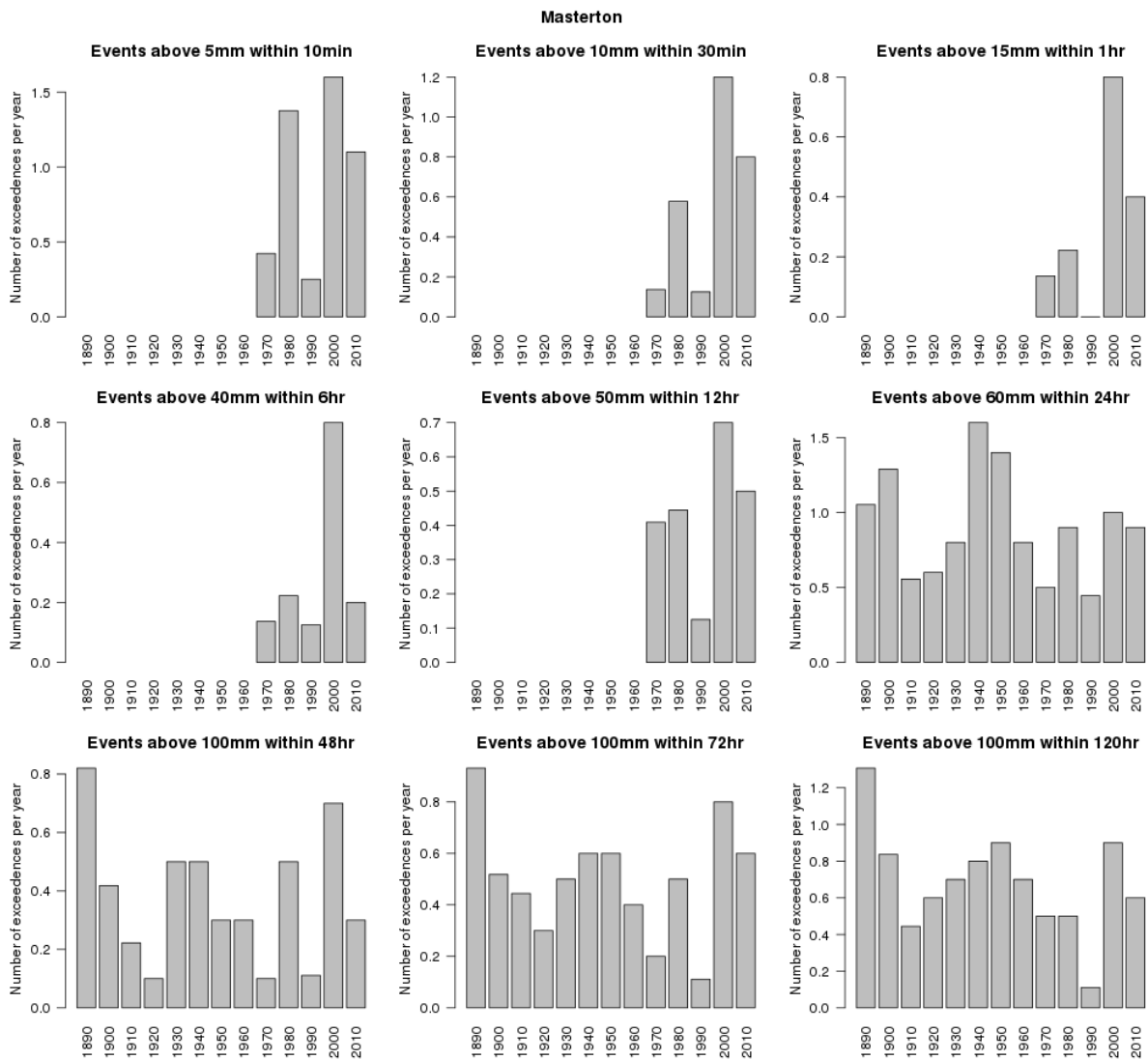


**Figure 3-4: Average annual rainfall threshold exceedances per decade for Masterton.** Where no bar is shown, data is not available for this decade. Where there is a thin horizontal line (e.g. the decade starting in 1990 for the 1-hour duration) data is available, but the threshold was not reached.

The large inter-decadal variability means that the number of exceedances per decade can be very different at different locations, so in order to compare the frequency of these events between locations it is necessary to average over a longer period. Figure 3-5 shows the average rainfall threshold exceedances per year over the entire period of record for each of the four sites. This shows that Kelburn generally has the largest number of exceedances of the extreme rainfall thresholds per year (i.e. this site experiences the most extreme rainfall events under the definitions used here), and Masterton generally has the least (i.e. this site experiences the fewest extreme rainfall events). Table 3-3 shows the same data as Figure 3-5.

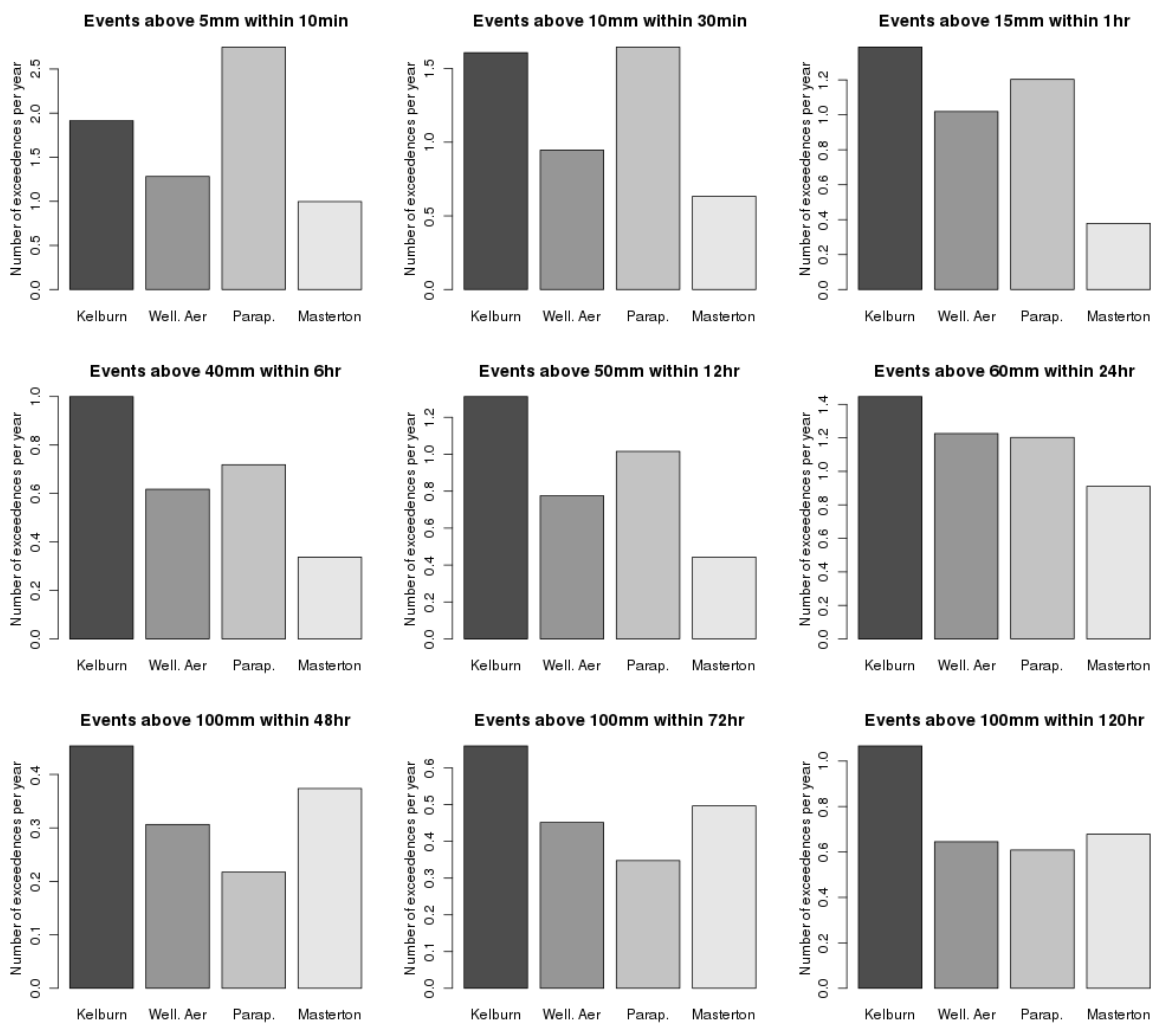


**Figure 3-5: Average annual rainfall threshold exceedances for all four Wellington Region locations, for the entire period of record.**

**Table 3-3: Average annual rainfall threshold exceedances for all four Wellington Region sites, for the entire period of record.**

	Average exceedances per year			
	Kelburn	Wellington Aero	Paraparaumu	Masterton
5mm/10 min	1.92	1.28	2.75	1.00
10mm/30 min	1.61	0.95	1.65	0.63
15mm/1 hour	1.39	1.02	1.20	0.38
40mm/6 hour	1.00	0.62	0.72	0.34
50mm/12 hour	1.31	0.78	1.02	0.44
60mm/24 hour	1.45	1.23	1.20	0.91
100mm/48 hour	0.45	0.31	0.22	0.37
100mm/72 hour	0.66	0.45	0.35	0.50
100mm/120 hour	1.07	0.65	0.61	0.68



## 3.2 Future changes in rainfall threshold exceedances

Intense rainfall events are expected to increase in magnitude in a warmer climate. When expressed as the number of events exceeding a (fixed) high threshold, this would equate to a larger number of these events in the warmer climate. To assess how the observed rainfall threshold exceedances given in Table 3-3 will change in the future, two different methodologies have been implemented, one applying rainfall augmentation factors to the historical record and the second estimating changes based on regional climate model projections.

The first method relies on the climate change analysis done as part of the 2019 update to the High Intensity Rainfall Design System (HIRDS<sup>4</sup>; Carey-Smith et al., 2018). This study provided augmentation factors that can be applied to extreme rainfall depths (or intensities) to estimate the increase in rainfall due to given increases in temperature. However, these factors were only estimated for events with return periods of two years or greater which corresponds to a 50% annual exceedance probability (or 0.5 exceedances per year). As can be seen from Table 3-3, the majority of the thresholds of interest occur more often than this, and in a warming climate are likely to become more frequent, meaning that the augmentation factors from HIRDS may no longer be directly applicable.

Despite this caveat, for the first method we have re-estimated the observed frequency of threshold exceedances after increasing the historical observations by factors appropriate for different representative concentration pathways (RCPs) and future time slices. All rainfall values in the gauge records were increased by the same factor for this analysis, but only the rainfall events just below the relevant threshold will have been affected as only these will have been pushed over the threshold.

The factors used (percentage increase in rainfall depth per degree of warming) were those estimated for the 2-year return period and vary for the different event durations as shown in Table 3-4. The temperature deltas used for the different scenarios and future periods were also taken from the HIRDS analysis and are reproduced in Table 3-5. The results from this (first) analysis are shown by the dashed lines in Figure 3-6 to Figure 3-9.

**Table 3-4: Percentage change factors for a 2-year return period event to project rainfall depths derived from the current climate to a future climate that is 1 degree warmer. The values in brackets show the expected variability across New Zealand based on Regional Climate Modelling results (from Table 6 and Table 7 in Carey-Smith et al., 2018).**

10 min	30 min	1 hour	6 hours	12 hours	24 hours	2 day	3 day	5 day
12.2% (9.8-17.5%)	12.2% (9.8-17.5%)	12.2% (9.8-17.5%)	9.8% (7.5-14.9%)	8.5% (5.7-13.5%)	7.2% (4-11.9%)	6.1% (2.6-11%)	5.5% (2.1-10.5%)	4.8% (1.3-9.6%)

**Table 3-5: New Zealand land-average temperature increase (°C) relative to 1986—2005 for four future greenhouse gas concentration scenarios. Each projection is an average of six regional climate model simulations (from Table 8 in Carey-Smith et al., 2018).**

Period	RCP 2.6	RCP 4.5	RCP 6.0	RCP 8.5
2031—2050	0.59	0.74	0.68	0.85
2081—2100	0.59	1.21	1.63	2.58

<sup>4</sup> The High Intensity Rainfall Design System (HIRDS) can be accessed as an online tool from <https://hirds.niwa.co.nz/>

To assess the impact of using 2-year return period augmentation factors for events more common than this, we have also estimated the change in threshold exceedance from direct rainfall projections from NIWA's regional climate modelling (RCM) programme. This programme provided 6 different RCM 130-year projections for each representative concentration pathway (RCP), providing rainfall output down to hourly temporal resolution. Changes in the number of rainfall threshold exceedances were estimated by counting the number of exceedances in each of three different 30-year periods; 1976—2005 (historical), 2031—2060 (mid-century) and 2071—2100 (end-century) and averaging across all six different projections for each RCP.

Due to biases in model precipitation amounts, the threshold used for the different events at each site was adjusted so that the frequency of exceedances in the RCM historical period closely matched the observed event frequencies (Table 3-3). As can be seen in Table 3-6, in most cases this adjustment was not large, however for the 1-hour duration event, the threshold is reduced by nearly one half suggesting that the RCM is not able to capture the rainfall intensity for very short duration events.

Results from this second method are shown by the solid lines in Figure 3-6 to Figure 3-9. No information from this method is shown for sub-hourly durations as this data is not available from the RCM output. In general, the two methods show similar results, however for the thresholds leading to less common events (i.e. less than 1 event per year), there is more variability between methods and the trends are less clear. This variability is mainly a result of the low sampling rate and can be seen most clearly for Masterton where the chosen thresholds correspond to relatively rare events (and also, in the HIRDS-based method, because the sub-daily observation record is relatively short).

Note that for the mid-century period, the relative difference between the current number of exceedances (red) and the future (green) is not very large, especially for longer duration events. It is not until end-century under the higher greenhouse gas concentration pathways that the differences become large (e.g. more than double the current rate). This slow emergence aligns with the observed records where significant trends in threshold exceedances are rarely found. For the Wellington region, the only location that shows a significant trend is Kelburn, for its short duration events. This is also the longest of the Wellington region sub-daily records lending some credence to the result. However, while this is consistent with the model results (short duration events increasing quicker than others), given its isolated nature, it is also possible this observed trend is not due to climate change, but simply a result of climate and weather variability.

**Table 3-6: Adjusted thresholds (in mm) used to account for model biases when estimating changes in event frequency from RCM rainfall.**

Duration	Observed Threshold (mm)	Adjusted RCM threshold (mm) to match observed frequency			
		Kelburn	Wellington Air	Paraparaumu	Masterton
1 hour	15	8.2	9	8.7	8.6
6 hours	40	37	41	41	39
12 hours	50	48	54	55	57
24 hours	60	56	58	69	64
48 hours	100	99	108	132	101
72 hours	100	92	101	130	100
120 hours	100	86	97	130	103

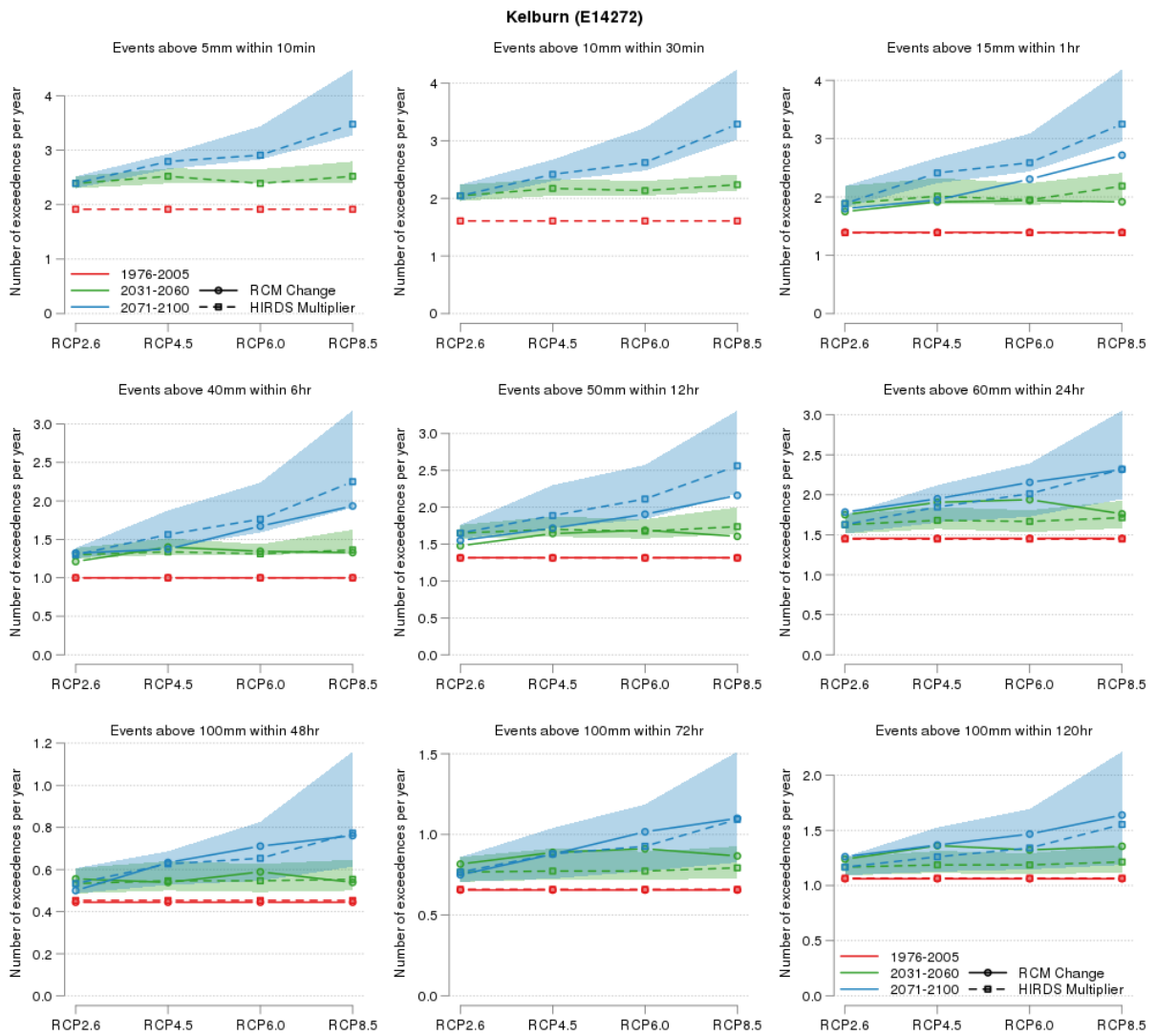


**Figure 3-6: The change in rainfall exceedances with climate change for Kelburn. The results from the first (HIRDS-based) analysis are shown by the dashed lines where the red lines are for the current climate and reproduce the numbers in Table 3-3. The shading shows the range produced when using the climate change factors in brackets in Table 3-4. The solid lines show results from the direct RCM analysis, where the red line is number of exceedances above a threshold adjusted to closely match the observed number of exceedances. For both methods, the green line is the mid-century time slice and the blue line is for the end of century period.**

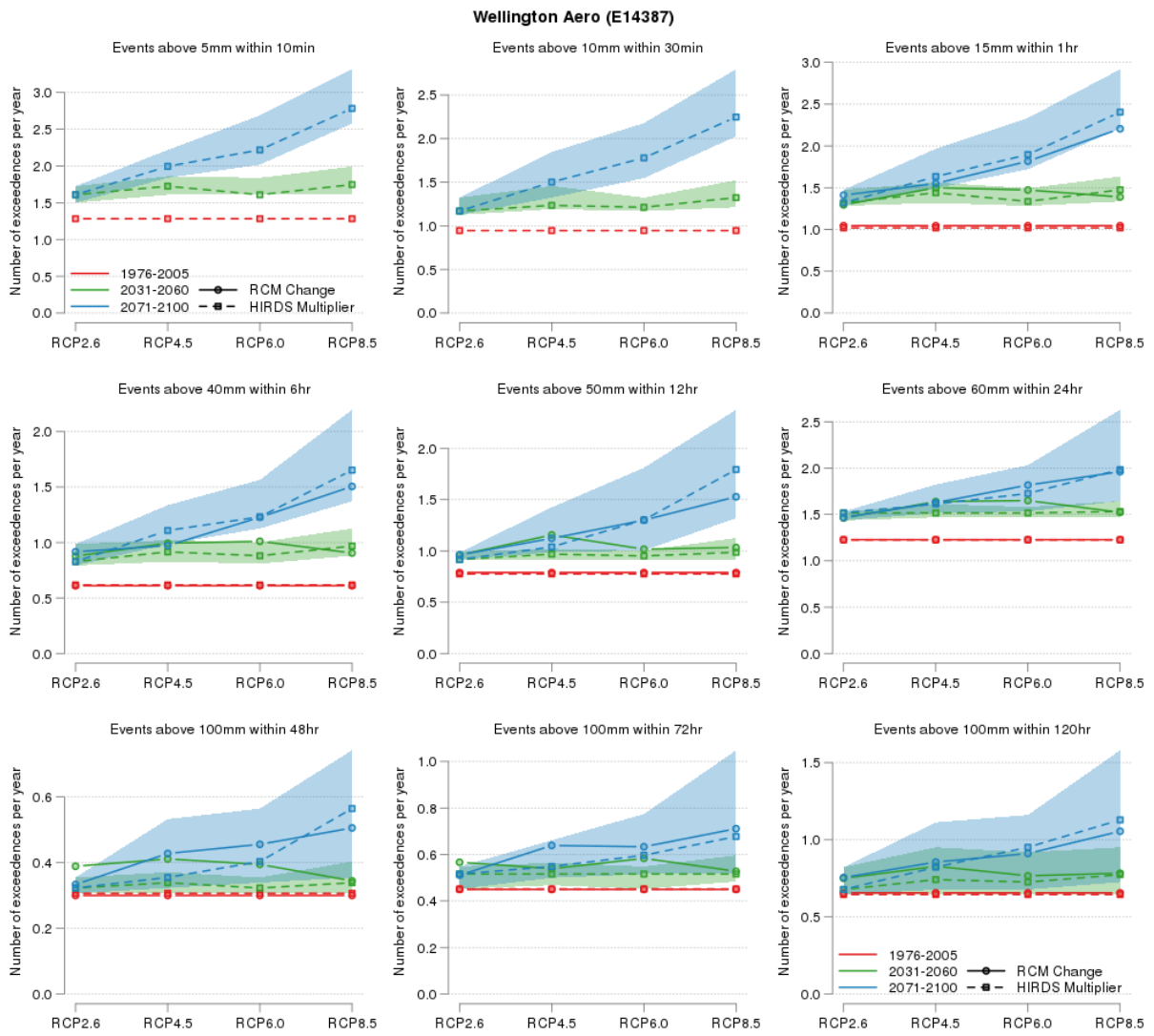


**Figure 3-7:** As Figure 3-6 but for Wellington Aero.

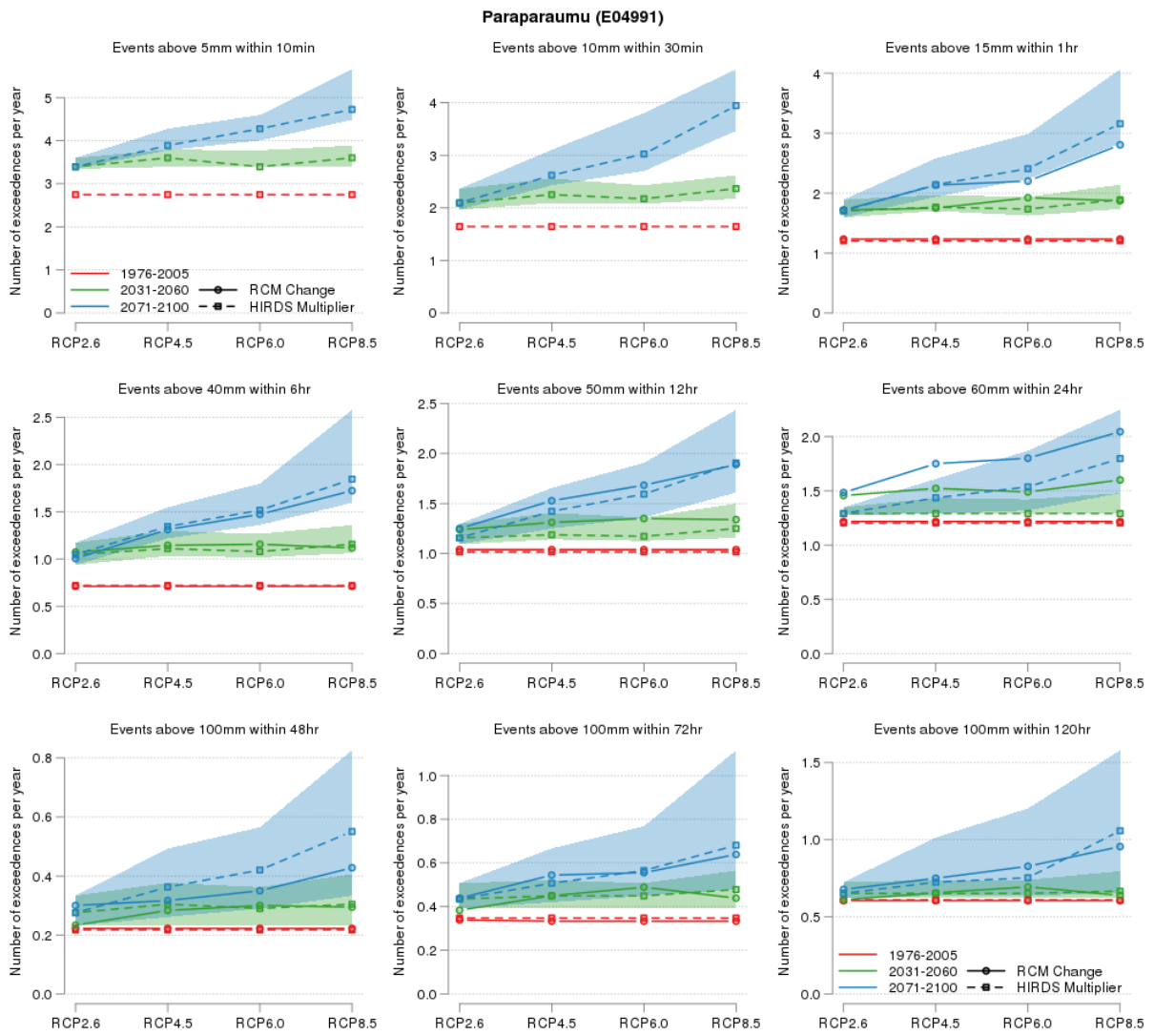


**Figure 3-8: As Figure 3-6 but for Paraparaumu.**

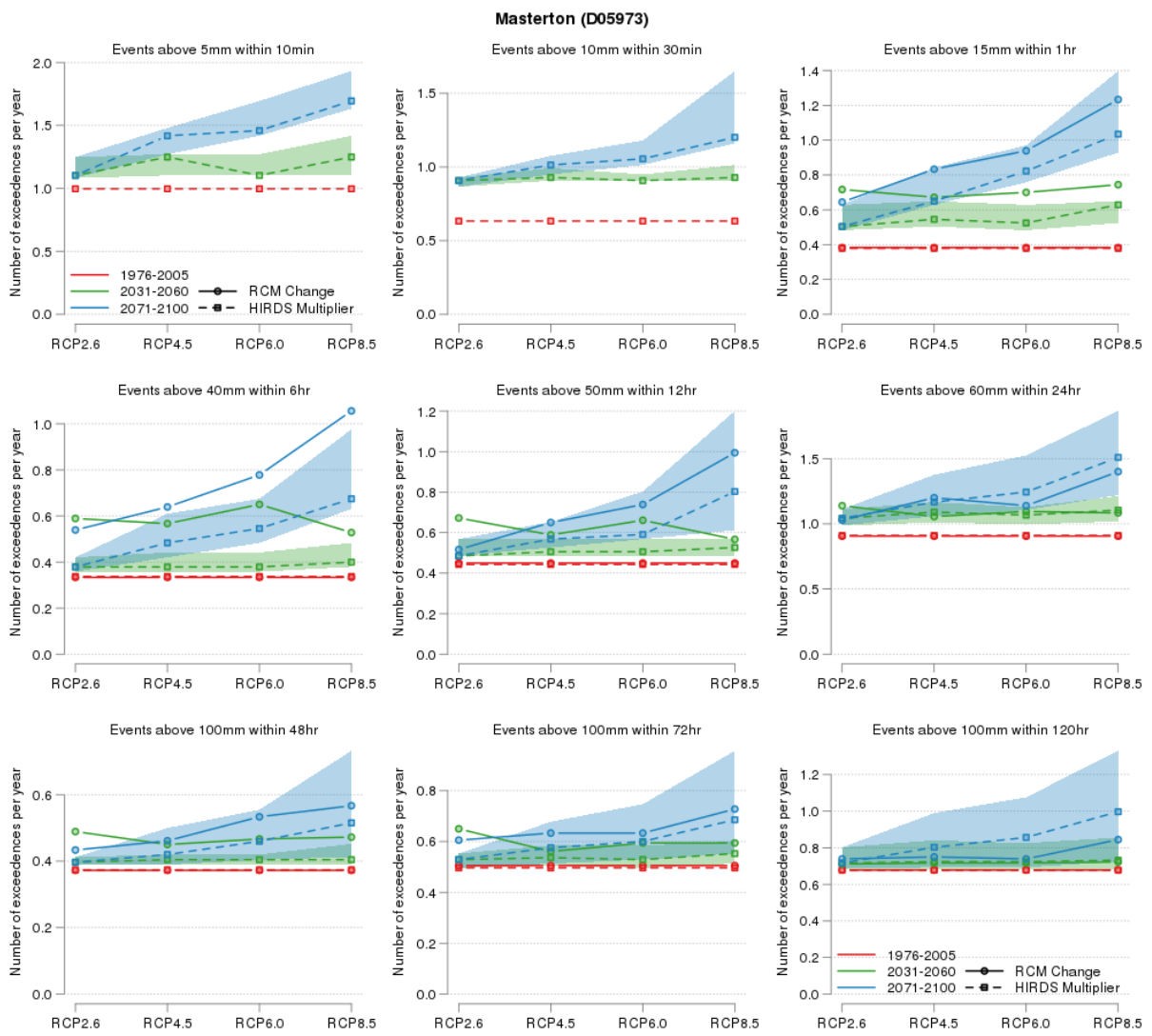


**Figure 3-9: As Figure 3-6 but for Masterton.**

## 4 Mean sea level pressure

Atmospheric pressure has been recorded in Wellington since the 1860's, making it one of New Zealand's longest-running meteorological records. NIWA is the custodian of New Zealand's historic climate data archives, and much of the handwritten data on paper forms has been digitised in the National Climate Database (CliDB<sup>5</sup>). However, some of the earlier daily data has not been digitised and ingested into CliDB (although monthly sums or means have been ingested). Daily data from the early Wellington period were recently digitised and submitted to the International Surface Pressure Databank (ISPD<sup>6</sup>) and contribute to the 20<sup>th</sup> Century Reanalysis (20CR<sup>7</sup>). These data have been made available for analysis in this report. The more recent daily data (post ~1950) were obtained from CliDB. Note however that full homogenisation of the data was not undertaken, and biases may therefore exist in the combined pressure record.

This analysis aims to understand extremes of mean sea level pressure (MSLP) for Wellington, i.e. incidences of high and low pressure which indicate periods of calm or stormy weather respectively.

### 4.1 Methodology and data

In the early period of the Wellington pressure records, the observation locations were moved frequently (Table 4-1), but all observation sites were within ~3.5 km of each other (Figure 4-1). All data were converted to hectopascals (hPa; early data were in inches of mercury). No further data corrections were made – the corrected data as transcribed were used. Due to some sites having slightly different corrections applied at the time of measurement (e.g. including gravity as a factor in the correction or not), there may be small differences, however these potential differences were deemed to be minor. Data for all sites had been corrected for temperature and sea level.

**Table 4-1: Listing of Climate stations where 9 am (NZST) mean sea level pressure records were obtained for this section.**

Station name	Date range	Frequency	Comment	Percentage complete (%)
Knowles Observatory	1862-1868	Daily	Corrected to 0°C and sea level	83.7
Old Museum	1868-1869	Daily	Corrected to 0°C and sea level	100.0
Bolton Street Cemetery	1869-1906	Daily	Corrected to 0°C , sea level and gravity	99.2
		Daily	Corrected to 0°C and sea level	99.6
Mt Cook	1906-2012			
Thorndon Esplanade	1912-1927	Daily	Corrected to 0°C and sea level	100.0
Kelburn	1928-1960	Daily	Corrected to 0°C , sea level and gravity	99.9
		3-Hourly	Corrected to 0°C , sea level and gravity	100.0
		Hourly	Corrected to 0°C , sea level and gravity	94.0
		Daily	Corrected to 0°C , sea level and gravity	99.1
Kelburn AWS	2004-2020	Hourly	Corrected to 0°C , sea level and gravity	99.6
		Hourly, 3-Hourly,		97.4
Total Record	1862-2020	Daily		

<sup>5</sup> The National Climate Database (CliDB) can be accessed publicly through [www.cliflo.niwa.co.nz](http://www.cliflo.niwa.co.nz)

<sup>6</sup> <https://reanalyses.org/observations/international-surface-pressure-databank>

<sup>7</sup> [https://www.psl.noaa.gov/data/20thC\\_Rean/](https://www.psl.noaa.gov/data/20thC_Rean/)



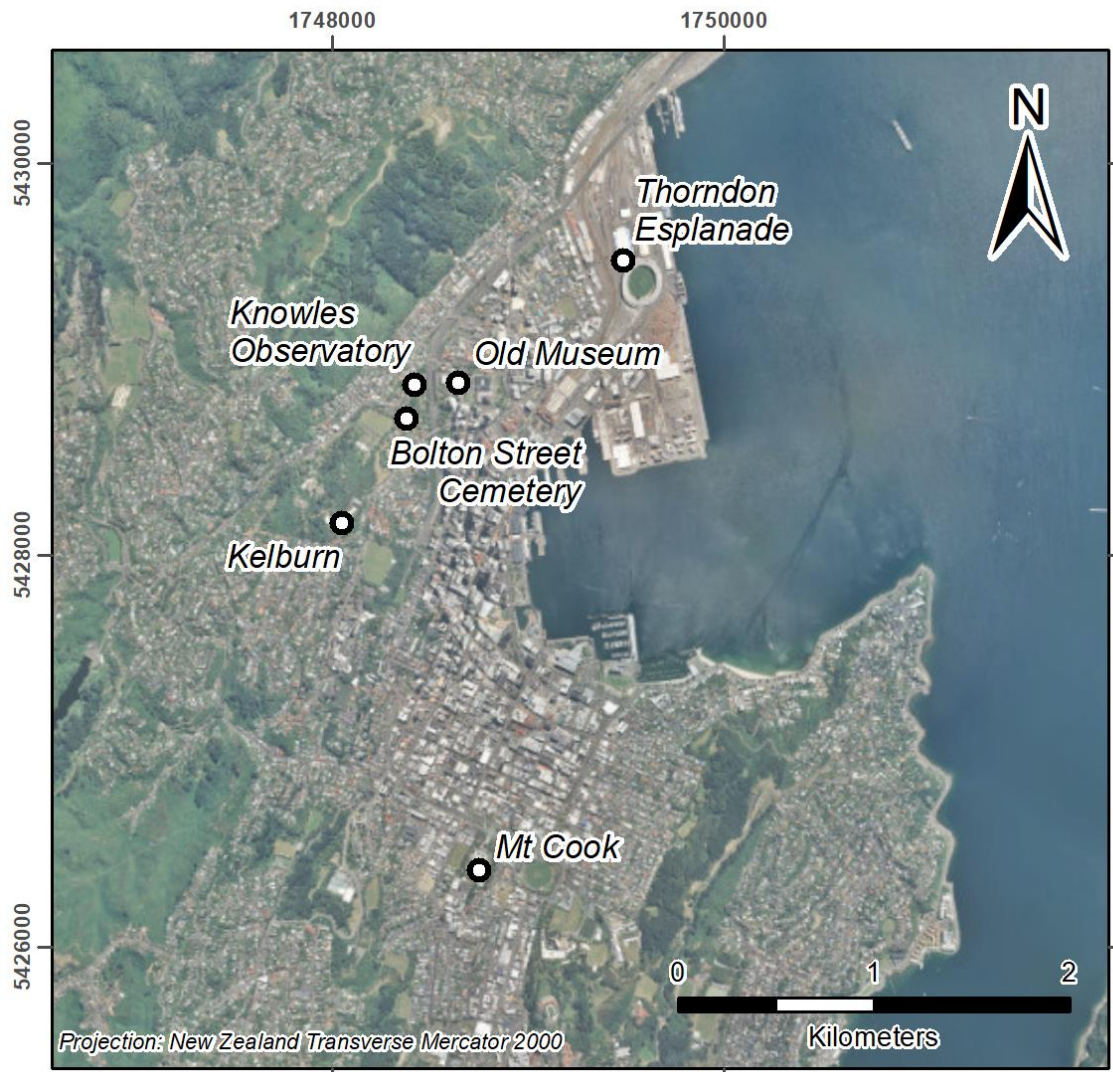


**Figure 4-1: Approximate locations of Wellington climate stations used in the pressure analysis.**

To determine the relative frequency of anomalously high- and low-pressure events, the percentage of observations that exceed the 90<sup>th</sup> percentile and fall below the 10<sup>th</sup> percentile on a monthly basis were computed as shown in Table 4-2 and visualised in Figure 4-2. The sampling frequency of the record was highly variable and inconsistent throughout the record. Observations prior to 1961 were sampled at 9:00 am (local time), while after 1961 they are predominately hourly with a few time intervals of daily and 3-hourly sampling.

To ensure consistency across the entire record, pressure observations are only sampled from 7:00 am to 11:00 am (two-hour window around 9:00 am). The combined record of all observations is shown in Figure 4-3.

**Table 4-2: Pressure thresholds used for the analysis on a monthly basis.**

Types of pressure events	Description	Pressure threshold value (hPa)
High pressure events	% of observations > 90 <sup>th</sup> percentile per month	1025.6 hPa
Low pressure events	% of observations < 10 <sup>th</sup> percentile per month	1001.3 hPa

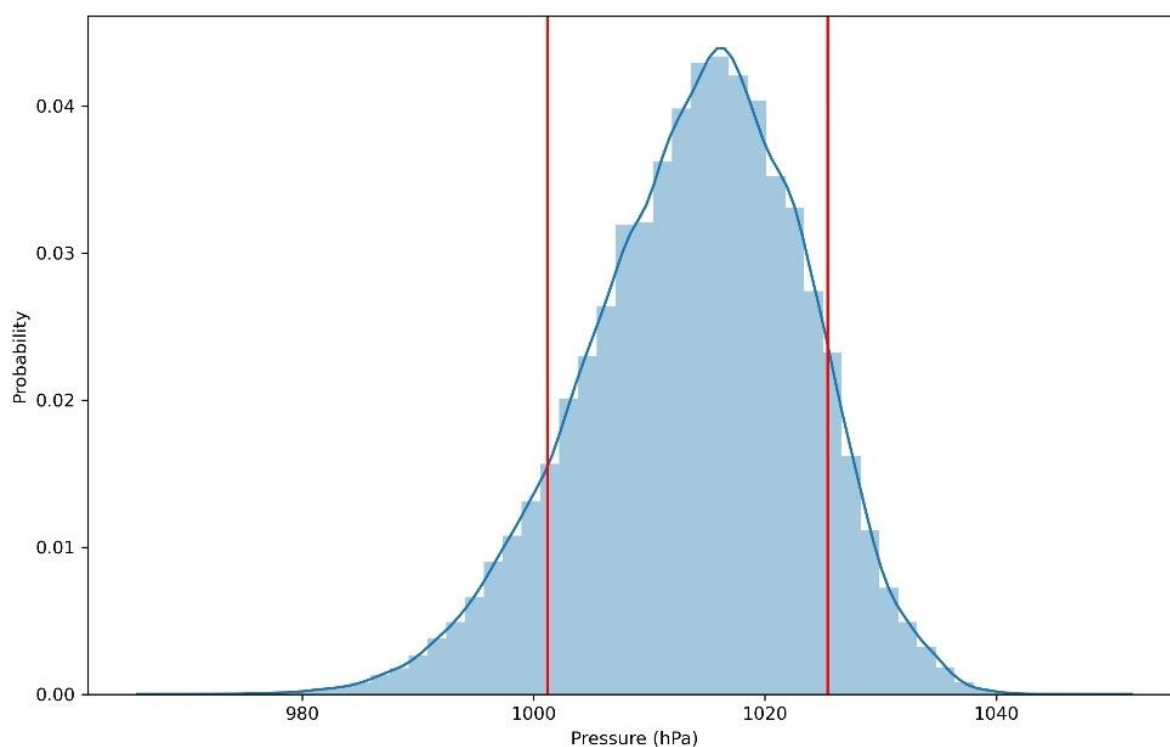


**Figure 4-2: The probability distribution of all pressure observations from the combined pressure record. The 10th and 90th percentiles are outlined as red vertical lines.**

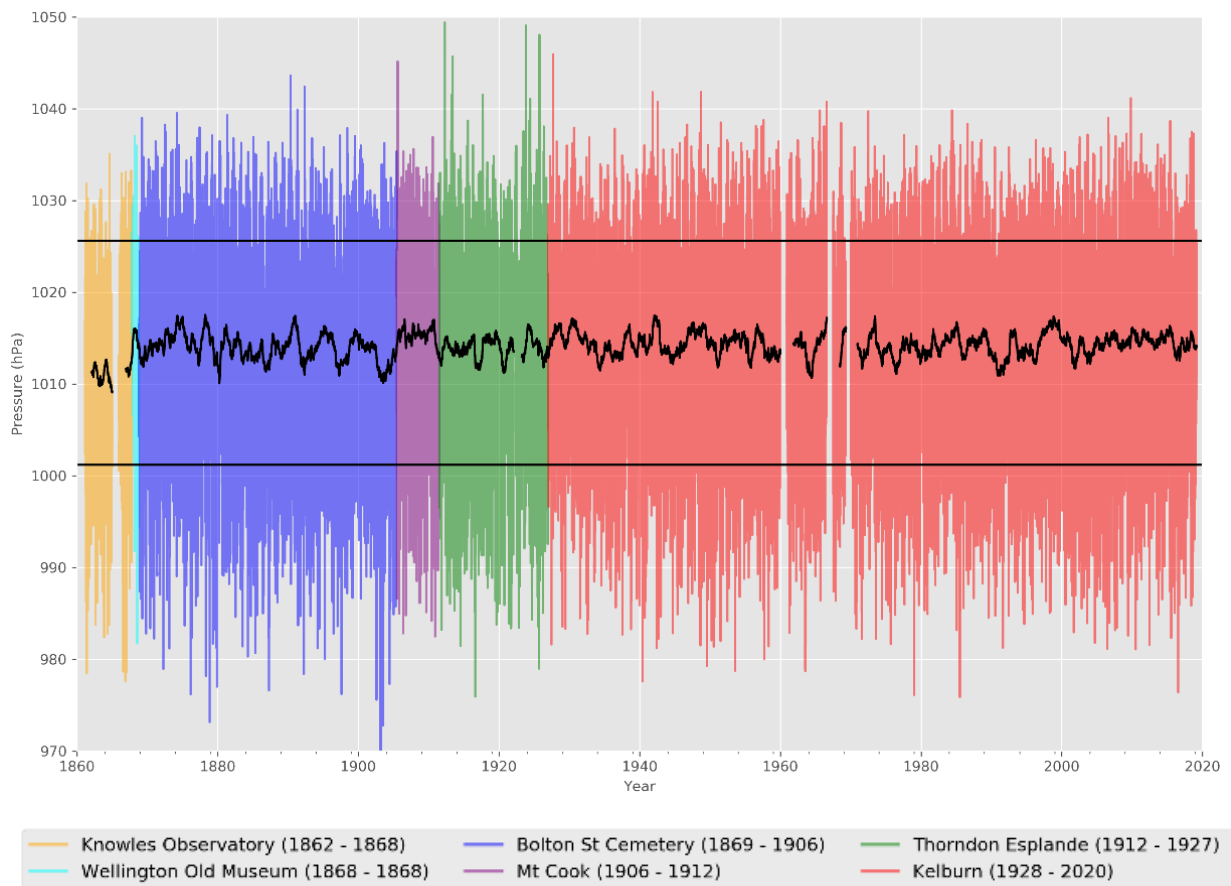


**Figure 4-3:** An illustration of the aggregated Wellington pressure record (hPa), with the records of each individual site color-coded. Thick black line represents a rolling 1-year average. Horizontal straight lines above and below the rolling 1-year average represent the 90<sup>th</sup> and the 10<sup>th</sup> percentile thresholds for all observations. Note that pressure observations were only sampled from 7:00 am to 11:00 am.

## 4.2 Annual trends in pressure

Trends of both maximum and minimum annual pressure are presented in Figure 4-4: An illustration of the aggregated Wellington pressure record (hPa) as show in Figure 4-3, with the trend analysis for annual minimum pressure (red) and annual maximum pressure (blue). and Figure 4-5 (Figure 4-5 also includes the trend analysis for mean annual pressure) and Table 4-3 and Table 4-4 show the five highest and lowest years of mean annual pressure respectively. Both annual maximum and minimum pressure contain a high degree of variability associated with interannual and interdecadal variability, and thus are likely to obscure a temporal trend. For annual maximum pressure, there is a weakly negative trend although this is not statistically significant ( $p = 0.26$ ). For annual minimum pressure, it appears that there is a statistically significant ( $p = 0.01$ ) increase of approximately 0.2 hPa per decade, or 2 hPa per century, however this result should be taken with caution due to the large amount of interdecadal variability. Additionally, the extent to which changes in instrumentation and/or site exposure influence these trends remains unclear and further work would therefore be required to assess any apparent changes in pressure.

It is also noted that trends in the spread of observed MSLP through time were briefly explored during this research. A slight decrease in the standard deviation of MSLP through time was indicated across all three moving time window intervals used for the analysis (moving time window intervals of 1, 3, and 5 years were used) however the statistical significance of these results was notably different

between analyses (significant only for the 3-year analysis interval). Further work is therefore required to understand trends in the distribution of MSLP, which is beyond the scope of this report. The results of these exploratory analyses are however presented as supplementary figures in Section 7 and may serve as a starting point for further research on this front.

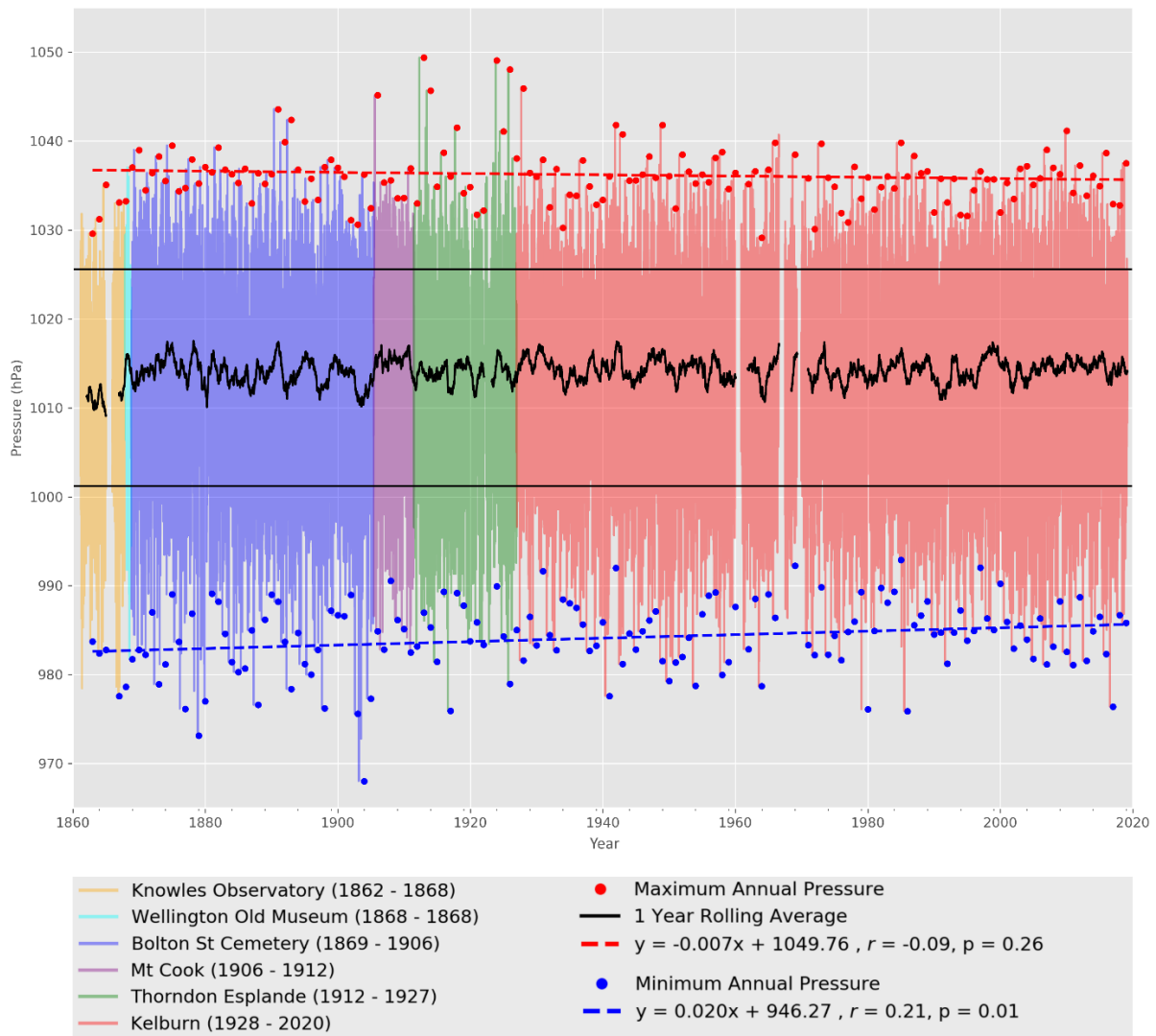


**Figure 4-4: An illustration of the aggregated Wellington pressure record (hPa) as show in Figure 4-3, with the trend analysis for annual minimum pressure (red) and annual maximum pressure (blue).** The points represent the maximum (red) and minimum (blue) pressure within the plotted calendar year (years 15 days or more of missing data were not included in the trend analysis). Dashed lines are trend lines obtained by linear regression. Note that pressure observations were only sampled from 7:00 am to 11:00 am.

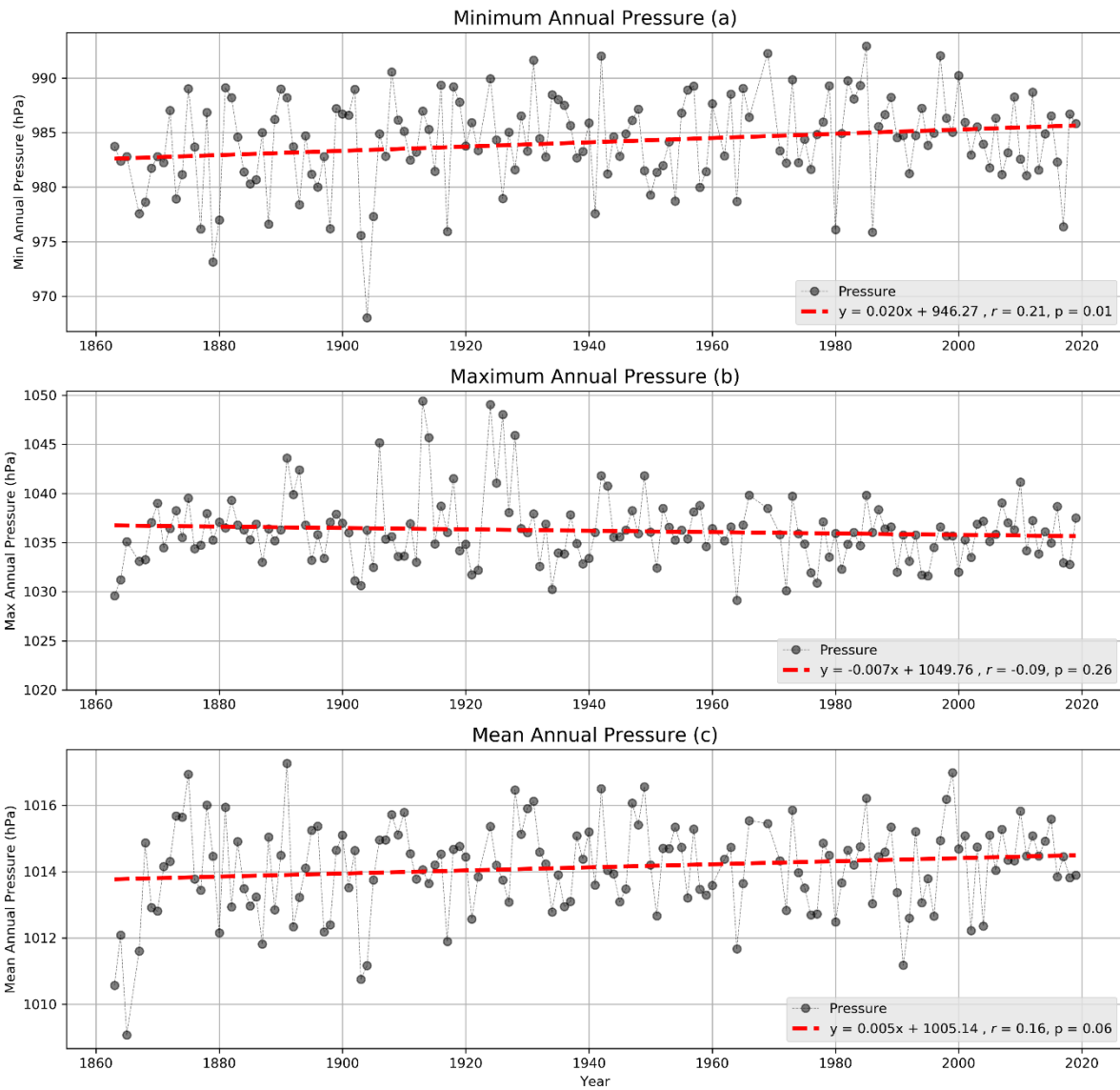


**Figure 4-5: Trend analysis for annual minimum pressure (hPa, top), annual maximum pressure (middle), and annual mean pressure (bottom).** The top two plots for maximum and minimum pressure are the same as the red (max) and blue (min) data points and trendlines presented in Figure 4-4. Dashed lines are trend lines obtained by linear regression. Note that pressure observations were only sampled from 7:00 am to 11:00 am. Years with 15 days or more of missing data were not included in this analysis.

**Table 4-3: 5-highest years of annual mean pressure (hPa, Jan-Dec average) and associated relative humidity (RH, %), temperature (°C), and wind speed anomalies.** Pressure values correspond to the 1-year rolling average in Figure 4-3. Some RH and wind data were not available in the National Climate Database.

Year	Mean Pressure (hPa)	RH anomaly (change in %)	Temp anomaly (°C)	Wind speed (% of average)
1891	1017.3	-	-0.1	-
1999	1017.0	2.2	1.0	94
1875	1016.9	-	0.3	-
1949	1016.6	-3.7	-0.5	-
1942	1016.5	-2.6	-0.4	-

**Table 4-4: 5-lowest years of annual mean pressure (hPa, Jan-Dec average) and associated relative humidity (RH, %), temperature (°C), and wind speed anomalies.** Pressure values correspond to the 1-year rolling average in Figure 4-3. Some RH and wind data were not available in the National Climate Database.

Year	Mean Pressure (hPa)	RH anomaly (change in %)	Temp anomaly (°C)	Wind speed (% of average)
1903	1010.8	-	-0.2	-
1904	1011.2	-	-0.2	-
1991	1011.2	0.9	-0.2	117
1964	1011.7	-3.1	-0.3	103
1887	1011.8	-	0.1	-

### 4.3 Seasonal variability in pressure

Pressure varies on numerous temporal scales – ranging from sub-daily to inter-decadal variations. One of the most significant temporal modes in variability of pressure is associated with the seasonal cycle.

The seasonal cycle of the frequency of high-pressure extremes (90th percentile) appears to have a moderate-strength positive correlation ( $r = 0.6$ ) with the seasonal cycle of mean sea level pressure (MSLP), as illustrated in Figure 4-6. There is also a weak-moderate strength correlation between the frequency of low-pressure extremes (10th percentile) and MSLP ( $r = -0.4$ ). This indicates that when the MSLP is higher-than-average (e.g. between March – April) there tends to be a reduction of low-pressure extremes and an increase of high-pressure extremes. The seasonal cycles for the frequency of low- and high-pressure extremes are very weakly correlated, with an approximate lag of three-months. Also, the amplitude or the change from the month of minimum to maximum of low- and high-pressure extremes is very different, and asymmetric.



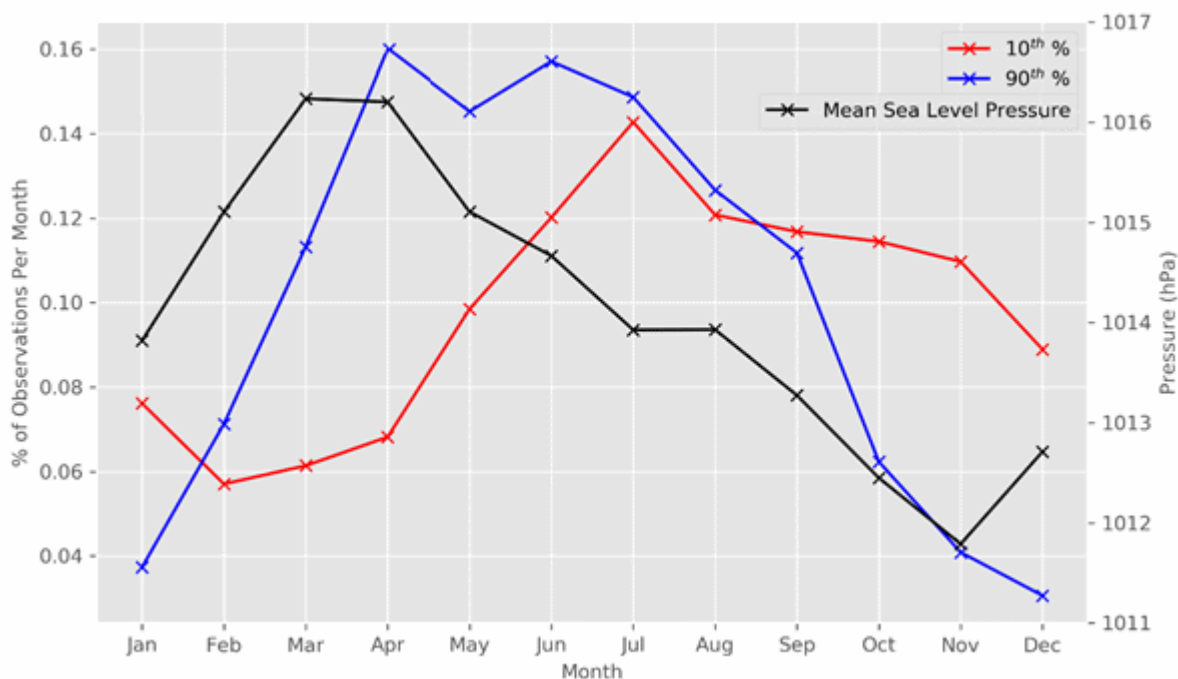


**Figure 4-6: The mean seasonal cycle (1868 – present) of the % of observations that fall below or exceed the 10<sup>th</sup> and 90<sup>th</sup> percentile, respectively .**

This difference or asymmetry between the seasonal cycles of the low- and high-pressure extremes is largely driven by the seasonal changes in distributions of pressure. During the summer, the distribution of pressure has lower variance or is narrower in comparison to the winter. This is illustrated in Figure 4-7, as the range between the 10<sup>th</sup> and 90<sup>th</sup> percentiles of pressure is significantly larger for winter. However, these changes are largely asymmetric, and the increase is larger for the 90<sup>th</sup> percentile of pressure during winter, and thus why there is a difference in the seasonal cycle amplitude between low- and high-pressure extremes.

This analysis indicates that pressure extremes tend to have a significant seasonal cycle. The proportion of observations falling below the 10<sup>th</sup> percentile undergoes a relatively modest seasonal cycle. In comparison, the proportion of observations exceeding the 90<sup>th</sup> percentile undergoes a significantly stronger seasonal cycle. In other words, extreme low pressure events are more evenly distributed across the seasons whereas extreme high pressure events are more concentrated in some seasons than others.

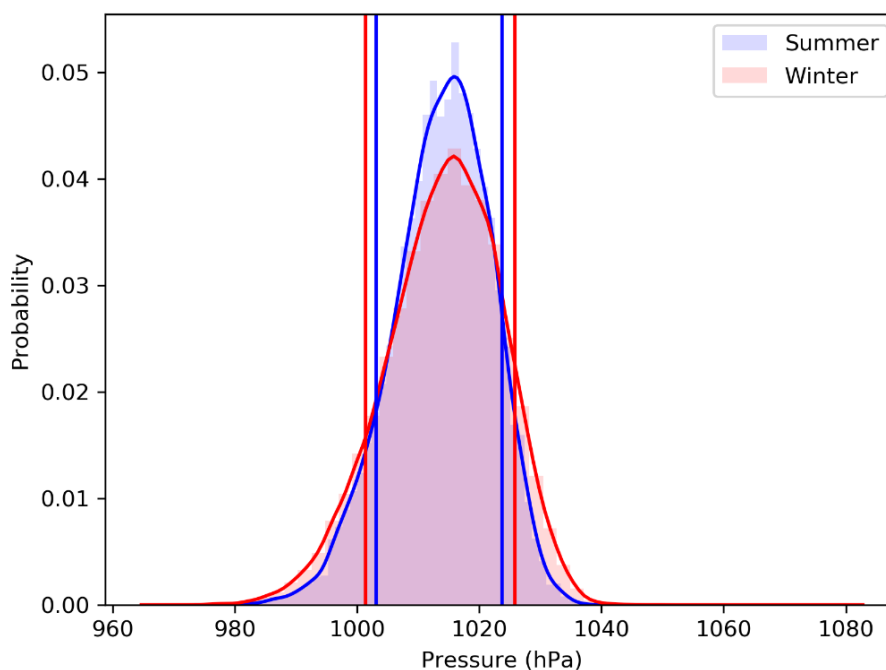


**Figure 4-7:** A comparison of the distribution of pressure for Summer (Dec-Feb) and Winter (Jun-Aug). The bold vertical lines mark the 10<sup>th</sup> and the 90<sup>th</sup> percentiles of the distribution for Summer (blue) and Winter (red), respectively.

#### 4.4 Multi-year and Inter-decadal variability

In addition to the seasonal mode, there appears to be a strong mode of temporal variability in extreme pressure that is associated with longer time scales such as multi-year and inter-decadal variability. To observe temporal variability associated with these time scales, high frequency variability must be removed from the signal. This high frequency variability represents the seasonal cycle and random noise - which obscures long-term trends and fluctuations.

Long-term variability in climatological signals are often linked to processes that change atmospheric or oceanic circulation. Such processes include the El Niño Southern Oscillation (ENSO) and the Inter-decadal Pacific Oscillation (IPO). Variations in the IPO occur on interdecadal timescales (20-30 years), whereas ENSO variability (between phases) typically occurs on timescales between 2-7 years. In this analysis, to determine the strength of the IPO and the ENSO we use the Pacific Decadal Oscillation (PDO) Index and the Southern Oscillation Index (SOI), respectively. These indices are obtained from the National Oceanic and Atmospheric Administration (NOAA<sup>8,9</sup>). Note, there are some differences in the PDO amongst the various providers. However, the analysis remains relatively invariant across different indices.

Research into the influence of the IPO on New Zealand climate has indicated that during the positive phase of the IPO, sea surface temperatures around New Zealand tend to be lower, and westerly winds stronger, resulting in drier conditions for eastern areas of both North and South Islands (Salinger et al., 2001). The opposite effects generally occur during the negative phase of the IPO.

During El Niño events, weakened trade winds cause New Zealand to experience a stronger than normal south-westerly airflow. This generally brings lower seasonal temperatures to the country and

<sup>8</sup> <https://www.ncdc.noaa.gov/teleconnections/pdo/>

<sup>9</sup> <https://www.ncdc.noaa.gov/teleconnections/enso/indicators/soi/>



drier than normal conditions to the north and east of New Zealand (Salinger and Mullan, 1999). During La Niña conditions, strengthened trade winds cause New Zealand to experience more north-easterly airflow than normal, higher-than-normal temperatures (especially during summer), and wetter conditions in the north and east of the North Island.

The analyses in the section outlined below are averaged over all months (January – December). Our analysis indicates that multi-year variability in the proportion of observations exceeding or falling below the 90<sup>th</sup> and 10<sup>th</sup> percentiles respectively appears to be linked to variability in ENSO, as illustrated in Figure 4-8. A negative correlation between the percentage of observations below the 10<sup>th</sup> percentile and the Southern Oscillation Index (SOI) indicates that during El Niño (ENSO positive phase or negative SOI) there tends to be a greater-than-average occurrence of extreme low-pressure events in Wellington. Conversely, during La Niña there tends to be a lower-than-average occurrence of low-pressure events in Wellington. Similarly, for 90<sup>th</sup> percentile exceedance there tends to be a higher-than-average occurrence of high-pressure events in Wellington during La Niña and a lower-than-average occurrence of pressure events during El Niño. Note that the SOI does not extend back beyond 1950 therefore this analysis only covers the 1950-2020 period.

With further signal smoothing (10-year running mean), inter-decadal variability for the proportion of observations exceeding or falling below the 90<sup>th</sup> and 10<sup>th</sup> percentiles respectively appears to be strongly linked to variability in the IPO index (Table 4-5 and Figure 4-9). Our results show that during the positive phase of the IPO (IPO > 0.0), the proportion of observations falling below the 10<sup>th</sup> percentile tends to be higher-than-average while the converse occurs in the negative phase of the IPO (i.e. lower proportion during the negative phase; Figure 4-9a). A somewhat negative correlation occurs for the observations above the 90<sup>th</sup> percentile and there tends to be a lower than average proportion of observations exceeding this threshold during positive phases of the IPO and vice versa (higher proportion during negative IPO; Figure 4-9b). The decades associated with the most frequent exceedances of these extreme pressure thresholds (top-5 ranked decades) are shown in Table 4-6 and Table 4-7. The ranking of these decades is consistent with our analysis of the IPO signal and extreme pressure.

Our analysis indicates that pressure extremes are associated with both multi-year variability (ENSO) and the inter-decadal variability (IPO). Furthermore, the amplitude associated with these temporal scales is significant (comparable to the amplitude of the seasonal cycle) and obscures long-term or time-dependent statistical trends.

**Table 4-5: The correlation coefficient between the % of pressure events above and below the 90<sup>th</sup> and 10<sup>th</sup> percentile and the SOI (left column) and IPO (right column) indexes, respectively.**

	Correlation Coefficient ( <i>r</i> ) with SOI (summer) with a 2-year running mean.	Correlation Coefficient ( <i>r</i> ) with IPO (summer) with 10-year running mean.
10th Percentile	-0.47	0.31
90th Percentile	0.31	-0.28

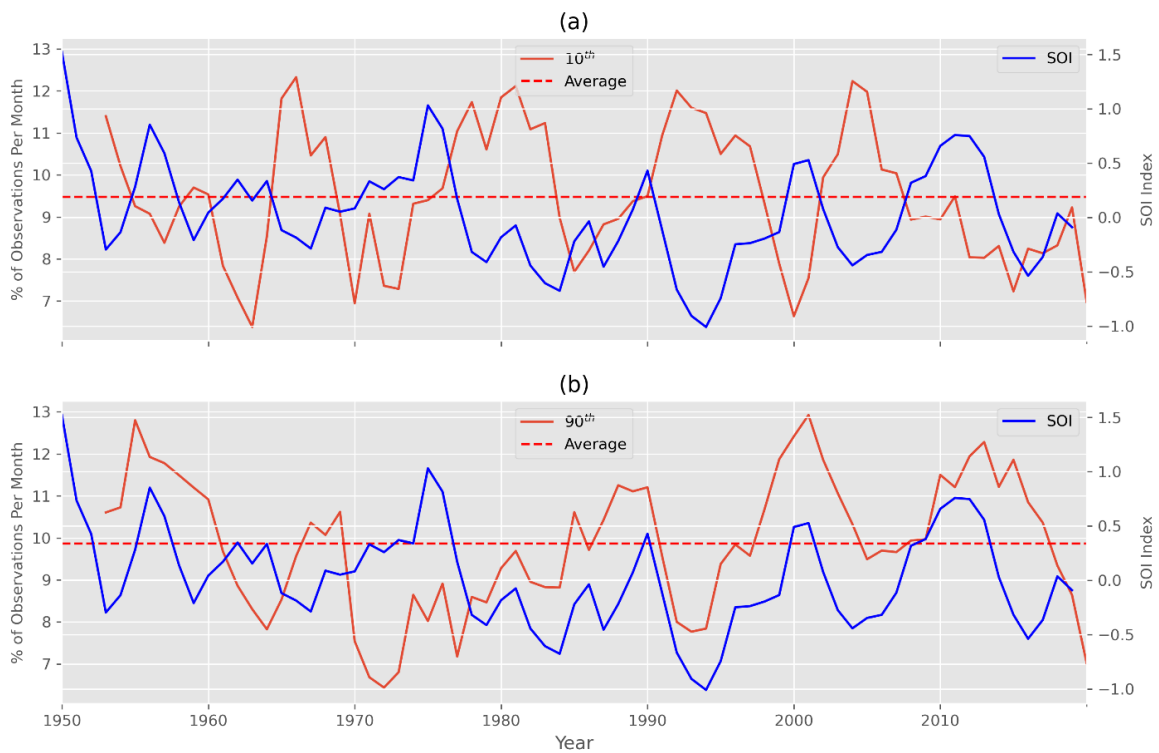


**Figure 4-8: The annual mean time-series for the SOI and percentage of observations of mean sea level pressure in Wellington below the 10th percentile (a) and above the 90th percentile (b) over the period 1950-2020. A two-year running mean is applied to both time-series. Dashed lines are trend lines obtained by linear regression.**

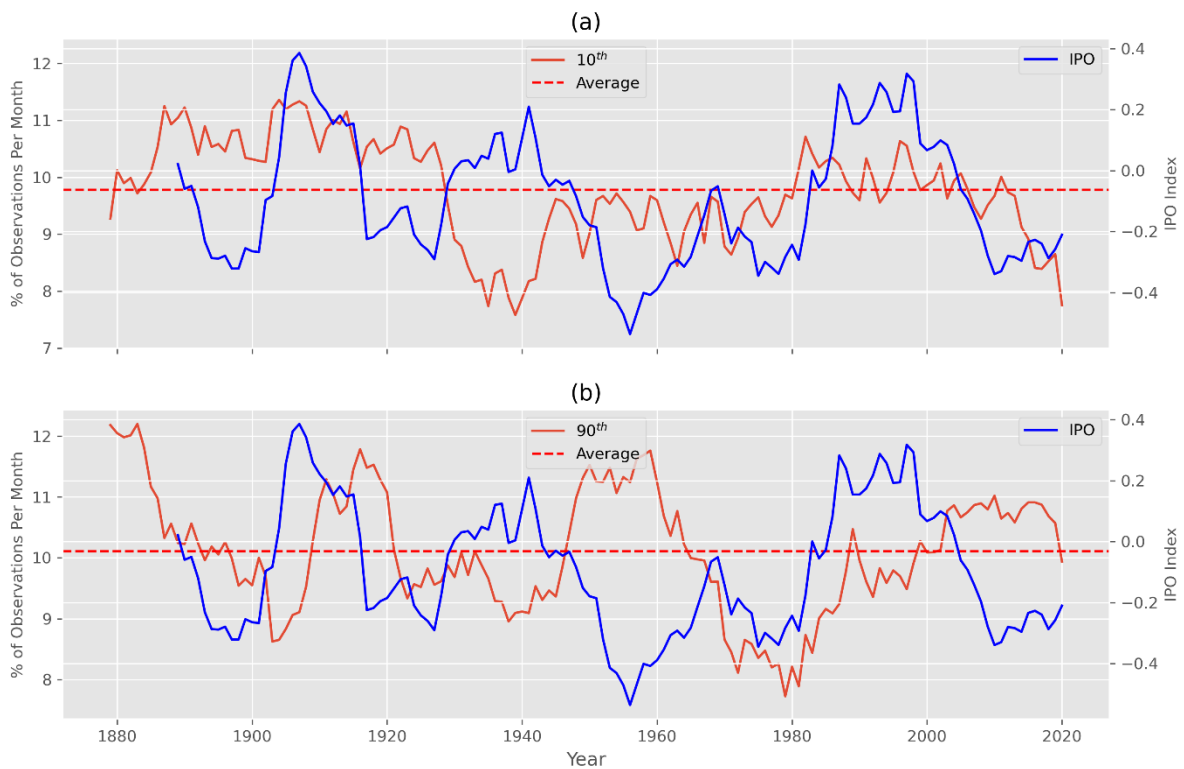


**Figure 4-9: The annual mean time-series (10-year running mean) for the IPO and percentage of observations of mean sea level pressure in Wellington below the 10th percentile (a) and above the 90th percentile (b) over the period 1870 – 2020. Dashed lines are trend lines obtained by linear regression.**

**Table 4-6: Decades with the highest percentage of pressure observations falling below the 10<sup>th</sup> percentile (All Seasons). Top five, ordered highest to lowest.**

Decade	Percentage of pressure observations less than the 10 <sup>th</sup> percentile
1880-1890	11.7
1900-1910	11.0
1910-1920	10.7
2000-2010	10.3
1950-1960	10.3

**Table 4-7: Decades with the highest percentage of pressure observations exceeding the 90<sup>th</sup> percentile (All Seasons). Top five, ordered highest to lowest.**

<b>Decade</b>	<b>Percentage of pressure observations exceeding the 90<sup>th</sup> percentile</b>
1870-1880	12.1
1940-1950	11.6
1950-1959	11.4
1900-1910	11.0
2010-2020	10.6

## 5 Dew point temperature

### 5.1 Methodology and data

In New Zealand long-term (historic) climate records relating to moisture content of air masses (i.e., Relative Humidity ( $RH$ ), Dewpoint Temperature ( $T_d$ ), and Wet Bulb Temperature ( $T_w$ )) are typically only available from daily 9 am observations. Hourly records of these variables are more commonplace from the early 1990's with the introduction of automated weather stations (AWS). Typically, only one of the three variables ( $RH$ ,  $T_d$ ,  $T_w$ ) was reported. This is because when one of these is known along with the dry bulb air temperature ( $T_a$ ) (which is almost always reported), the other two variables can be reasonably determined. Abbot and Tabony (1985), Alduchov and Eskridge (1996), August (1828), Magnus (1844), and Stull (2011) provide background and various methods to do these calculations. Additionally, there are online calculators and resources which can be utilised to these conversions, a listing of some of these sites is provided within the reference section of this report.

A survey of NIWA station histories (Fouhy et al., 1992) and New Zealand's national climate database (CliDB) identified that for Wellington the Kelburn site could be used to derive dew-point temperature records back to 1928, and that a collection of sites could be used for Masterton (see Table 5-1). The locations of the Masterton area sites are shown in Figure 5-1. The longest records were for 9 am records and so this time was chosen for the analysis here. Early daily maximum and minimum temperature records do not have coincident humidity records so were unsuitable. Digitization, and quality control of many of the older records, especially those prior to 1972 was also required for this analysis. Quality control consisted of visual inspection of records checking for obviously spurious values, unphysical values, e.g. when dew-point or wet-bulb temperatures exceeded dry-bulb air temperatures, and also the conversion from Fahrenheit to Celsius when required. Prior to automated stations the observing method typically involved the observer recording the dry-bulb temperature and wet-bulb temperature then using psychrometric charts to determine Relative Humidity and dew-point temperature. At times a sling psychrometer may also have been used to determine the wet-bulb temperature by a trained observer. The psychrometric chart determination also requires barometric pressure to be known (or assumed).

One complication in this analysis, due to daylight savings, was that there were periods in the past where only 9 am local records were available. These periods are noted in Table 5-1. This meant that only 8 am New Zealand Standard Time (NZST) records were available in these periods. To account for this, regression relationships between 8 am and 9 am NZST observations were developed from nearby stations where, or from a later period, when hourly observations were available, and adjustments made. Further details about the adjustment are provided in Table 5-2. It should also be noted that the current NZST was adopted in 1941. In the period 1927-1941 New Zealand did have daylight savings in the summer months and in 1941 this daylight savings time was adopted all-year round and became the current NZST. The old standard time (NZMT) between 1927 and 1941 was 30 minutes behind our current NZST or +11:30 ahead of UTC. The period of daylight savings from 1928 to 1933 was from the 2<sup>nd</sup> Sunday in October to the 3<sup>rd</sup> Sunday in March and from 1933 to 1941 it was from the 1<sup>st</sup> Sunday in September until the last Sunday in April. Adjustments were made to account for the half-hour shift during the period of NZMT – this tended to result in a slight cooling of average dew-point temperatures on the order of 1 °C at Masterton, but only a slight cooling of around 0.1 °C at Kelburn.

Wet-bulb temperature, dew-point temperature or relative humidity are measures of the moisture content of air-mass characteristics and are most meaningful when combined with other parameters such as dry-bulb temperature to provide apparent temperature (heat indices), e.g., where high humidity and high temperatures are uncomfortable for humans or livestock as it limits the ability to regulate the cooling of the body. Physically, dew-point temperature is, in the absence of a change of air-mass, often a useful indicator of what the overnight temperatures may drop to and when high in the summer are associated with sub-tropical air-masses and so can be used to assess climatic risk of spread of some potentially invasive insect pests from warmer climates, e.g., Red Imported Fire Ant (RIFA; Turner et al., 2006). Low dew-point temperatures near zero or below will also be associated with frost occurrence and extended periods of low-humidities in warmer months associated with drought risk. Thus in this section we present annual time series of seasonal average variables of Relative Humidity (*RH*), Dewpoint Temperature (*T<sub>d</sub>*), Wet Bulb Temperature (*T<sub>w</sub>*), and Dry bulb air-temperature (*T<sub>a</sub>*), along with time-series of the monthly maximum, minimum and average values of dew-point temperature and relative humidity.

**Table 5-1: Listing of Climate stations where 9 am (NZST) temperature and humidity records were obtained for this section.**

Station Name	Begin Date (analysis)	End Date (analysis)	Comment
<b>Wairarapa</b>			
Masterton, Essex St	2-Sep-1928	30-Nov-1942	Digitized from paper records
Masterton Waingawa <sup>1</sup>	2-Jan-1943	31-Dec-1971	Digitized from paper records
Masterton Waingawa <sup>2</sup>	1-Jan-1972	31-Mar-1991	8 am records in NZDT 1974 – 1991
East Taratahi <sup>1,2</sup>	28-Oct-1991	4-Nov-2009	8 am records in NZDT 1991 - 1995
Masterton Aero AWS	5-Nov-2009	25-Mar-2020	
<b>Wellington</b>			
Kelburn <sup>3</sup>	1-Dec-1928	30-Jan-1961	Digitized from paper records
Kelburn <sup>4,5</sup>	1-Dec-1961	1-Sep-2005	8 am records in NZDT 1989 – 2004
Kelburn AWS	2-Sep-2005	25-Mar-2020	

1 – Dec 1996: Stevenson Screen Replaced

2 – May 2001: Humidity Probe replaced due to overheating

3 – Jul 1949: Exposure increased and improved.

4 – Apr 1970: Equipment replaced due to vandalism

5 – Dec 1989: Thermometer replaced



**Figure 5-1:** Map showing location of Masterton climate stations with records used in the Dewpoint Temperature analysis.

**Table 5-2:** Regression relationships and correlations between 8 am and 9 am temperature and humidity variables for stations where hourly records available. Ta = dry bulb air temperature, Tw = wet bulb air temperature, RH = relative humidity, Td = dew point temperature.

Station	Years	Ta			Tw		
		slope	intercept	r <sup>2</sup>	slope	intercept	r <sup>2</sup>
East Taratahi	1995-2009	0.9180	2.7207	0.926	0.8571	2.6097	0.929
Masterton AWS	2009-2020	0.9198	2.8088	0.925	0.8562	2.6016	0.938
Kelburn	1972-1988	1.0231	0.3251	0.943	0.9593	0.7802	0.958
Kelburn AWS	2004-2020	0.9839	1.0393	0.949	0.9578	0.9370	0.968
		RH			Td		
		slope	intercept	r <sup>2</sup>	slope	intercept	r <sup>2</sup>
East Taratahi	1995-2009	1.0051	-5.1407	0.812	0.8295	2.1485	0.897
Masterton AWS	2009-2020	0.9753	-4.1650	0.811	0.8410	1.8891	0.907
Kelburn	1972-1988	0.8504	10.2570	0.591 <sup>10</sup>	0.8991	1.0695	0.899
Kelburn AWS	2004-2020	1.0122	-4.2783	0.834	0.9671	0.4719	0.959

<sup>10</sup> The lower correlation between 8 am and 9 am RH at Kelburn is suspected to be due to different precisions in reported values at these times of the day.



## 5.2 Wellington

Average values for each season (summer, autumn, winter, and spring) for each year from 1928 to 2019 for Kelburn for  $RH$ ,  $T_a$ ,  $T_w$ , and  $T_d$  are provided in Figure 5-2 to Figure 5-5. Potential breakpoints in the time-series due to an exposure change in 1949 and the station change in 2004 are indicated in these figures but visually these appear to have little effect on trends. While this section is focused on trends and extremes in dew-point temperatures, the other variables are presented also as a check on consistency and to aid physical interpretation. The other point to note about the other variables is that the dry-bulb air temperatures ( $T_a$ ) are 9 am temperatures and so trends and rankings presented here may not precisely match those of daily maximum, minimum or average temperatures derived elsewhere.

From these seasonal plots, it is apparent that the year-to-year variation and longer-term trends in  $T_a$ ,  $T_w$ , and  $T_d$  are all very similar. Overall, the trend in winter is strongest where there is an increase (linear regression) in 9 am dew-point temperatures of 1.7 °C over the 90 years, and an increase in relative humidity of around 3.6% over the period (Figure 5-4). For autumn there is also an increase of around 0.8 °C in  $T_d$  and around 2.1% in RH (Figure 5-3), and for summer these increases are 0.4°C and 0.4% (Figure 5-2). Meanwhile, for spring the increases to  $T_d$  and RH are 0.1 °C and 0.1% respectively (Figure 5-5). The increases in relative humidity are interesting since relative humidity decreases as dry-bulb temperature increases (if all other air-mass parameters remain unchanged) and so it appears that in this instance, increases to dew-point temperature are more influential than the increases in dry bulb air temperature in determining the trend in relative humidity. It is noted that there is a sudden increase in RH during summer between 1990 and 2004 which doesn't occur for the other seasons (Figure 5-2), and this appears consistent with the observed temperature changes at the time (which show a drop in 9am temperatures). While no information in the station histories was found that indicated any relevant station issues during this period, it is noted that the end of the period aligns with a station change and it is therefore possible that there could be some underlying data issues during this period.

The top-ten and bottom-ten ranked months for average dew-point temperatures are provided in Table 5-4 and Table 5-5. Interesting points from these tables are that January 2018 had the highest average  $T_d$  values of 16.6°C and February 1998 was ranked third, where these two years are tied for 2<sup>nd</sup> warmest years for New Zealand (according to NIWA's 7 station temperature series<sup>11</sup>). Also interesting is that, in spite of the long-term upward trend, February 1938 (2<sup>nd</sup>) and February 1935 (10<sup>th</sup>) are ranked within the top ten. In terms of bottom ranked years, seven of the ten months occurred in the 1930's and 1940's.

---

<sup>11</sup> <https://niwa.co.nz/our-science/climate/information-and-resources/nz-temp-record/seven-station-series-temperature-data>



**Table 5-3: Change in average seasonal values in “9 am” dew-point temperature (Td), Relative Humidity (RH), dry bulb air temperature (Ta) and wet-bulb air-temperature (Tw) for the Kelburn, Wellington site between 1928 and 2020.**

Change between 1928 and 2019				
Season	T <sub>d</sub> (°C)	RH (%)	T <sub>a</sub> (°C)	T <sub>w</sub> (°C)
Summer	+0.4	+0.4	+0.3	+0.3
Autumn	+0.8	+2.1	+0.3	+0.6
Winter	+1.7	+3.6	+0.9	+1.2
Spring	+0.1	+0.1	+0.1	+0.1

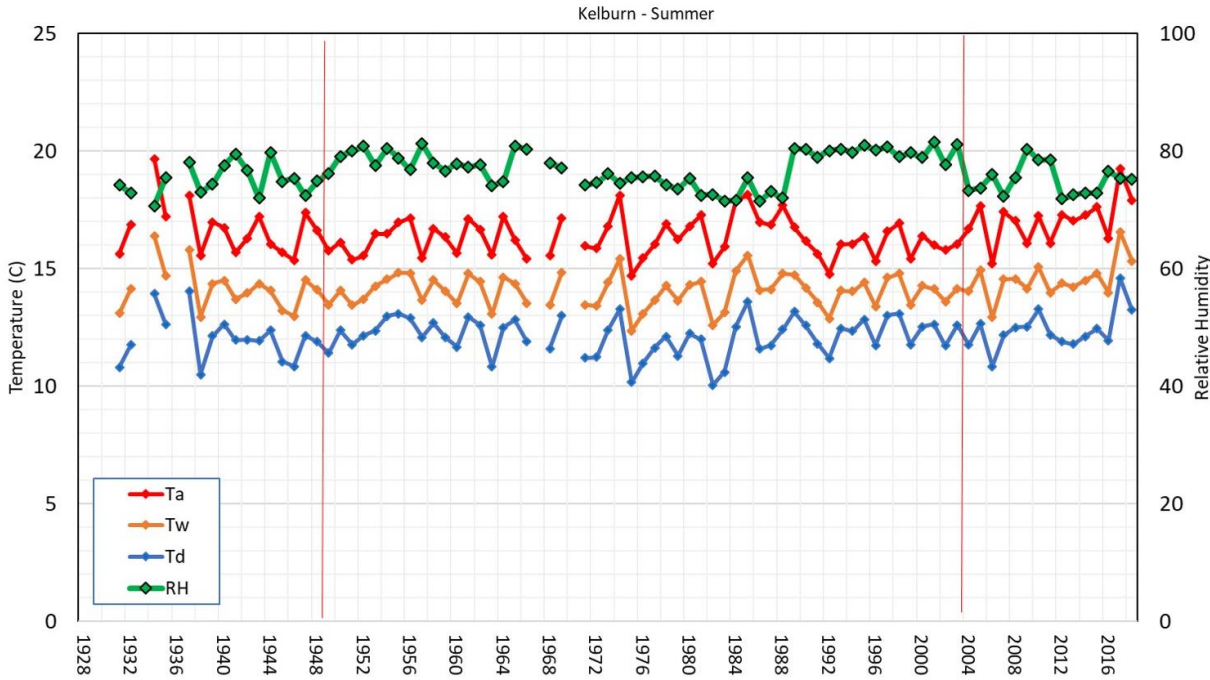


**Figure 5-2: Time series of summer “9 am” averages for dry bulb air temperature (T<sub>a</sub>; red-line), wet-bulb air-temperature (T<sub>w</sub>; orange line), dew-point temperature (T<sub>d</sub>; blue line) and Relative Humidity (RH; green line) for the Kelburn, Wellington site for the period 1928 to 2020. The red vertical lines mark an exposure change in 1949 and the switch to records from Kelburn (CliDB agent no. 3385) to Kelburn AWS (25354) in 2004.**

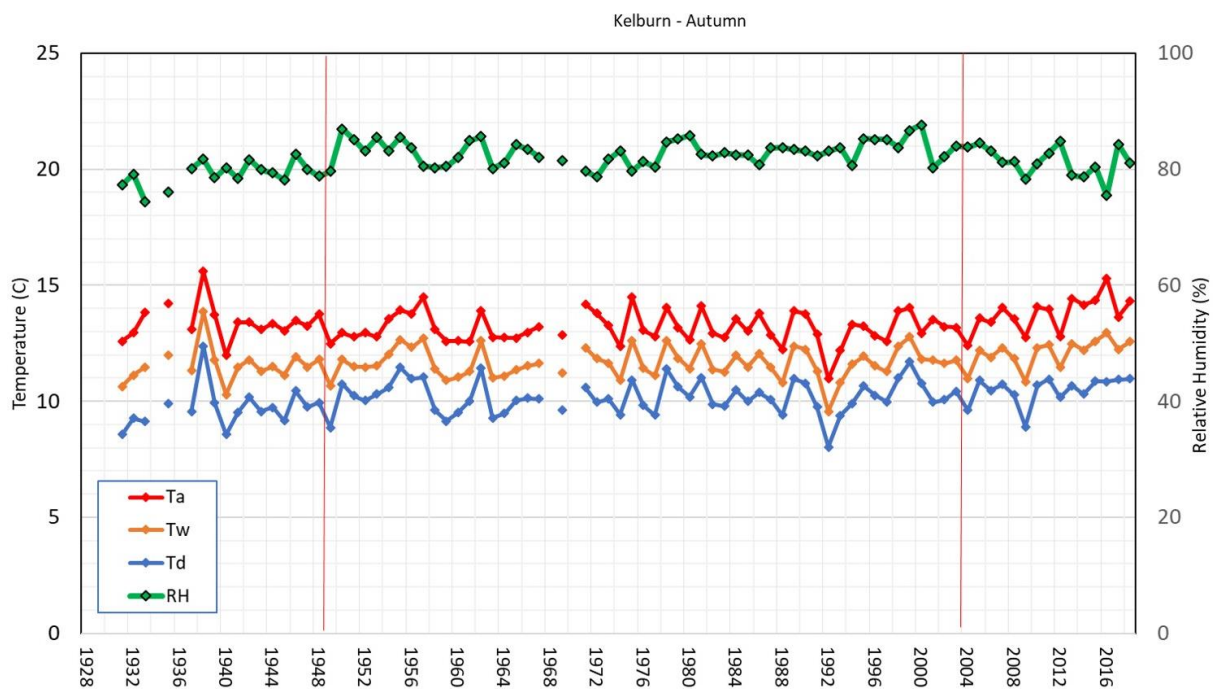


**Figure 5-3:** Time series of autumn “9 am” averages for dry bulb air temperature ( $T_a$ ; red-line), wet-bulb air temperature ( $T_w$ ; orange line), dew-point temperature ( $T_d$ ; blue line) and Relative Humidity ( $RH$ ; green line) for the Kelburn, Wellington site for the period 1928 to 2020. The red vertical lines mark an exposure change in 1949 and the switch to records from Kelburn (CliDB agent no. 3385) to Kelburn AWS (25354) in 2004.

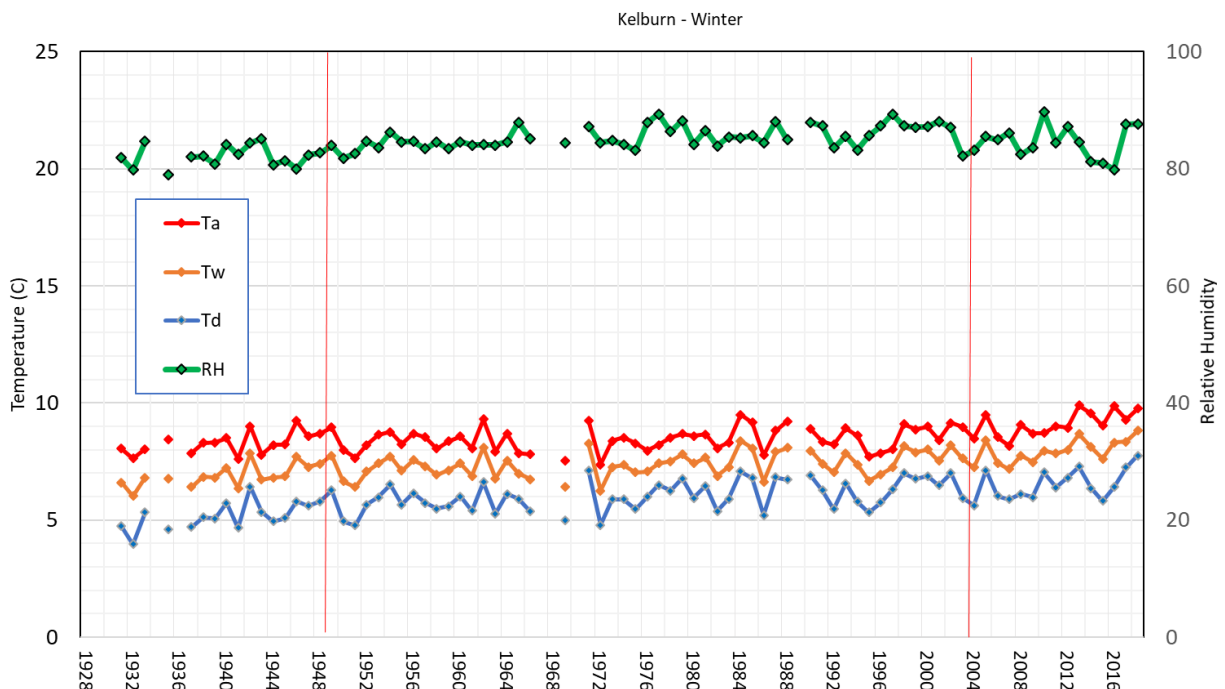


**Figure 5-4:** Time series of winter “9 am” averages for dry bulb air temperature ( $T_a$ ; red-line), wet-bulb air temperature ( $T_w$ ; orange line), dew-point temperature ( $T_d$ ; blue line) and Relative Humidity ( $RH$ ; green line) for the Kelburn, Wellington site for the period 1928 to 2020. The red vertical lines mark an exposure change in 1949 and the switch to records from Kelburn (CliDB agent no. 3385) to Kelburn AWS (25354) in 2004.

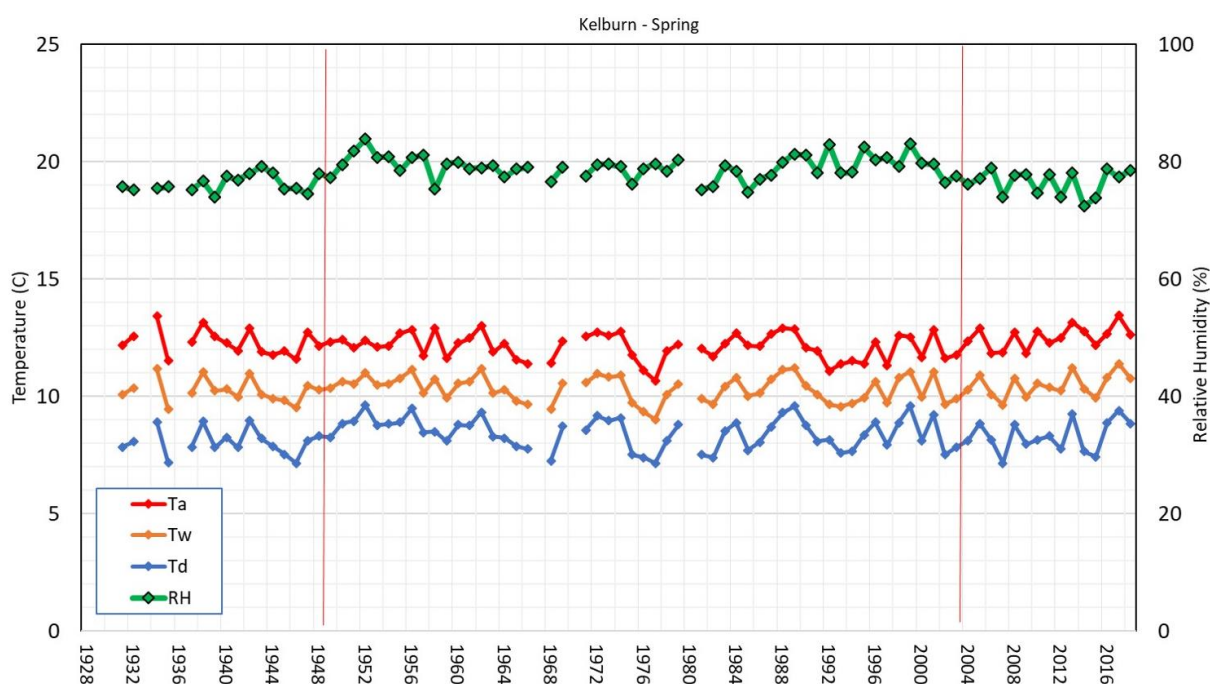


**Figure 5-5:** Time series of spring “9 am” averages for dry bulb air temperature ( $T_a$ ; red-line), wet-bulb air-temperature ( $T_w$ ; orange line), dew-point temperature ( $T_d$ ; blue line) and Relative Humidity (RH; green line) for the Kelburn, Wellington site for the period 1928 to 2020. The red vertical lines mark an exposure change in 1949 and the switch to records from Kelburn (CliDB agent no. 3385) to Kelburn AWS (25354) in 2004.

**Table 5-4:** Top ten ranked months with highest average 9 am  $T_d$  (6<sup>th</sup> column) in the period 1928 to 2019 at Kelburn. Also listed are the average values  $T_a$ ,  $T_w$ , RH in these months.

Date	Rank	$T_a$	$T_w$	RH	$T_d$
Jan-18	1	20.6	18.2	78.8	16.6
Feb-38	2	19.2	17.2	81.4	15.8
Feb-98	3	18.2	16.7	87.0	15.7
Jan-56	4	18.3	16.4	82.9	15.1
Feb-90	5	18.2	16.3	82.8	14.9
Feb-55	6	17.4	15.9	85.1	14.8
Feb-74	7	17.9	16.0	82.4	14.7
Feb-66	8	17.8	16.0	82.3	14.6
Jan-86	9	19.2	16.5	74.7	14.5
Feb-35	10	18.9	16.4	76.6	14.5

**Table 5-5: Bottom ten ranked months with lowest average 9 am  $T_d$  (6<sup>th</sup> column) in the period 1928 to 2019 at Kelburn. Also listed are the average values  $T_a$ ,  $T_w$ , RH in these months.**

<b>Date</b>	<b>Rank</b>	<b><math>T_a</math></b>	<b><math>T_w</math></b>	<b>RH</b>	<b><math>T_d</math></b>
Jul-39	1	6.3	4.8	76.6	<b>3.0</b>
Jun-72	2	6.4	5.1	81.6	<b>3.3</b>
Jul-32	3	7.0	5.6	79.6	<b>3.6</b>
Jun-41	4	7.6	6.0	77.7	<b>3.7</b>
Jul-45	5	7.1	5.7	80.3	<b>3.8</b>
Aug-32	6	7.7	6.1	77.1	<b>3.8</b>
Jun-69	7	7.0	5.7	81.2	<b>3.8</b>
Jun-37	8	7.6	6.1	79.5	<b>4.1</b>
Jul-95	9	7.1	5.8	82.1	<b>4.1</b>
Jun-44	10	8.5	6.6	74.5	<b>4.1</b>

Monthly averages, minimums, and maximum of dry bulb air temperature ( $T_a$ ), wet bulb temperature ( $T_w$ ), relative humidity (RH) and dew-point temperature ( $T_d$ ) for Kelburn are shown in Figure 5-6 to Figure 5-9. The thick bold lines are running 12 month means of the average, minimum and maximum. Trends in the averages correspond to the overall annual trends in these values and are +0.8 °C for  $T_a$ ,  $T_w$ , and  $T_d$  and +1.3% for RH over the 90 years.

The ten most extreme maximum values of 9 am dew-point temperature and the dates on which these occurred are provided in Table 5-6 while the values of the extreme minimums and dates are provided in Table 5-7. The most extreme high 9 am dew-point temperature was 20.3 °C on 10 March 1981. Interestingly, only the events of 18 February 1955 and 30 January 1956 occurred in months that had averages ranked in the top-ten. Extreme minimum events occurred in winter, with the record minimum of -6.8 °C on 7 June 1944. Again 7 of the 10 bottom ranked events occurred in the 1930's and 1940's.

It is noted that this analysis only captures extremes in "9 am" dew-point temperatures and therefore will have missed other significant observations that might have occurred at different times of the day. The maximum dew-point temperature across the entire record for Kelburn was 22.0 °C observed at 1800 hours on 11 Feb 2018 (part of the notably hot and wet summer of 2018).

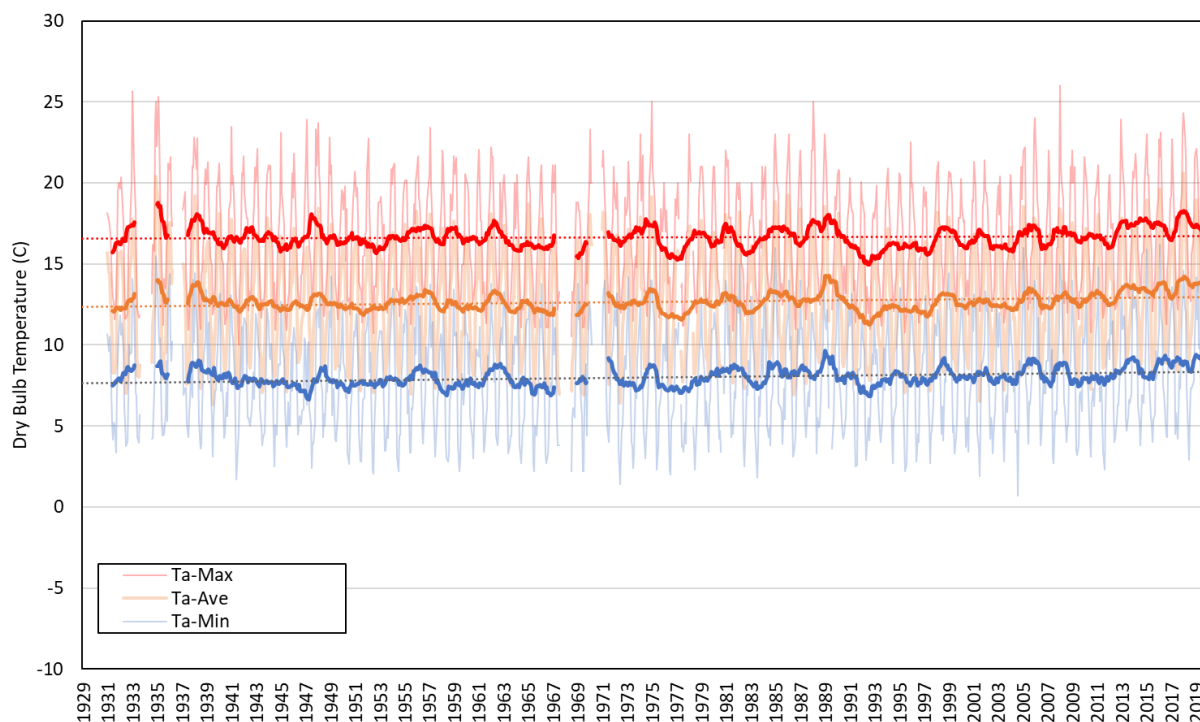


**Figure 5-6: Monthly “9 am” average (orange lines), minimum (blue lines), and maximum (red lines) time series (thin lines) of dry bulb air temperature ( $T_a$ ) for Kelburn, Wellington for the period 1929 to 2019. The thick bold lines are running 12 month means of the average, minimum and maximum. Trendlines are represented by the faint dotted lines.**

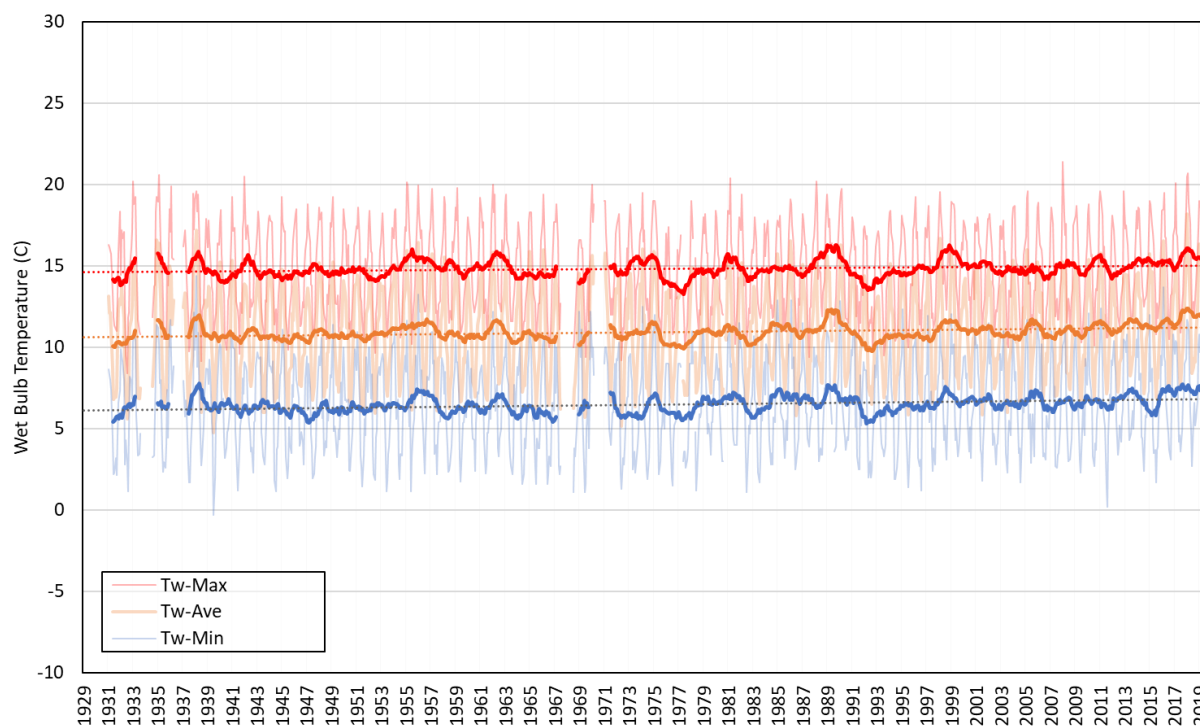


**Figure 5-7: Monthly “9 am” average (orange lines), minimum (blue lines), and maximum (red lines) time series (thin lines) of wet bulb temperature ( $T_w$ ) for Kelburn, Wellington for the period 1929 to 2019. The thick bold lines are running 12 month means of the average, minimum and maximum. Trendlines are represented by the faint dotted lines.**



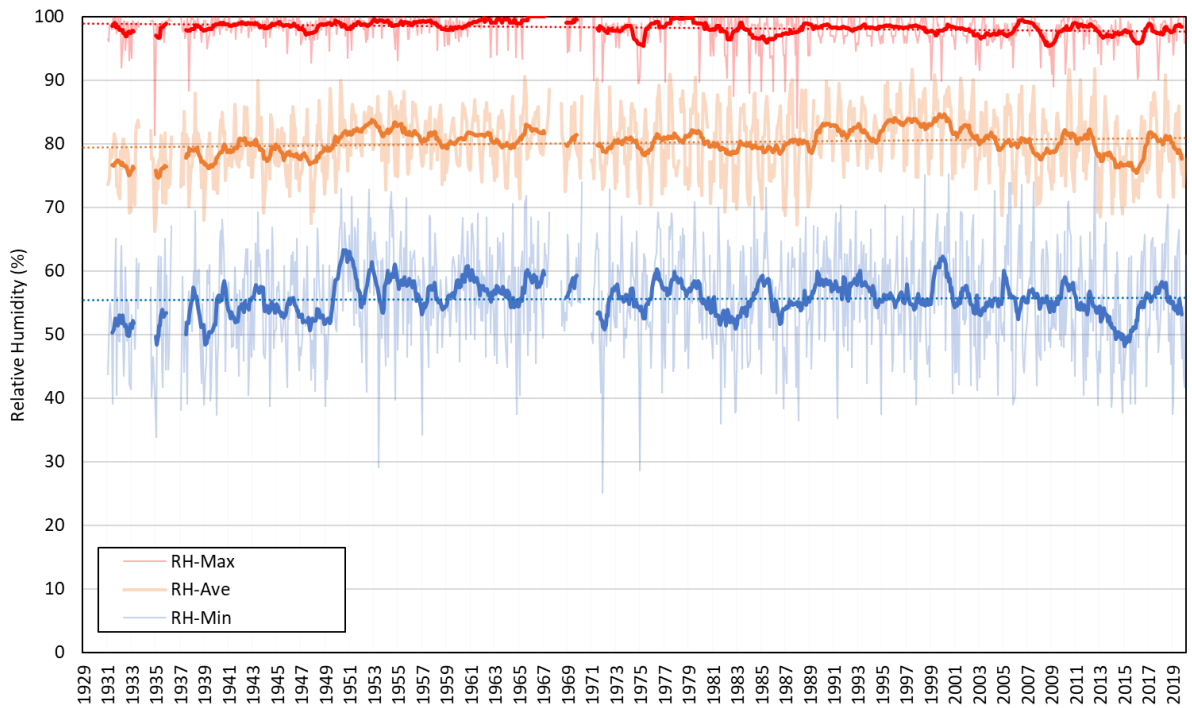


**Figure 5-8: Monthly “9 am” average (orange lines), minimum (blue lines), and maximum (red lines) time series (thin lines) of relative humidity (RH) for Kelburn, Wellington for the period 1929 to 2019. The thick bold lines are running 12 month means of the average, minimum and maximum. Trendlines are represented by the faint dotted lines.**

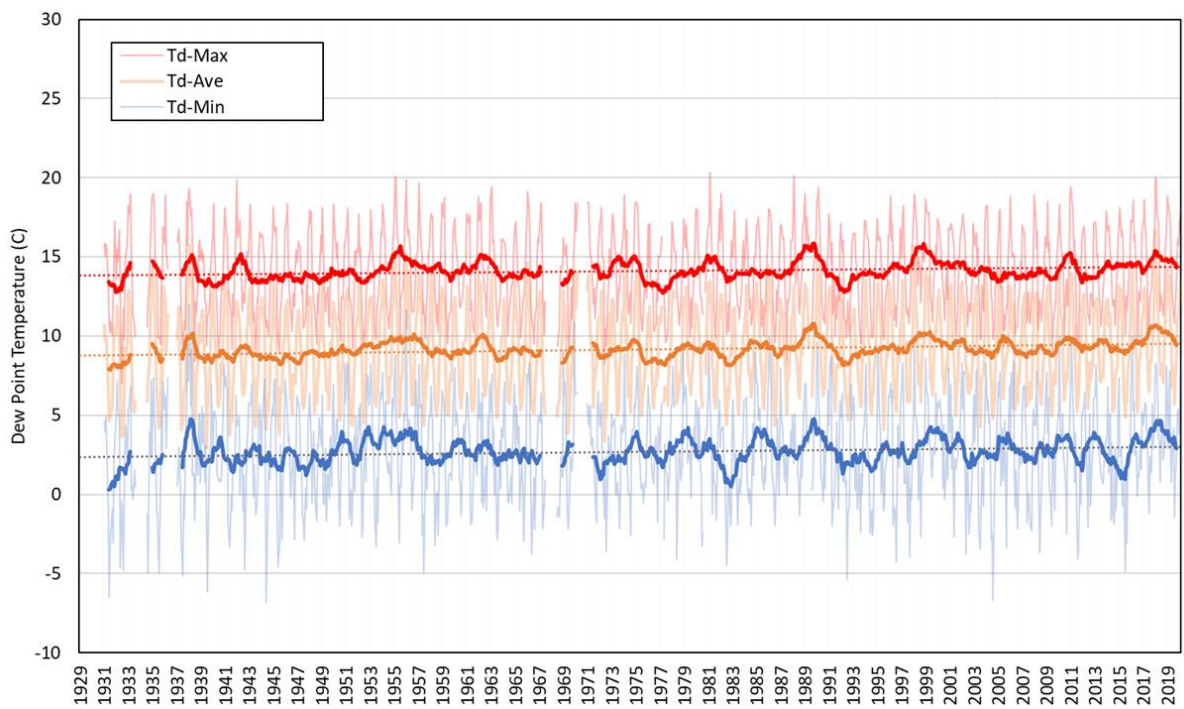


**Figure 5-9: Monthly “9 am” average (orange lines), minimum (blue lines), and maximum (red lines) time series (thin lines) of dew-point temperature ( $T_d$ ) for Kelburn, Wellington for the period 1929 to 2019. The**

thick bold lines are running 12 month means of the average, minimum and maximum. Trendlines are represented by the faint dotted lines.

**Table 5-6: Dates of extreme high values (top ten) of “9 am”  $T_d$  (6th column) in the period 1928 to 2019 at Kelburn. Also listed are the values  $T_a$ ,  $T_w$ , RH and Dew-point depression ( $DPP = T_a - T_d$ ) on these dates.**

Date	Rank	$T_a$	$T_w$	RH	$T_d$	DPP
10/3/1981	1	20.6	20.4	98.1	<b>20.3</b>	0.2
12/2/1988	2	20.4	20.2	98.1	<b>20.1</b>	0.2
18/2/1955	3	20.2	20.1	99.5	<b>20.1</b>	0.1
15/3/1955	4	19.9	19.9	100.0	<b>19.9</b>	0.0
30/1/1956	5	20.1	19.9	98.9	<b>19.9</b>	0.1
30/1/1942	6	21.7	20.5	89.4	<b>19.9</b>	1.2
4/2/1957	7	19.7	19.7	100.0	<b>19.7</b>	0.0
10/3/1990	8	19.6	19.6	100.0	<b>19.6</b>	0.0
14/3/1955	9	20.2	19.8	96.3	<b>19.6</b>	0.4
17/2/1963	10	19.4	19.4	100.0	<b>19.4</b>	0.0

**Table 5-7: Dates of extreme low values (bottom ten) of “9 am”  $T_d$  (6th column) in the period 1928 to 2019 at Kelburn. Also listed are the values  $T_a$ ,  $T_w$ , RH and Dew-point depression ( $DPP = T_a - T_d$ ) on these dates.**

Date	Rank	$T_a$	$T_w$	RH	$T_d$	DPP
7/6/1944	1	6.1	1.9	39.0	<b>-6.8</b>	12.9
24/8/2004	2	0.7	1.7	40.5	<b>-6.7</b>	7.4
5/6/1931	3	6.4	2.2	39.1	<b>-6.5</b>	12.1
13/8/1939	4	5.9	1.9	41.6	<b>-6.1</b>	12.0
27/7/1992	5	5.7	2.0	44.8	<b>-5.4</b>	11.1
19/7/2015	6	4.8	1.5	48.6	<b>-5.1</b>	9.9
7/7/1937	7	5.1	1.7	47.5	<b>-5.1</b>	10.2
25/8/1935	8	7.2	3.0	41.7	<b>-4.9</b>	12.1
2/9/1934	9	7.8	3.3	40.2	<b>-4.9</b>	12.7
28/7/1957	10	5.8	2.2	46.0	<b>-4.9</b>	10.7

### 5.3 Wairarapa

Average values for each season (summer, autumn, winter, and spring) for each year from 1928 to 2019 for Masterton of  $RH$ ,  $T_a$ ,  $T_w$ , and  $T_d$  are provided in Figure 5-10 to Figure 5-13. Potential breakpoints in the time-series due to station changes are also indicated in these figures. Unfortunately, there are no overlaps of the records from which to make adjustments, so no attempts at adjustments were made. Brown and DeGaetano (2009) describe a method to detect inhomogeneities in historical dewpoint temperature series, but their method relies on hourly records being available which were not available in this record prior to 1991.

As was found for Wellington, it is apparent that the year-to-year variation and longer-term trends in  $T_a$ ,  $T_w$ , and  $T_d$  are all very similar. Again, the trend in winter is strongest where there is an increase (linear regression) in 9 am dew-point temperatures of 1.8°C and an increase in winter relative humidity of around 5.8% for the 90-year period. For autumn there is also an increase of around 0.8°C in  $T_d$  and around 3.2% in RH, and for spring they are +0.4°C and +1.7% while for summer there is an

increase of 0.5°C, and a small increase of 0.2% in RH. The smaller increases in summer relative humidity is likely impacted by recent increases in  $T_a$ . It is noted however, if records prior to 1942 are ignored due to a potential breakpoint due to the station move, the trends in  $T_d$  are +0.9 °C for winter, +0.2 °C for autumn, -0.4 °C for summer (decrease), and -0.2 °C (decrease) for spring. The trends in RH become +5.8% for winter, +2.0% for autumn, -3.9% (decrease) for summer, and -2.8% (decrease) for spring, and the trends in  $T_a$  become -0.02 °C for winter, +0.05 °C for spring, +0.58 °C for summer, and -0.21 °C for autumn.

The top-ten and bottom-ten ranked months for average dew-point temperatures are provided in Table 5-9 and Table 5-10. As was the case for Wellington, January 2018 in Masterton had the highest average  $T_d$  values of 16.1 °C. Four of the top ten ranked months for average  $T_d$  occurred in the 1950's. Six of the bottom ranked months occurred in the 1930's and all occurred before 1972. Extreme high summer and autumn values of  $T_d$  occurred in the 1930's where there seems to be considerable year to year variability during those seasons.

**Table 5-8: Change in average seasonal values in “9 am” dew-point temperature ( $T_d$ ), Relative Humidity (RH), dry bulb air temperature ( $T_a$ ) and wet-bulb air-temperature ( $T_w$ ) for the Masterton, Wairarapa site between 1928 and 2019.**

Season	Change between 1928 and 2019			
	$T_d$ (°C)	RH (%)	$T_a$ (°C)	$T_w$ (°C)
Summer	+0.5	+0.2	+0.5	+0.3
Autumn	+0.8	+3.2	-0.1	+0.3
Winter	+1.8	+5.8	0.0	+0.5
Spring	+0.4	+1.7	-0.2	+0.1



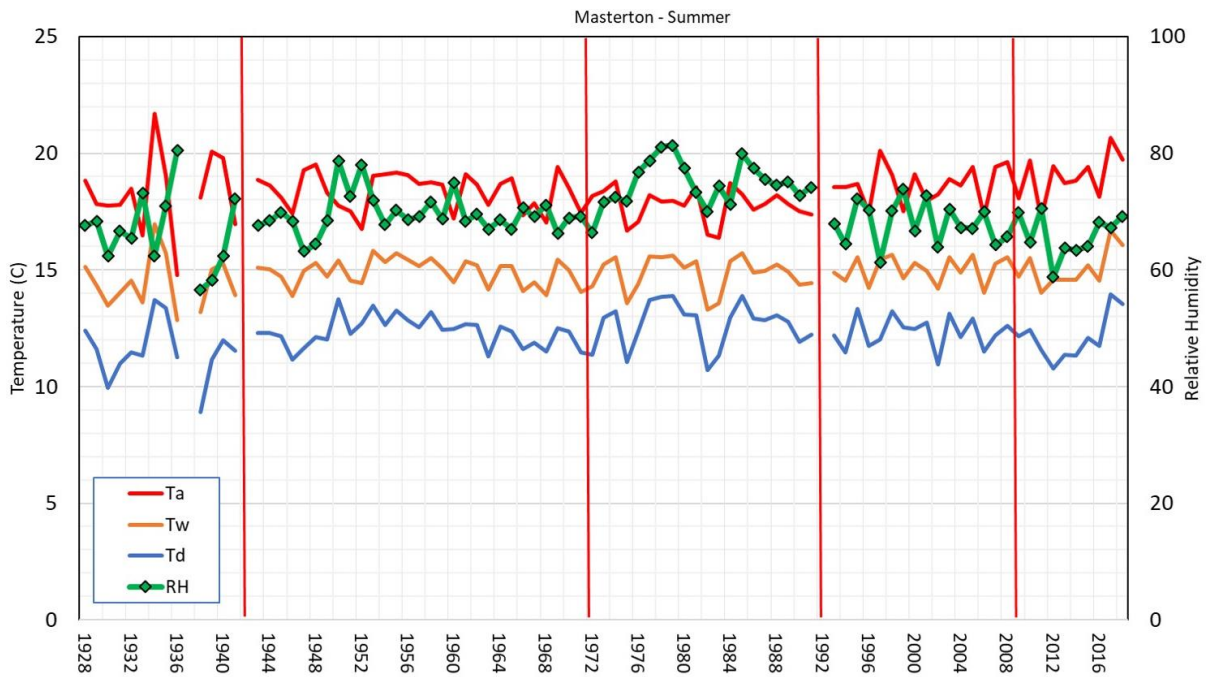


**Figure 5-10: Time series of “9 am” summer averages for dry bulb air temperature ( $T_a$ ; red-line), wet-bulb air-temperature ( $T_w$ ; orange line), dew-point temperature ( $T_d$ ; blue line) and Relative Humidity ( $RH$ ; green line) for the Masterton, Wairarapa site for the period 1928 to 2020. The red vertical lines mark station moves and the red line at 1972 marks the switch from earlier records recently digitized from meteorological charts to records retrieved from the national Climate Database (CliDB).**

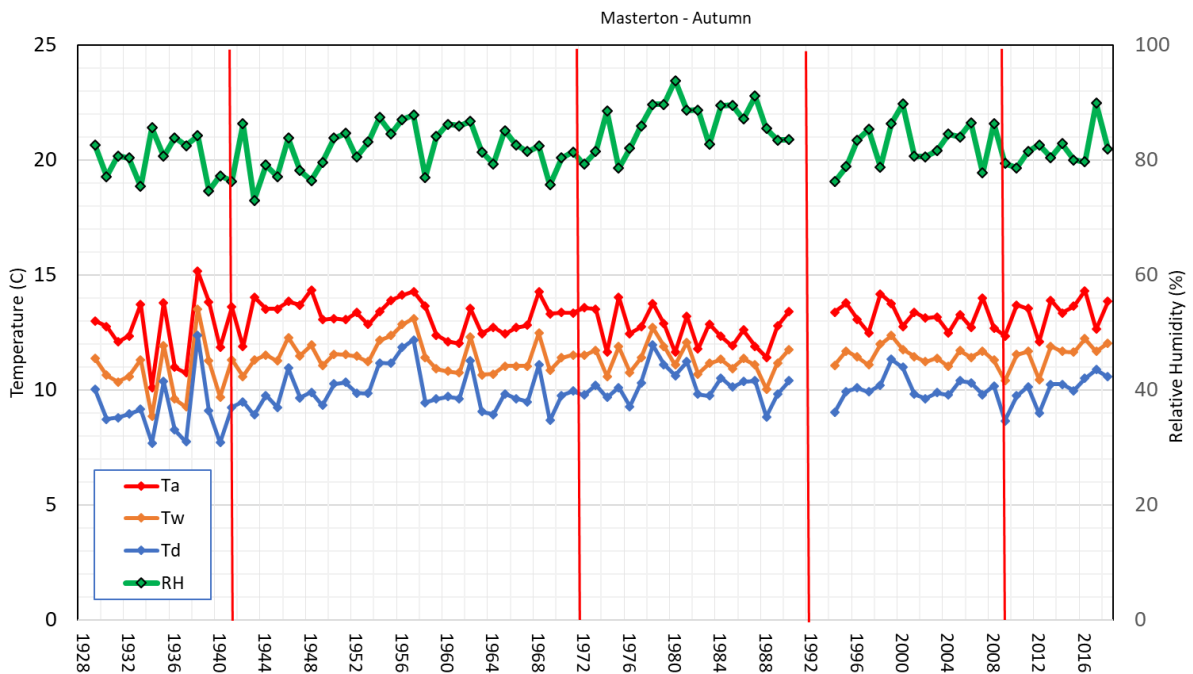


**Figure 5-11: Time series of “9 am” autumn averages for dry bulb air temperature ( $T_a$ ; red-line), wet-bulb air-temperature ( $T_w$ ; orange line), dew-point temperature ( $T_d$ ; blue line) and Relative Humidity ( $RH$ ; green line) for the Masterton, Wairarapa site for the period 1928 to 2020. The red vertical lines mark station moves and the red line at 1972 marks the switch from earlier records recently digitized from meteorological charts to records retrieved from the national Climate Database (CliDB).**

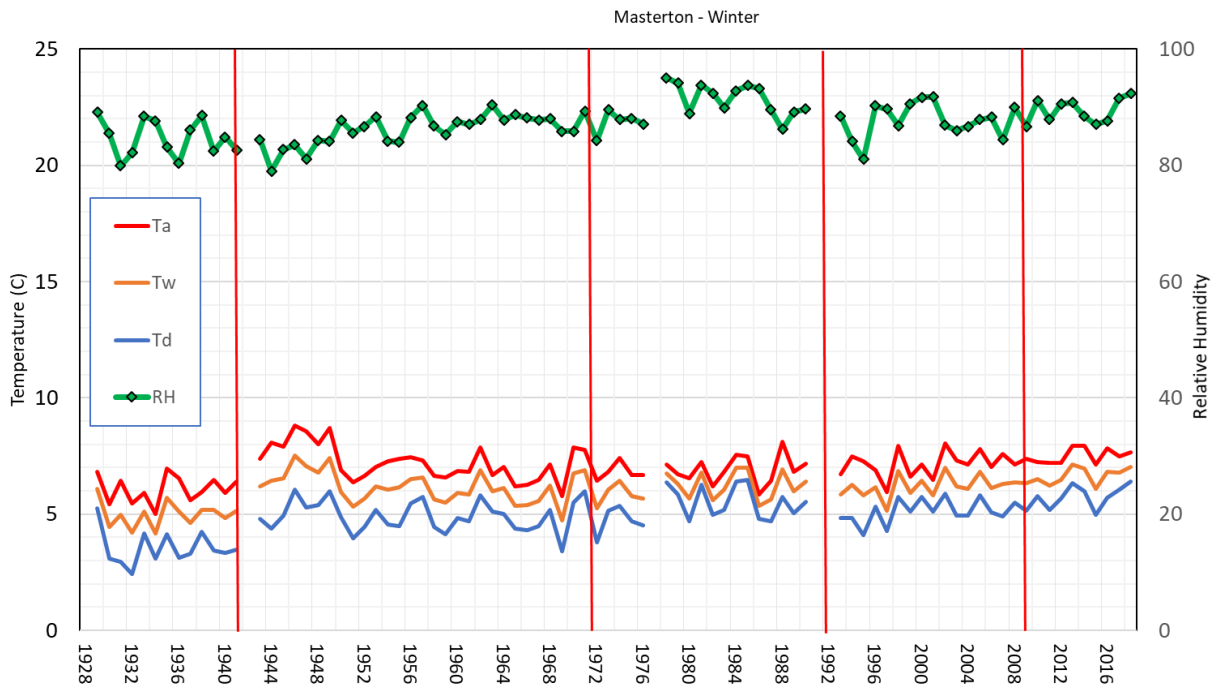


**Figure 5-12: Time series of “9 am” winter averages for dry bulb air temperature ( $T_a$ ; red-line), wet-bulb air-temperature ( $T_w$ ; orange line), dew-point temperature ( $T_d$ ; blue line) and Relative Humidity ( $RH$ ; green line) for the Masterton, Wairarapa site for the period 1928 to 2020. The red vertical lines mark station moves and the red line at 1972 marks the switch from earlier records recently digitized from meteorological charts to records retrieved from the national Climate Database (CliDB).**

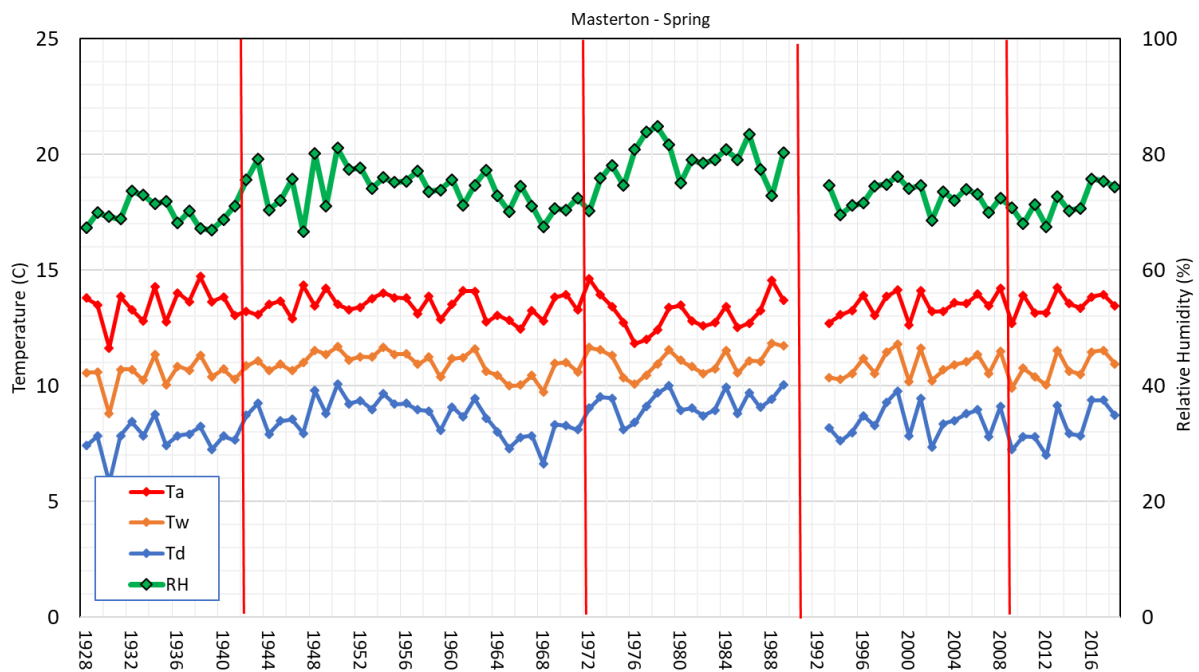


**Figure 5-13: Time series of “9 am” spring averages for dry bulb air temperature ( $T_a$ ; red-line), wet-bulb air-temperature ( $T_w$ ; orange line), dew-point temperature ( $T_d$ ; blue line) and Relative Humidity ( $RH$ ; green line) for the Masterton, Wairarapa site for the period 1928 to 2020. The red vertical lines mark station moves and the red line at 1972 marks the switch from earlier records recently digitized from meteorological charts to records retrieved from the national Climate Database (CliDB).**

**Table 5-9: Top ten ranked months with highest average “9 am” T<sub>d</sub> (6<sup>th</sup> column) in the period 1928 to 2019 at Masterton. Also listed are the average values T<sub>a</sub>, T<sub>w</sub>, RH in these months.**

Date	Rank	T <sub>a</sub>	T <sub>w</sub>	RH	T <sub>d</sub>
Jan-18	1	22.0	18.5	70.7	<b>16.1</b>
Mar-57	2	17.4	16.5	90.7	<b>15.8</b>
Feb-54	3	19.9	17.3	78.6	<b>15.7</b>
Feb-74	4	19.9	17.1	75.6	<b>15.2</b>
Jan-56	5	20.9	17.5	71.5	<b>15.0</b>
Mar-79	6	16.4	15.4	90.8	<b>14.7</b>
Feb-58	7	20.1	17.0	72.6	<b>14.7</b>
Feb-35	8	20.2	16.9	71.5	<b>14.6</b>
Mar-81	9	17.2	15.7	85.3	<b>14.6</b>
Jan-78	10	19.2	16.5	77.8	<b>14.5</b>

**Table 5-10: Bottom ten ranked months with lowest average “9 am” T<sub>d</sub> (6<sup>th</sup> column) in the period 1928 to 2019 at Masterton. Also listed are the average values T<sub>a</sub>, T<sub>w</sub>, RH in these months.**

Date	Rank	T <sub>a</sub>	T <sub>w</sub>	RH	T <sub>d</sub>
Jul-32	1	5.6	4.1	76.7	<b>1.5</b>
Jul-30	2	4.5	3.5	83.6	<b>1.9</b>
Jul-39	3	5.3	4.0	80.4	<b>2.0</b>
Jul-69	4	4.3	3.5	86.7	<b>2.1</b>
Jul-34	5	4.9	3.8	82.9	<b>2.1</b>
Jul-52	6	4.5	3.6	85.6	<b>2.1</b>
Jun-36	7	6.5	4.8	75.5	<b>2.2</b>
Jun-72	8	5.5	4.1	81.5	<b>2.2</b>
Jul-37	9	6.0	4.6	79.3	<b>2.3</b>
Jun-69	10	5.0	4.0	84.9	<b>2.3</b>

Monthly averages, minimums, and maximum of dry bulb air temperature (T<sub>a</sub>), wet bulb temperature (T<sub>w</sub>), relative humidity (RH) and dew-point temperature (T<sub>d</sub>) for Masterton are shown in Figure 5-14 to Figure 5-17. Trends in the averages correspond to the overall annual trends in these values and are +0.2 °C for T<sub>a</sub>, +0.4 °C T<sub>w</sub>, and +0.7 °C T<sub>d</sub> and +3.3% for RH over the 90 years. An interesting feature is the late 1970's where minimum relative humidity values below 60% were not observed and average relative humidity was above 80% - this seems mainly due to humid summers and autumns at this time although it is noted that this signal is not present in the Wellington record, and it corresponds with a block marked by station changes at the beginning and at the end.

The ten most extreme maximum values of 9 am dew-point temperature and the dates on which these occurred are provided in Table 5-11 while the values of the extreme minimums and dates are provided in Table 5-12. The most extreme maximum  $T_d$  value was 23.7 °C, on 23 January 1958. Extreme minimum events again occurred in winter, with the record minimum of -10.3 °C of 3 August 1932. All the 10 bottom ranked events occurred prior to 1945.

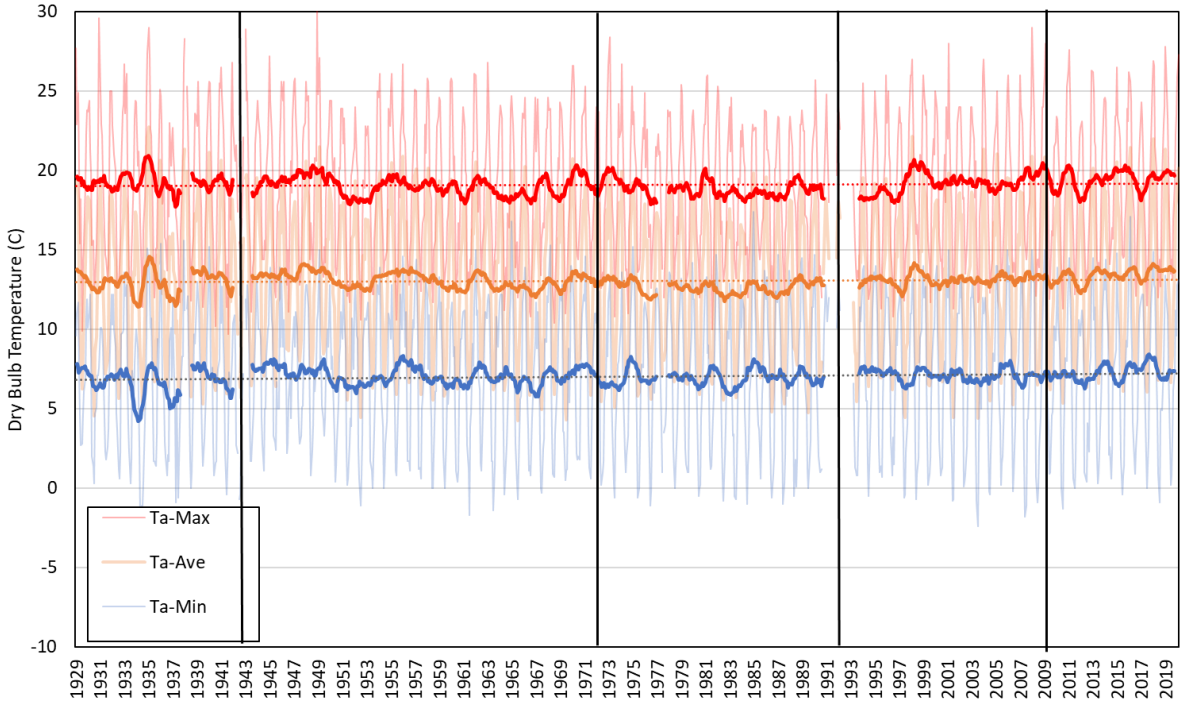


**Figure 5-14: Monthly “9 am” average (orange lines), minimum (blue lines), and maximum (red lines) time series (thin lines) of dry bulb air temperature ( $T_a$ ) for Masterton, Wairarapa for the period 1929 to 2019. The thick bold lines are running 12 month means of the average, minimum and maximum. Trendlines are represented by the faint dotted lines.**



**Figure 5-15: Monthly “9 am” average (orange lines), minimum (blue lines), and maximum (red lines) time series (thin lines) wet bulb temperature ( $T_w$ ) for Masterton, Wairarapa for the period 1929 to 2019. The thick bold lines are running 12 month means of the average, minimum and maximum. Trendlines are represented by the faint dotted lines.**

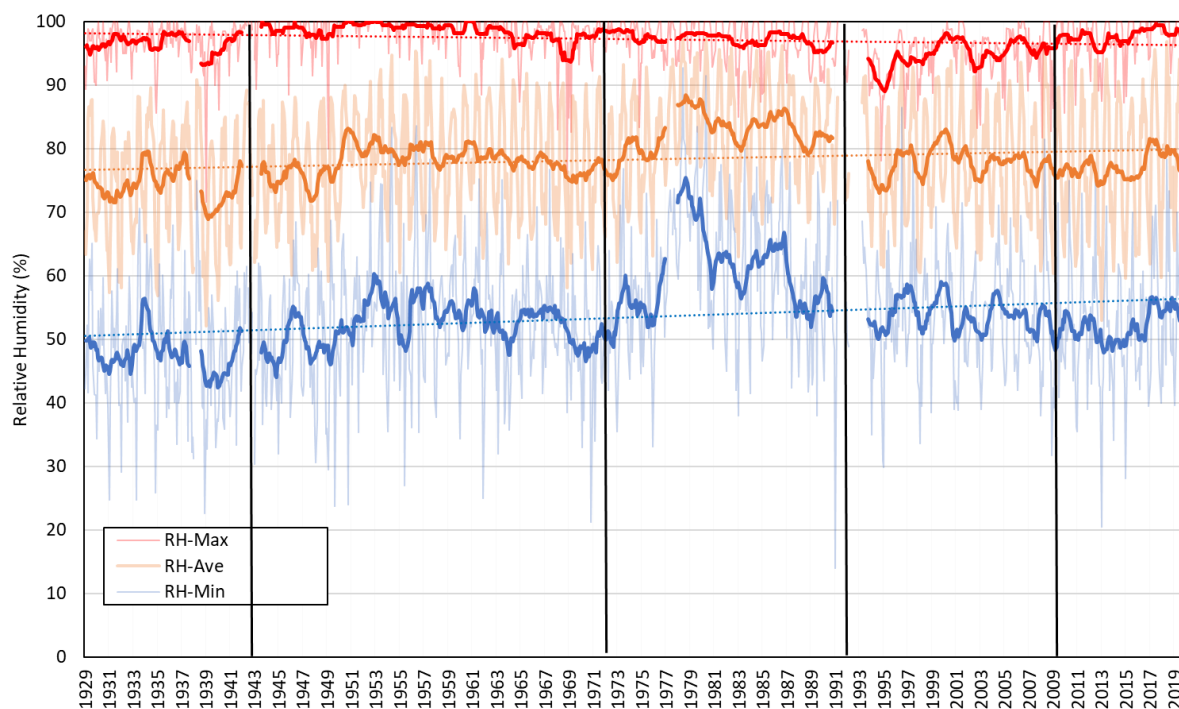


**Figure 5-16: Monthly “9 am” average (orange lines), minimum (blue lines), and maximum (red lines) time series (thin lines) of relative humidity (RH) for Masterton, Wairarapa for the period 1929 to 2019. The thick bold lines are running 12 month means of the average, minimum and maximum. Trendlines are represented by the faint dotted lines.**

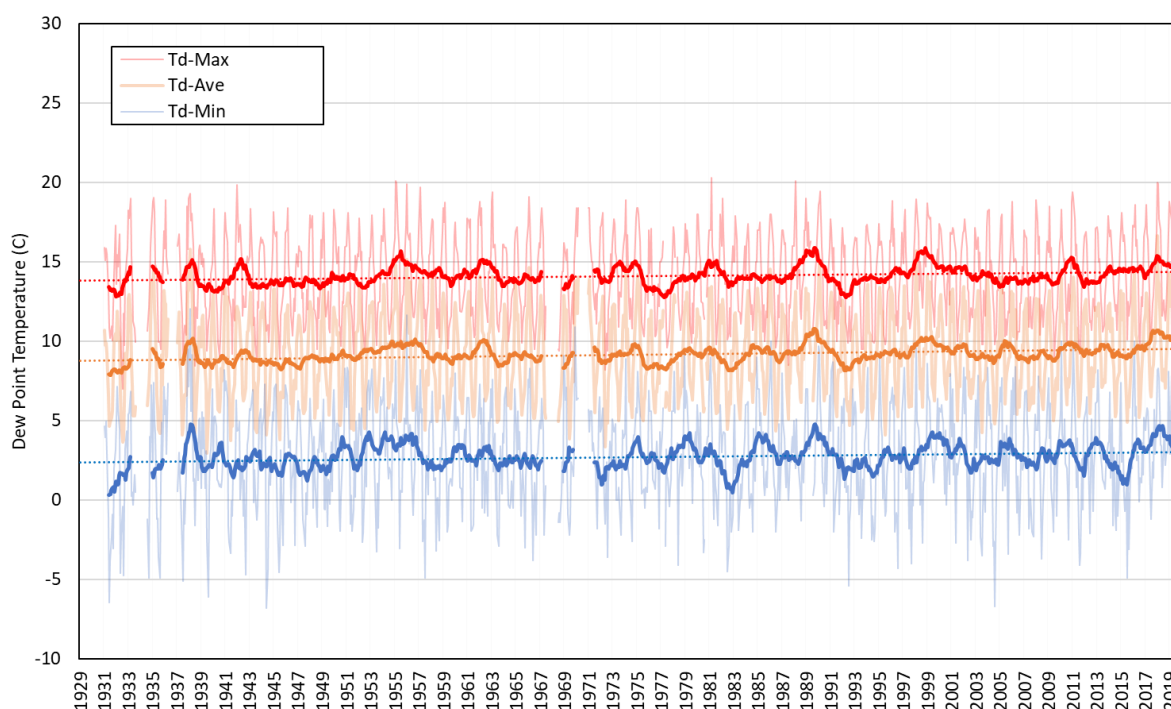


**Figure 5-17: Monthly “9 am” average (orange lines), minimum (blue lines), and maximum (red lines) time series (thin lines) of dew-point temperature ( $T_d$ ) for Masterton, Wairarapa for the period 1929 to 2019. The thick bold lines are running 12 month means of the average, minimum and maximum. Trendlines are represented by the faint dotted lines.**

**Table 5-11: Dates of extreme high values (top ten) of “9 am”  $T_d$  (6th column) in the period 1928 to 2019 at Masterton. Also listed are the values  $T_a$ ,  $T_w$ , RH and Dew-point depression ( $DPP = T_a - T_d$ ) on these dates.**

Date	Rank	$T_a$	$T_w$	RH	$T_d$	DPP
23/01/1958	1	24.4	23.9	95.4	<b>23.7</b>	0.7
27/01/1956	2	24.0	22.9	90.7	<b>22.4</b>	1.6
22/01/1937	3	22.7	22.2	96.1	<b>22.0</b>	0.7
12/02/2018	3	23.9	22.6	89.2	<b>22.0</b>	1.9
17/12/1946	5	23.3	22.2	90.6	<b>21.7</b>	1.6
14/02/1958	6	25.6	22.8	78.3	<b>21.5</b>	4.1
10/03/1981	7	26.0	22.8	75.4	<b>21.3</b>	4.7
7/02/1943	8	21.9	21.1	95.8	<b>21.1</b>	0.8
4/02/1957	8	21.1	21.1	100.0	<b>21.1</b>	0.0
30/01/1956	18	24.6	22.2	80.8	<b>21.1</b>	3.5

**Table 5-12: Dates of extreme low (bottom ten) values of “9 am”  $T_d$  (6th column) in the period 1928 to 2019 at Masterton. Also listed are the values  $T_a$ ,  $T_w$ , RH and Dew-point depression ( $DPP = T_a - T_d$ ) on these dates.**

<b>Date</b>	<b>Rank</b>	<b><math>T_a</math></b>	<b><math>T_w</math></b>	<b>RH</b>	<b><math>T_d</math></b>	<b>DPP</b>
22/07/1932	1	4.2	0.0	33.8	<b>-10.3</b>	14.5
8/08/1936	2	5.2	0.5	30.2	<b>-9.6</b>	14.8
24/07/1937	3	5.3	0.7	30.7	<b>-9.3</b>	14.6
21/07/1931	4	2.8	-0.6	43.6	<b>-8.4</b>	11.2
6/06/1936	5	4.2	0.2	37.1	<b>-8.2</b>	12.4
10/07/1937	6	4.2	0.2	37.8	<b>-8.0</b>	12.2
8/06/1944	7	6.1	1.7	36.0	<b>-8.0</b>	14.1
27/06/1930	8	1.8	-1.0	50.4	<b>-7.4</b>	9.2
13/06/1936	9	3.3	0.1	46.7	<b>-7.0</b>	10.3
31/07/1937	10	5.3	1.2	37.7	<b>-7.0</b>	12.3



## 6 Conclusions

This report presents analyses for historic extremes of wind, rainfall, air pressure, and dew point temperature data for the Wellington Region.

Long-term homogenised records of daily maximum gust speeds, noon gust speeds and daily wind-run were analysed for Wellington airport and for Masterton. For Wellington, 58 of the peak annual maximum gusts over the last 60 years are northerly (winds from NW through NE). The other two events were southerly, one of which was the most extreme event of the record (the *Wahine* Storm of 1968). For Masterton, the annual maximum gusts are dominated by Northerly sector winds which were primarily (> 90%) directed between WNW and NNW. There is little in terms of temporal trends in strength of annual maxima, however examination of seasonal trends at Wellington Airport shows that average daily maximum gust speeds have increased in spring by around 0.5 m/s (1.8 km/hr) since 1972. The other seasons had little in terms of a temporal trend. Spring also had an increase in days with maximum gusts exceeding the 90th, 95th, and 99th percentiles while the other seasons show a slight decrease.

The changes in the frequency of extreme precipitation events for Kelburn, Wellington Airport, Paraparaumu and Masterton were considered and there were no obvious consistent temporal trends within or between the sites. Of the four sites, Kelburn generally has the largest number of exceedances of extreme rainfall thresholds per year while Masterton has the least. We also considered future changes in rainfall threshold exceedances under four climate change scenarios (Representation Concentration Pathways; RCPs) and for two future 30-year periods (2031-2060 and 2071-2100). At all four sites, the number of exceedances of all thresholds considered were indicated to increase for the 2071-2100 period under all RCPs (with few exceptions), with the largest increases projected under the RCP 8.5 scenario.

The analysis of atmospheric pressure in Wellington since 1862 indicated that there is significant temporal variability in pressure extremes in the record (both high and low). The proportion of observations exceeding the 90<sup>th</sup> percentile and falling below the 10<sup>th</sup> percentile follow a seasonal cycle, which is significantly stronger for high pressure extremes. The El Niño-Southern Oscillation (ENSO) was shown to play an important role with extreme pressure, with more high-pressure extremes occurring during La Niña and more low-pressure extremes during El Niño. It was also shown that inter-decadal variability in extreme pressure observations is largely driven by the Interdecadal Pacific Oscillation (IPO). During the positive phase of the IPO there tended to be more extreme low-pressure events whereas more frequent extreme high-pressure events tend to occur during the negative phase of the IPO.

The construction and analysis of a dew point temperature ( $T_d$ ) record for Wellington and Masterton revealed an overall increase in dew point temperature since 1928 when averaged over all seasons. The strongest increasing trend occurs for the winter season at both locations, while the second strongest is during autumn. Summer and spring saw smaller increases or even a decrease. Unsurprisingly, many monthly average  $T_d$  values that were ranked in the bottom ten for each location occurred during the 1930's (and 1940's for Wellington). However, despite the long-term upward trend, average  $T_d$  values for February 1938 and February 1935 are ranked 2<sup>nd</sup> and 10<sup>th</sup> highest respectively in the Kelburn record, while February 1935 is also ranked 8<sup>th</sup> highest in the Wairarapa record. Finally, the records show that extreme high summer and autumn values of  $T_d$  occurred in the 1930's where there seems to be considerable year to year variability.



## 7 Supplementary figures

The figures presented in this section relate to a very brief exploratory analysis of the spread of observed MSLP through time (noted in Section 4.2). The standard deviation of MSLP was calculated for rolling time intervals of 1, 3, and 5 years, the results of which are presented in Figures 7-1, 7-2 and 7-3 respectively. For each of the chosen intervals there is a slight decreasing trend in standard deviation however the statistical significance of these results was notably different between analyses and significant only when computed at the 3-year interval. Further work is therefore required to understand trends in the distribution of MSLP however the results presented in this section may serve as a starting point for further research on this front.

Note that same as for the data presented in Section 4, the analysed pressure observations in the following figures are only sampled from 7:00 am to 11:00 am (i.e. a two-hour window around 9:00 am). Data gaps exist where there were 15 days or more of missing data in the analysed time interval.

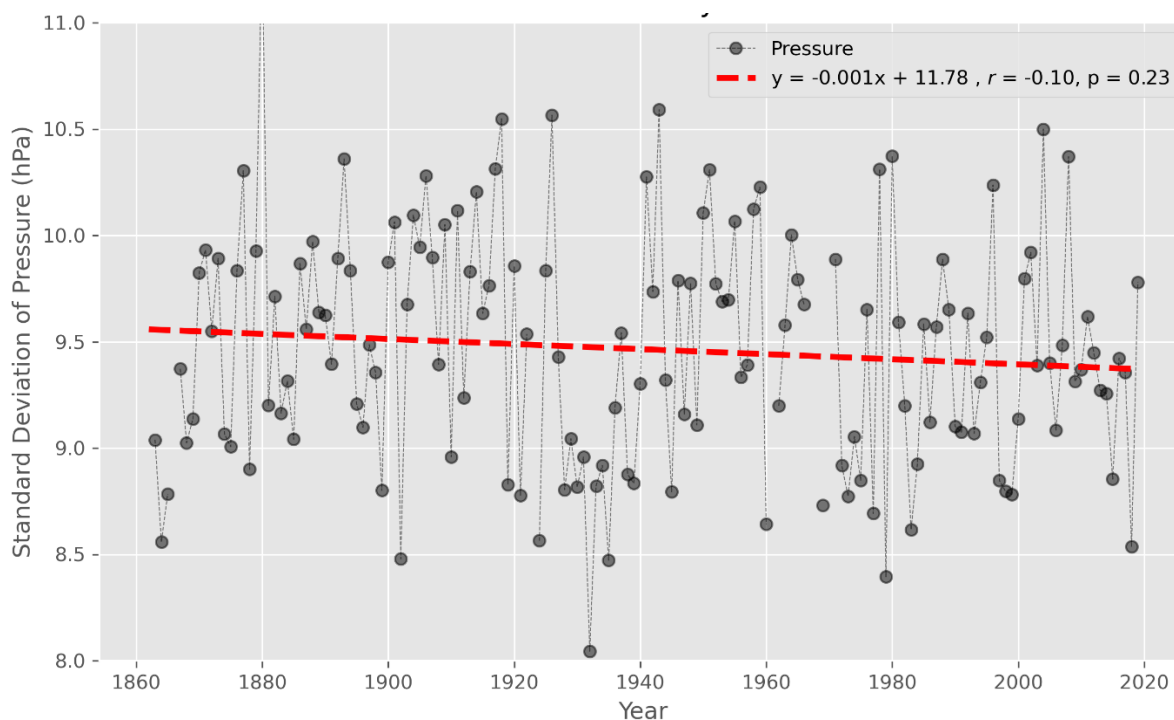


**Figure 7-1: Standard deviation of annual mean sea level pressure through time (i.e. standard deviation using a 1-year rolling time window).** Each data point represents the standard deviation calculated from the distribution of MSLP values for the given calendar year. One-year time windows associated with each data point do not overlap. The dashed red trendline suggests decreasing variability through time however the results of the trend analysis presented in the legend indicate that this trend is not statistically significant ( $p = 0.23$ ).

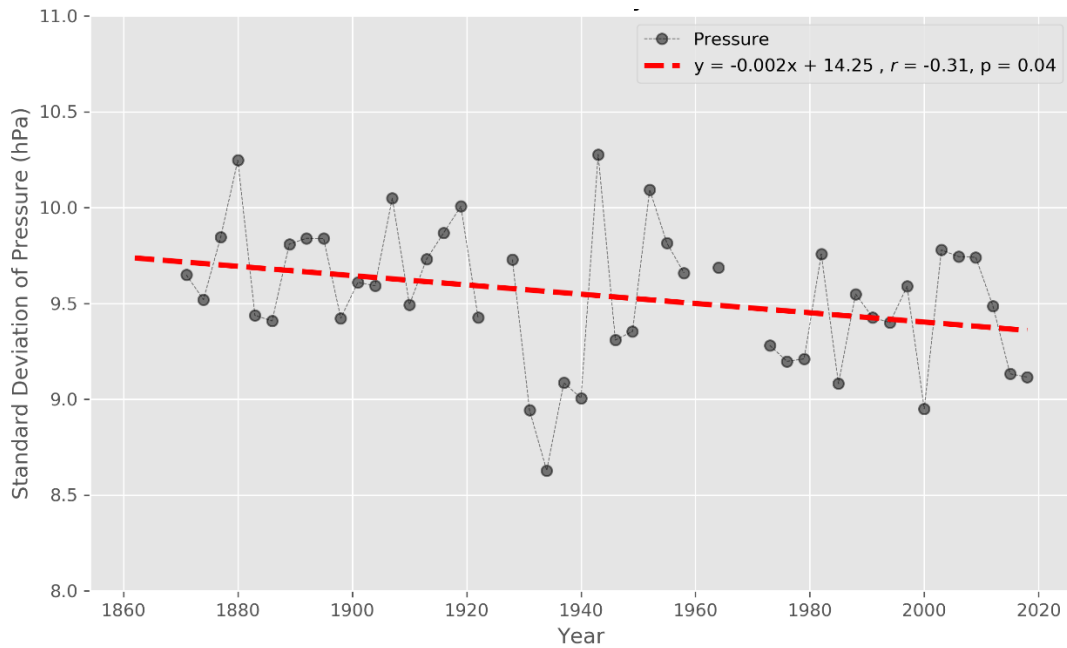


**Figure 7-2: Standard deviation of 3-year mean sea level pressure through time computed using 3-year bins.** Each data point represents the end year of the computation period (i.e. the 3 years leading up to the plotted year were used to calculate the standard deviation). The 3-year bins associated with each data point do not overlap. The dashed red trendline suggests decreasing variability through time. The results of the trend analysis presented in the legend indicate that this trend is statistically significant ( $p = 0.04$ ).

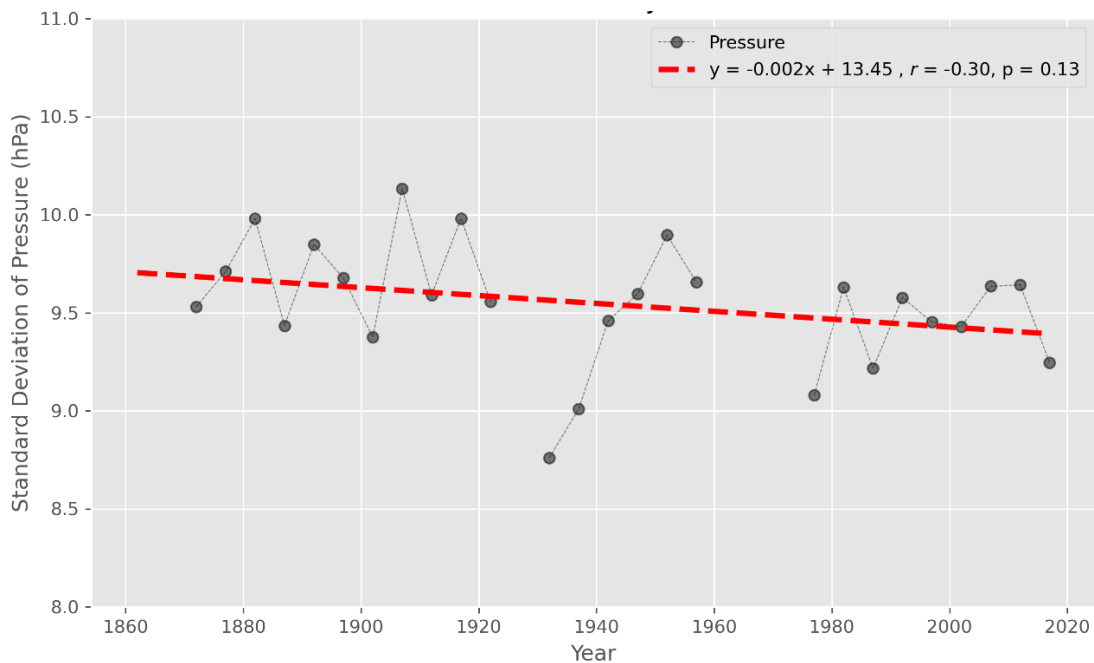


**Figure 7-3: Standard deviation of mean sea level pressure through time computed using a 5-year bins.** Each data point represents the end year of the computation period (i.e. the 5 years leading up to the plotted year were used to calculate the standard deviation). Time 5-year bins associated with each data point do not overlap. The dashed red trendline suggests decreasing variability through time. The results of the trend analysis presented in the legend indicate that this trend is not statistically significant ( $p = 0.13$ ).

## 8 Acknowledgements

Katie Baddock is acknowledged for rapidly digitising the early period daily temperature and humidity data for this project. Dr Alex Pezza from Greater Wellington Regional Council is thanked for providing feedback on the draft version of the report.

## 9 References

- Abbott, P.F., and Tabony, R.C. 1985. The estimation of humidity parameters. *Met. Mag.*, 114, 49-56.
- Bureau of Meteorology. 2003. Equipment Specification A2669. 215pp
- Alduchov, O. A., and R. E. Eskridge, 1996: Improved Magnus' form approximation of saturation vapor pressure. *J. Appl. Meteor.*, 35, 601–609.
- August, E. F., 1828: Ueber die Berechnung der Expansivkraft des Wasserdunstes. *Ann. Phys. Chem.*, 13, 122–137.
- Australian Bureau of Meteorology Official Website, 2020:  
<http://www.bom.gov.au/climate/averages/climatology/relhum/calc-rh.pdf>
- Brown, P. J., and A. T. DeGaetano, 2009, A method to detect inhomogeneities in historical dewpoint temperature series. *J. Appl. Meteor. Climatol.*, 48, 2362-2376.
- Carey-Smith, T., Henderson, R. and Singh, S., 2018. High Intensity Rainfall Design System, Version 4. NIWA Client Report 2018022CH, NIWA. Available at:  
[https://niwa.co.nz/sites/niwa.co.nz/files/2018022CH\\_HIRDSv4\\_Final.pdf](https://niwa.co.nz/sites/niwa.co.nz/files/2018022CH_HIRDSv4_Final.pdf) (Accessed: 7 May 2020).
- Cenek, P., R. Turner, R. Flay, A. Safeei-Pirooz, N. Jamieson, and P. Carpenter, 2019, Tools and knowledge to improve New Zealand's long-term resilience to wind-storms. Final research report by WSP (OPUS) and collaborators to Natural Hazards Research Platform. 64 pp.
- Fouhy, E., L. Coutts, R. McGann, B. Collen, and J. Salinger, 1992, South Pacific Historical Climate Network. *Climate Station Histories. Part 2: New Zealand and Offshore Islands.* 221 pp. ISBN 0-477-01583-2
- Magnus, G., 1844: Versuche über die Spannkräfte des Wasserdampfes. *Ann. Phys. Chem.*, 61, 225–247.
- McNoldy, B., 2019, Temperature Dewpoint, and Relative Humidity Calculator.  
<https://bmcnoldy.rsmas.miami.edu/Humidity.html>
- Omni, 2020, Wet Bulb Calculator, <https://www.omnicalculator.com/physics/wet-bulb>
- Pearce, P., Fedaeff, N., Mullan, B., Rosier, S., Carey-Smith, T., and Sood, A., 2019. Wellington Region climate change extremes and implications. NIWA client report 2019134AK prepared for Greater Wellington Regional Council. Available at: <https://www.gw.govt.nz/assets/Climate-change/GWRC-NIWA-climate-extremes-FINAL3.pdf>
- Salinger, M. J. & Mullan, A. B. 1999. New Zealand climate: temperature and precipitation variations and their links with atmospheric circulation 1930–1994. *International Journal of Climatology*, 19, 1049-1071.
- Salinger, M. J., Renwick, J. A. & Mullan, A. B. 2001. Interdecadal Pacific oscillation and south Pacific climate. *International Journal of Climatology*, 21, 1705-1721.
- Stull, R., 2011, Wet bulb temperature from relative humidity and air temperature. *J. Appl. Meteor. Climatol.*, 51, 2267-2269. <https://doi.org/10.1175/JAMC-D-11-0143.1>

Turner, R., T. Bromley, A. Tait, 2006, Potential aerial spread of Red Imported Fire Ant (RIFA) (*Solenopsis Invicta*) at Whirinaki Hawkes Bay. NIWA client report for MAF Biosecurity, WLG2006-68, 24 pp.

Turner, R., A.A. Safaei Pirooz, R.G. Flay, S. Moore, and M. Revell, 2019: Use of High-Resolution Numerical Models and Statistical Approaches to Understand New Zealand Historical Wind Speed and Gust Climatologies. *J. Appl. Meteor. Climatol.*, 58, 1195–1218, <https://doi.org/10.1175/JAMC-D-18-0347.1>